

UNCLASSIFIED

---

---

AD 296 240

*Reproduced  
by the*

ARMED SERVICES TECHNICAL INFORMATION AGENCY  
ARLINGTON HALL STATION  
ARLINGTON 12, VIRGINIA



---

---

UNCLASSIFIED

NOTICE: When government or other drawings, specifications or other data are used for any purpose other than in connection with a definitely related government procurement operation, the U. S. Government thereby incurs no responsibility, nor any obligation whatsoever; and the fact that the Government may have formulated, furnished, or in any way supplied the said drawings, specifications, or other data is not to be regarded by implication or otherwise as in any manner licensing the holder or any other person or corporation, or conveying any rights or permission to manufacture, use or sell any patented invention that may in any way be related thereto.

**CIVIL ENGINEERING STUDIES**

STRUCTURAL RESEARCH SERIES NO. 261



CATALOGUE OF ASTIA 296240  
AS 11110.

296 240

**INTERACTION OF PLANE ELASTIC WAVES  
WITH AN ELASTIC CYLINDRICAL SHELL**



By  
T. YOSHIHARA  
A. R. ROBINSON  
and  
J. L. MERRITT

A Technical Report  
of a Research Program  
Sponsored by  
THE OFFICE OF NAVAL RESEARCH  
DEPARTMENT OF THE NAVY  
Contract Nonr 1834(03)  
Project NR-064-183

UNIVERSITY OF ILLINOIS  
URBANA, ILLINOIS  
JANUARY 1963

INTERACTION OF PLANE ELASTIC WAVES  
WITH AN ELASTIC CYLINDRICAL SHELL

By

T. Yoshihara

A. R. Robinson

and

J. L. Merritt

A Technical Report  
of a Research Program  
Sponsored by

THE OFFICE OF NAVAL RESEARCH  
DEPARTMENT OF THE NAVY  
Contract Nonr 1834(03)  
Project NR-064-183

UNIVERSITY OF ILLINOIS  
URBANA, ILLINOIS  
JANUARY 1963

## ABSTRACT

The purpose of this study was to investigate the interaction of plane elastic waves with a thin, hollow, cylindrical shell embedded in an elastic medium.

The cylindrical shell is considered to be elastic, isotropic, homogeneous, and of infinite length. It is surrounded by an elastic, isotropic, and homogeneous medium whose motions conform to the ordinary theory of elasticity. A plane stress wave, either dilatational or shear, with a step variation in time, whose wave front travels in a direction perpendicular to the cylinder axis, envelops the shell. Later, a Duhamel integral is used to study other wave shapes for the incident stress.

The response of the shell is studied by expressing the two components of displacement, radial and tangential, in terms of Fourier series, each term of which is called a mode. The equations of motion of the shell in vacuo are derived from expressions giving the strain and kinetic energies due to generalized external forces. Forces on the shell result from the stresses in the medium at the boundary. Stresses in the medium are taken to be the sum of the stresses due to the incoming stress wave expressed in terms of Fourier series whose coefficients are known, and those due to the reflected and diffracted effects expressed in terms of a pair of displacement potentials representing waves diverging from the axis of the shell.

The equations to be solved consist of two pairs of coupled integro-differential equations in the generalized coordinates of the shell and the displacement potentials. By use of a digital computer they are solved mode-wise by a step-by-step iterative integration technique known as the Newmark Beta Method, with which values for the potential functions, and the acceler-

ations, velocities, and displacements of the shell are determined. Stresses in the shell are found from the displacements, and the values of the potential functions permit determination of stresses for any point in the medium.

Although the equations are written to include an infinite number of modes, only the first three modes are considered in detail. The computed solution is compared with values obtained from a series expansion of the equations, which is valid for short times, and with the static solution based on the theory of elasticity to which the general solution should approach asymptotically. In addition, the results of two particular problems are compared with results given in another study.

Numerical solutions are obtained to determine the effect of the several parameters which describe the relative physical properties of the shell and medium. Results are presented in tabular and graphical form.

## ACKNOWLEDGMENT

The study reported herein was conducted under a program sponsored by the United States Navy Bureau of Yards and Docks and administered by the Superintendent, U. S. Naval Postgraduate School. The report is based upon a thesis prepared by T. Yoshihara in partial fulfillment of the requirements for the degree of Doctor of Philosophy in Civil Engineering.

The report was prepared under the general direction of Dr. N. M. Newmark, Head, Department of Civil Engineering. The assistance of Dr. S. L. Paul, Instructor in Civil Engineering, is gratefully acknowledged.

Appreciation is also expressed to the personnel of the University of Illinois Digital Computer Laboratory for their cooperation.

## TABLE OF CONTENTS

|   | Page |
|---|------|
| I. INTRODUCTION . . . . .                                     | 1    |
| 1.1 General Remarks . . . . .                                 | 1    |
| 1.2 Statement of Problem. . . . .                             | 1    |
| 1.3 Basic Assumptions . . . . .                               | 2    |
| 1.4 Method of Approach. . . . .                               | 3    |
| 1.5 Previous Work . . . . .                                   | 4    |
| 1.6 Notation. . . . .   | 5    |
| II. BASIC EQUATIONS. . . . .                                  | 9    |
| 2.1 Equations for the Medium. . . . .                         | 9    |
| 2.11 Dilatational Wave . . . . .                              | 12   |
| 2.12 Shear Wave. . . . .                                      | 18   |
| 2.2 Equations for the Shell . . . . .                         | 21   |
| 2.21 Dilatational Wave . . . . .                              | 23   |
| 2.22 Shear Wave. . . . .                                      | 25   |
| 2.23 Effect of Additional Mass . . . . .                      | 26   |
| 2.3 Boundary Conditions . . . . .                             | 28   |
| 2.4 Summary of Equations in Non-Dimensionalized Form. . . . . | 29   |
| 2.5 Other Equations of Interest . . . . .                     | 32   |
| III. METHOD OF SOLUTION . . . . .                             | 34   |
| 3.1 General . . . . .   | 34   |
| 3.2 Numerical Integration of the Potential Functions. . . . . | 34   |
| 3.3 Solution of the Basic Equations . . . . .                 | 40   |
| 3.4 Stresses of the Shell and Medium. . . . .                 | 43   |
| 3.5 Time Dependent Stress Wave. . . . .                       | 46   |
| 3.6 Description of the Computer Program . . . . .             | 46   |
| 3.7 Short-Time Approximation. . . . .                         | 48   |
| IV. DISCUSSION OF RESULTS. . . . .                            | 53   |
| 4.1 General . . . . .   | 53   |
| 4.2 Modal Response of Shell and Medium. . . . .               | 54   |
| 4.3 Short-Time and Asymptotic Comparison. . . . .             | 56   |
| 4.4 Effect of Parameters. . . . .                             | 59   |
| 4.5 Response to Time Varying Incident Wave. . . . .           | 61   |
| 4.6 Comparison with Previous Work . . . . .                   | 61   |
| 4.7 Conclusions . . . . .                                     | 62   |
| BIBLIOGRAPHY . . . . .  | 64   |

## TABLE OF CONTENTS (Cont'd)

|   | Page |
|---|------|
| APPENDIX A. DERIVATION OF THE EXPRESSIONS INVOLVING THE POTENTIAL FUNCTIONS . . . . . | 65   |
| A.1 General Form of the Potential Function . . . . .                                  | 65   |
| A.2 Velocity Terms . . . . .  | 68   |
| A.3 Stress Terms . . . . .  | 69   |
| APPENDIX B. STATIC SOLUTION . . . . .   | 71   |
| B.1 Dilatational Wave. . . . .  | 71   |
| B.11 $n = 0$ Mode . . . . .   | 72   |
| B.12 $n = 2$ Mode . . . . .   | 74   |
| B.2 Shear Wave . . . . .  | 76   |

## CHAPTER I

### INTRODUCTION

#### 1.1 General Remarks

The problem of designing underground protective structures to resist the effects of nuclear weapons has become increasingly important in recent years with the development of modern weapons whose destructive capacity is overwhelming. Engineers in this field are hampered to a great extent by a lack of theoretical information on how structures in media such as soil or rock behave when subjected to dynamic loads. Even for static loads alone, much of the design practice today is of a semi-empirical nature.

When a nuclear explosion occurs, stress waves are transmitted through the air and ground. How are they transmitted and how are they modified by the presence of a structure embedded in the medium? How does the structure respond?

The purpose of this report is to study one aspect of the problem, the interaction between the medium and structure.

#### 1.2 Statement of Problem

The problem considered here consists of analyzing the elastic response of a hollow cylindrical shell (tunnel lining) embedded in an elastic medium when subjected to an incident plane stress wave traveling in a direction perpendicular to the axis of the shell. Some questions with which this problem may be associated are: Do tunnel linings in contact with rock afford a measure of protection significantly higher than an unlined opening? What magnitude and time variation of displacement, velocity, and acceleration would equipment mounted within such a structure be subjected to? How are stress waves within

the medium modified in the vicinity of the shell? This study was conducted in an attempt to find some qualitative and quantitative answers to these questions within the limitations imposed by the assumptions noted below.

### 1.3 Basic Assumptions

The cylindrical shell is considered to be of infinite length, and is embedded in an elastic medium of infinite extent in all directions. A plane stress wave whose front travels in a direction perpendicular to the cylinder axis envelops the shell. Strains parallel to the axis in both the medium and shell are assumed to vanish; thus, since each cross section of the shell is exactly similar to every other, the problem is reduced to one of plane strain.

In the mathematical development of the problem certain basic assumptions were made, the most important of which are given here with a few explanatory remarks:

(1) The medium is considered to be homogeneous, isotropic, and linearly elastic. This implies that the ordinary theory of stress wave propagation applies. In view of the non-homogeneous, non-isotropic, and non-elastic characteristics of most materials encountered in nature, this is a severe limitation; however, current theories of stress propagation through such media have not advanced to the stage where this limitation can be readily overcome. In the case of some rocks, though, this assumption may be justified.

(2) The material in the shell is also considered to be homogeneous, isotropic, and linearly elastic. Generally speaking, this assumption is valid for values of stress below the so-called proportional limit of materials commonly used. In addition, the thickness of the shell relative to its radius

is assumed small; this permits expression of all stress components of the shell in terms of a function which describes the deflection of its middle surface. This deflection must satisfy a linear partial differential equation with the appropriate boundary conditions.

(3) The incident stress wave considered is either a plane dilatational or a plane distortional (shear) wave. Under actual conditions, both waves are propagated with the shear lagging the dilatational wave. The combined effect for elastic conditions may be determined through the principle of superposition.

(4) The radial and tangential particle velocities of the medium at the boundary are equal to that of the shell. This is the continuity relation insuring that the shell and the medium are in contact with no relative slip occurring at the boundary.

(5) Any additional mass within the shell is assumed to be distributed symmetrically about the axis. The significance of this assumption is found in the development of the equations of motion to account for any additional mass located within the shell.

Other assumptions are presented in the formal development of the mathematical expressions used to describe the behavior of shell and medium.

#### 1.4 Method of Approach

The two components of shell displacement, radial and tangential, are written in terms of Fourier series from which expressions giving the strain energy and kinetic energy of the shell in vacuo are derived. The equations of motion are derived from Lagrange's equations in terms of the displacement functions and forces acting on the shell. Forces on the shell result from the stresses in the medium at the boundary. Stresses in the

medium are taken to be the sum of the stresses due to the incoming stress wave expressed in terms of Fourier series whose coefficients are known, and those due to the reflected and diffracted effects expressed in terms of a pair of displacement potentials representing waves diverging from the axis of the shell. The form of these potentials as derived by Lamb (4)\*, is in terms of sine and cosine series, the nature and treatment of which has been studied by Paul (6).

The equations of motion, described as a pair of coupled integro-differential equations, are solved modewise using a numerical technique known as the Newmark Beta Method (5) which permits determination of the coefficients of the potentials and values of acceleration, velocity, and displacement of the shell.

The solution obtained is compared with values obtained from a series expansion of the equations, which is valid for short times, and with the static solution based on the theory of elasticity which the machine solution should approach asymptotically.

### 1.5 Previous Work

The problem stated above has been the subject of a recent report by Baron (1), whose analysis consists of first solving for the displacements caused at the boundary of an unlined cylindrical cavity subjected to a plane stress wave. This is done through an integral transform approach, the solution of the transformed equations being expressed using Hankel functions. The evaluation of the inverse transform is accomplished only with great computational effort. Values of displacements obtained are then used as influence coefficients in determining the displacements of the shell.

---

\* Numbers in parenthesis refer to the corresponding entry in the Bibliography.

Solutions obtained for two different sets of parameters by Baron are compared in Section 4.6 with results obtained by the method of solution outlined in this report.

The study by Paul (6) consisted of analyzing the effect of a plane stress wave incident on an unlined cylindrical cavity in an elastic medium. The reflected and diffracted waves are described in terms of displacement potentials which represent outgoing shear and dilatational waves. A method was developed for determining values of these potentials, and a similar method is used in this report.

### 1.6 Notation

Notation is defined throughout the text where it first appears; however, the following list summarizes the main uses of certain symbols. In discussions of special topics other meanings may be ascribed to the symbols, at which time they will be redefined.

|                                   |   |  |
|-----------------------------------|---|--|
| $A$                               | = | Area of cross section of the shell, per unit length.                         |
| $A_n, B_n, C_n$                   | = | Coefficients of Fourier series for stresses in the medium.                   |
| $\bar{A}_n, \bar{B}_n, \bar{C}_n$ | = | Coefficients of Fourier series for total stresses in the medium.             |
| $AM_m, EM_m$                      | = | Weighting factors.   |
| $a_n, b_n$                        | = | Generalized coordinates for the displacements of the medium at the boundary. |
| $a_{ns}, b_{ns}$                  | = | Generalized coordinates for displacements of the shell.                      |
| $c_1, c_2$                        | = | Velocities of wave propagation, dilatational and shear, respectively.        |
| $d$                               | = | Distance from neutral axis of shell to its outermost fiber.                  |

|                  |  |
|------------------|--|
| $E, \bar{E}_s$   | = Moduli of elasticity for the medium and shell, respectively. Bar over the symbol refers to the plane strain modulus. |
| $e$              | = Volumetric strain.   |
| $F, G$           | = Generalized coordinates of the displacement potentials.  |
| $I$              | = Moment of inertia of the shell, per unit length.   |
| $k$              | = Parameter which relates to the shape of a time dependent stress wave.  |
| $k_r$            | = $R/r$ , ratio of radii.  |
| $k_c$            | = $c_2/c_1$ , ratio of velocities.   |
| $m$              | = Mass of the shell per unit surface area.   |
| $m'$             | = Additional mass within the shell.  |
| $n$              | = Mode number.   |
| $Q_n, \bar{Q}_n$ | = Generalized forces.  |
| $R$              | = Radius of the shell.   |
| $R_m, Q_m$       | = Multiplying factors.   |
| $r, \theta$      | = Polar coordinates.   |
| $T$              | = Kinetic energy of the shell.   |
| $T'$             | = Kinetic energy of additional mass within the shell.  |
| $t$              | = Thickness of the shell; also, time.  |
| $U$              | = Strain energy of the shell.  |
| $\bar{u}$        | = Displacement vector.   |
| $u, v$           | = Components of the displacement vector in the radial and tangential directions, respectively.                         |
| $u_s, v_s$       | = Radial and tangential displacement components of the shell.  |
| $u_x, u_y$       | = Components of the displacement vector in the x and y directions, respectively.                                       |
| $x, y, z$        | = Rectangular coordinates.   |

|                            |   |   |
|----------------------------|---|---|
| $\alpha_n$                 | $= \frac{a_{sn} \bar{E}_s}{R \sigma_p}$ | , non-dimensionalized radial component of displacement.                   |
| $\beta_n$                  | $= \frac{b_{sn} \bar{E}_s}{R \sigma_p}$ | , non-dimensionalized tangential component of displacement.               |
| $\epsilon_x, \epsilon_y$   |   | = Strains along the x and y axes, respectively.                           |
| $\epsilon_\theta$          |   | = Circumferential strain.   |
| $\zeta$                    |   | = A variable of integration.  |
| $\eta_E$                   | $= \frac{\bar{E}_s}{E}$                 | , a parameter.  |
| $\eta_A$                   | $= \frac{A}{R}$                         | , a parameter.  |
| $\eta_I$                   | $= \frac{I}{R^3}$                       | , a parameter.  |
| $\eta_t$                   | $= \frac{t}{R}$                         | , a parameter.  |
| $\eta_\rho$                | $= \frac{\rho_s}{\rho}$                 | , a parameter.  |
| $\eta_\nu$                 | $= \frac{(1+\nu)(1-2\nu)}{(1-\nu)}$     | , a parameter.  |
| $\theta, r$                |   | = Polar coordinates.  |
| $\theta_1$                 |   | = Position angle of the incident wave.                                    |
| $k$                        |   | = Curvature of the shell.   |
| $\lambda, \mu$             |   | = Lamé constants.   |
| $\nu$                      |   | = Poisson's ratio.  |
| $\bar{\nu}$                | $= \frac{\nu}{1-\nu}$                   |   |
| $\xi_1, \xi_2$             |   | = Arguments of the functions F and G, respectively.                       |
| $\rho$                     |   | = Mass density of the medium.   |
| $\rho_s$                   |   | = Mass density of the shell.  |
| $\sigma_{xx}, \sigma_{yy}$ |   | = Normal components of stress parallel to the x and y axis, respectively. |
| $\sigma_{xy}$              |   | = Shearing stress component.  |

- $\sigma_{rr}, \sigma_{\theta\theta}$  = Radial and tangential normal stresses in polar coordinates. Additional subscripts s and m, when used, refer to the shell and medium.
- $\sigma_{r\theta}$  = Shearing stress in polar coordinates.
- $\sigma_{sb}$  = Bending stress in the shell.
- $\sigma_{smax}$  = Maximum stress in the shell.
- $\sigma_p$  = Amplitude of incident dilatational wave.
- $\sigma_s$  = Amplitude of incident shear wave.
- $\tau$  = Non-dimensionalized time in the case of the incident dilatational wave.
- $\tau_s$  = Non-dimensionalized time in the case of the incident shear wave.
- $\varphi, \psi$  = Displacement potentials, dilatational and shear, respectively.

CHAPTER II  
BASIC EQUATIONS

2.1 Equations for the Medium

The differential equation of motion of a particle in a homogeneous, isotropic, and linearly-elastic medium in terms of its displacement vector  $\bar{u}$  is given by Kolsky (3) in the form

$$(\lambda + 2\mu) \bar{\nabla} \bar{\nabla} \cdot \bar{u} - \mu \bar{\nabla} \times (\bar{\nabla} \times \bar{u}) = \rho \frac{\partial^2 \bar{u}}{\partial t^2} \quad (2-1)$$

where  $\lambda$  and  $\mu$  are the Lamé constants, and  $\rho$  is the density of the medium. The vector  $\bar{u}$  may be expressed as the sum of two displacements, the gradient of a scalar potential and the curl of a vector potential

$$\bar{u} = \bar{\nabla} \phi + \bar{\nabla} \times \bar{\Psi} \quad (2-2)$$

Here  $\phi$  is a potential giving rise to an irrotational displacement and  $\bar{\Psi}$  a potential leading to an equivoluminal displacement.

If the wave equations (2-3) are satisfied and  $\bar{u}$  expressed as in (2-2), the equations of motion (2-1) are automatically satisfied.

$$\nabla^2 \phi = \frac{1}{c_1^2} \frac{\partial^2 \phi}{\partial t^2} \quad (2-3)$$

$$\nabla^2 \bar{\Psi} = \frac{1}{c_2^2} \frac{\partial^2 \bar{\Psi}}{\partial t^2}$$

where the velocities of wave propagation are

$$c_1 = \sqrt{\frac{\lambda + 2\mu}{\rho}} \quad (2-4)$$

$$c_2 = \sqrt{\frac{\mu}{\rho}}$$

for the dilatational and shear waves, respectively.

Since the problem is essentially a two-dimensional one wherein only the rotation about the cylinder axis is considered, the expression for the propagation of shear waves can be written in terms of a scalar potential function

$$\nabla^2 \psi = \frac{1}{c_2^2} \frac{\partial^2 \psi}{\partial t^2} \quad ; \quad \text{with } \psi = \bar{\Psi}_z \quad (2-3a)$$

$\phi$  and  $\psi$  are functions of  $x$ ,  $y$ , and  $t$ . The components of the displacement vector  $\bar{u}$  can be expressed as

$$u_x = \frac{\partial \phi}{\partial x} + \frac{\partial \psi}{\partial y} \quad (2-5)$$

$$u_y = \frac{\partial \phi}{\partial y} - \frac{\partial \psi}{\partial x}$$

Stress components are

$$\sigma_{xx} = \lambda e + 2\mu \epsilon_x$$

$$\sigma_{xy} = \mu \gamma_{xy} \quad (2-6)$$

$$\sigma_{yy} = \lambda e + 2\mu \epsilon_y$$

where  $e$  represents volumetric strain,  $\epsilon_x$  and  $\epsilon_y$  strain along the  $x$  and  $y$  axis respectively, and  $\gamma_{xy}$  the shearing strain. The strain components for small displacement are

$$\epsilon_x = \frac{\partial u_x}{\partial x}$$

$$\epsilon_y = \frac{\partial u_y}{\partial y} \quad (2-6a)$$

$$\gamma_{xy} = \frac{\partial u_x}{\partial y} + \frac{\partial u_y}{\partial x}$$

In terms of the potential functions, the equations for the stress components become

$$\begin{aligned}\sigma_{xx} &= \lambda \left( \frac{\partial^2 \phi}{\partial x^2} + \frac{\partial^2 \phi}{\partial y^2} \right) + 2\mu \left( \frac{\partial^2 \phi}{\partial x^2} + \frac{\partial^2 \psi}{\partial x \partial y} \right) \\ \sigma_{xy} &= \mu \left( 2 \frac{\partial^2 \phi}{\partial x \partial y} - \frac{\partial^2 \psi}{\partial x^2} + \frac{\partial^2 \psi}{\partial y^2} \right) \\ \sigma_{yy} &= \lambda \left( \frac{\partial^2 \phi}{\partial x^2} + \frac{\partial^2 \phi}{\partial y^2} \right) + 2\mu \left( \frac{\partial^2 \phi}{\partial y^2} - \frac{\partial^2 \psi}{\partial x \partial y} \right)\end{aligned}\tag{2-7}$$

In polar coordinates

$$\nabla^2 = \frac{\partial^2}{\partial r^2} + \frac{1}{r} \frac{\partial}{\partial r} + \frac{1}{r^2} \frac{\partial^2}{\partial \theta^2}$$

and the wave equations expressed in polar coordinates are

$$\begin{aligned}\frac{\partial^2 \phi}{\partial r^2} + \frac{1}{r} \frac{\partial \phi}{\partial r} + \frac{1}{r^2} \frac{\partial^2 \phi}{\partial \theta^2} &= \frac{1}{c_1^2} \frac{\partial^2 \phi}{\partial t^2} \\ \frac{\partial^2 \psi}{\partial r^2} + \frac{1}{r} \frac{\partial \psi}{\partial r} + \frac{1}{r^2} \frac{\partial^2 \psi}{\partial \theta^2} &= \frac{1}{c_2^2} \frac{\partial^2 \psi}{\partial t^2}\end{aligned}\tag{2-8}$$

Displacements in polar coordinates become

$$\begin{aligned}u &= \frac{\partial \phi}{\partial r} + \frac{1}{r} \frac{\partial \psi}{\partial \theta} \\ v &= \frac{1}{r} \frac{\partial \phi}{\partial \theta} - \frac{\partial \psi}{\partial r}\end{aligned}\tag{2-9}$$

where  $u$  and  $v$  represent radial and tangential components of displacement, respectively.

Stress components may be written as

$$\begin{aligned}\sigma_{rr} &= (\lambda + 2\mu) \left[ \frac{\partial^2 \phi}{\partial r^2} + \frac{1}{r} \frac{\partial^2 \psi}{\partial r \partial \theta} - \frac{1}{r^2} \frac{\partial \psi}{\partial \theta} \right] + \frac{\lambda}{r} \left[ \frac{\partial \phi}{\partial r} + \frac{1}{r} \frac{\partial^2 \phi}{\partial \theta^2} + \frac{1}{r} \frac{\partial \psi}{\partial \theta} - \frac{\partial^2 \psi}{\partial r \partial \theta} \right] \\ \sigma_{r\theta} &= \mu \left[ \frac{2}{r} \frac{\partial^2 \phi}{\partial r \partial \theta} - \frac{2}{r^2} \frac{\partial \phi}{\partial \theta} - \frac{\partial^2 \psi}{\partial r^2} + \frac{1}{r^2} \frac{\partial^2 \psi}{\partial \theta^2} + \frac{1}{r} \frac{\partial \psi}{\partial r} \right] \\ \sigma_{\theta\theta} &= \left( \frac{\lambda + 2\mu}{r} \right) \left[ \frac{\partial \phi}{\partial r} + \frac{1}{r} \frac{\partial^2 \phi}{\partial \theta^2} + \frac{1}{r} \frac{\partial \psi}{\partial \theta} - \frac{\partial^2 \psi}{\partial r \partial \theta} \right] + \lambda \left[ \frac{\partial^2 \phi}{\partial r^2} + \frac{1}{r} \frac{\partial^2 \psi}{\partial r \partial \theta} - \frac{1}{r^2} \frac{\partial \psi}{\partial \theta} \right]\end{aligned}\tag{2-10}$$

where  $\sigma_{rr}$ ,  $\sigma_{r\theta}$ ,  $\sigma_{\theta\theta}$ , represent respectively the radial, shear and circumferential (hoop) stresses in the medium.

In the following development of the equations, the incoming wave, considered a step function of time, is either a dilatational or shear wave. The step wave was chosen as a convenient form from which, through the principle of superposition using Duhamel's integral, the effects of any time dependent wave may be approximated. It is shown by Kolsky (3) that for either the incoming dilatational or shear wave, the reflected wave from a plane body must have both dilatational and shear components in order to satisfy boundary conditions. The same holds in the present case.

### 2.11 Dilatational Wave

The orientation of the incoming dilatational (compressional) wave with respect to the spatial coordinates and time are shown in Fig. 1. Owing to symmetry about the x axis, the radial stress, hoop stress, and the radial component of displacement are even functions of  $\theta$ , while the shear stress and tangential component of displacement are odd functions of  $\theta$ .

In the expressions previously given, the dilatational potential may now be separated into two parts

$$\Phi = \Phi_{in} + \Phi_{out}$$

where

$$\Phi_{in} = -\sigma_p \chi(x+c_1 t)$$

represents the potential of the incoming step wave, and  $\Phi_{out}$  represents the potential of the outgoing dilatational wave.

The displacement and velocity of a particle behind the plane wave front can be derived from the potential of the incoming wave, with notation defined in Fig. 1

$$\begin{aligned}
 u_x &= -\sigma_p \chi'(x+c_1 t) \\
 \dot{u}_x &= -\frac{\sigma_p}{\rho c_1}
 \end{aligned}
 \tag{2-11}$$

The velocities in polar coordinates become

$$\begin{aligned}
 \dot{u} &= -\frac{\sigma_p}{\rho c_1} \cos \theta \\
 \dot{v} &= \frac{\sigma_p}{\rho c_1} \sin \theta
 \end{aligned}
 \tag{2-12}$$

The radial and tangential displacements at the boundary  $r = R$  due to the incoming plane stress wave are expanded in Fourier series as a function of time as

$$\begin{aligned}
 u(R, t, \theta) &= \sum_{n=0}^{\infty} a_n(R, t) \cos n\theta \\
 v(R, t, \theta) &= \sum_{n=1}^{\infty} b_n(R, t) \sin n\theta
 \end{aligned}
 \tag{2-13}$$

and the velocities as

$$\begin{aligned}
 \dot{u}(R, t, \theta) &= \sum_{n=0}^{\infty} \dot{a}_n(R, t) \cos n\theta \\
 \dot{v}(R, t, \theta) &= \sum_{n=1}^{\infty} \dot{b}_n(R, t) \sin n\theta
 \end{aligned}
 \tag{2-14}$$

The Fourier coefficients are determined as a function of  $\theta_1$ , a measure of the degree of envelopment of the shell by the incoming stress wave (Fig. 1), by evaluation of the integrals

$$\dot{a}_n = -\frac{2\sigma_p}{\pi\rho c_1} \int_0^{\theta_1} \cos \theta \cos n\theta \, d\theta$$

$$\dot{b}_n = \frac{2\sigma_p}{\pi\rho c_1} \int_0^{\theta_1} \sin \theta \sin n\theta \, d\theta$$

The indicated integrations are performed using the orthogonality properties of the sine and cosine functions to get the following result

$$\dot{a}_{n(\text{in})} = -\frac{\sigma_p}{\pi\rho c_1} \cdot \begin{cases} \sin \theta_1 & n = 0 \\ \theta_1 + \frac{\sin 2\theta_1}{2} & n = 1 \\ \frac{\sin(n-1)\theta_1}{n-1} + \frac{\sin(n+1)\theta_1}{n+1} & n = 2, 3, \dots \end{cases} \quad (2-15)$$

$$\dot{b}_{n(\text{in})} = \frac{\sigma_p}{\pi\rho c_1} \cdot \begin{cases} \theta_1 - \frac{\sin 2\theta_1}{2} & n = 1 \\ \frac{\sin(n-1)\theta_1}{n-1} - \frac{\sin(n+1)\theta_1}{n+1} & n = 2, 3, \dots \end{cases}$$

The subscript (in) has been added to designate the coefficients due to the incident wave.  $\theta_1$  is a time dependent variable which varies from 0 to  $\pi$  during the transit of the incoming wave across the cavity, after which it becomes a constant equal to  $\pi$ .

The stresses in the medium behind the wave front are as shown in Fig. 1, where  $\bar{\nu}$ ,\* a ratio relating the stress in a direction perpendicular to the direction of wave propagation, is derived from the assumption that there is no strain behind the wave front in the direction parallel to the wave front. It is related to Poisson's ratio,  $\nu$ , of the medium in the following way

---

\* The bar over the symbol does not indicate a vector quantity.

$$\bar{v} = \frac{v}{1-v} \quad (2-16)$$

The stresses behind the wave front are in polar coordinates

$$\begin{aligned} \sigma_{rr} &= -\sigma_p (\cos^2 \theta + \bar{v} \sin^2 \theta) \\ \sigma_{r\theta} &= \sigma_p \left( \frac{1-\bar{v}}{2} \right) \sin 2\theta \\ \sigma_{\theta\theta} &= -\sigma_p (\sin^2 \theta + \bar{v} \cos^2 \theta) \end{aligned} \quad (2-17)$$

Stresses in the medium as a function of radius and time are now expressed in terms of Fourier series

$$\begin{aligned} \sigma_{rr}(r,t,\theta) &= \sum_{n=0}^{\infty} A_n(r,t) \cos n\theta \\ \sigma_{r\theta}(r,t,\theta) &= \sum_{n=1}^{\infty} B_n(r,t) \sin n\theta \\ \sigma_{\theta\theta}(r,t,\theta) &= \sum_{n=0}^{\infty} C_n(r,t) \cos n\theta \end{aligned} \quad (2-18)$$

and the coefficients determined in the same manner as used previously for velocities are

$$\begin{aligned} A_n(\text{in}) &= -\frac{\sigma_p}{2\pi} \cdot \begin{cases} (1+\bar{v})\theta_1 + \left(\frac{1-\bar{v}}{2}\right) \sin 2\theta_1 & n = 0 \\ (1-\bar{v})\theta_1 + (1+\bar{v}) \sin 2\theta_1 + \left(\frac{1-\bar{v}}{4}\right) \sin 4\theta_1 & n = 2 \\ \frac{(1-\bar{v})\sin(n-2)\theta_1}{n-2} + \frac{(1-\bar{v})\sin(n+2)\theta_1}{n+2} + \frac{2(1+\bar{v}) \sin n\theta_1}{n} & n = 1,3,4,5,\dots \end{cases} \\ & \quad (2-19) \\ B_n(\text{in}) &= \frac{\sigma_p(1-\bar{v})}{2\pi} \cdot \begin{cases} \theta_1 - \frac{\sin 4\theta_1}{4} & n = 2 \\ \frac{\sin(n-2)\theta_1}{n-2} - \frac{\sin(n+2)\theta_1}{n+2} & n = 1,3,4,5,\dots \end{cases} \end{aligned}$$

$$C_{n(\text{in})} = -\frac{\sigma_p}{2\pi} \cdot \begin{cases} (1+\bar{\nu})\theta_1 - \left(\frac{1-\bar{\nu}}{2}\right) \sin 2\theta_1 & n = 0 \\ (\bar{\nu}-1)\theta_1 + (1+\bar{\nu}) \sin 2\theta_1 + \left(\frac{\bar{\nu}-1}{4}\right) \sin 4\theta_1 & n = 2 \\ \frac{(\bar{\nu}-1)\sin(n-2)\theta_1}{n-2} + \frac{(\bar{\nu}-1)\sin(n+2)\theta_1}{n+2} + \frac{2(1+\bar{\nu})\sin n\theta_1}{n} & n = 1, 3, 4, 5, \dots \end{cases}$$

where the subscript (in) again refers to the incident stress wave.

As noted earlier, the reflected and diffracted wave is represented as a diverging or outgoing cylindrical wave from a line source whose origin is the axis of the cylinder, and includes both dilatational and shear components. The outgoing potential functions are expressed as infinite series, each term of which will henceforth be called a mode

$$\begin{aligned} \varphi_{\text{out}} &= \sum_{n=0}^{\infty} f_n(r, t) \cos n\theta \\ \psi_{\text{out}} &= \sum_{n=1}^{\infty} g_n(r, t) \sin n\theta \end{aligned} \quad (2-20)$$

It is shown in the appendix that the coefficients are of the form

$$\begin{aligned} f_n &= \frac{(-1)^n}{c_1^n} \int_0^{\infty} F^n\left(t - \frac{r}{c_1} \cosh u_1\right) \cosh nu_1 \, du_1 \\ g_n &= \frac{(-1)^n}{c_2^n} \int_0^{\infty} G^n\left(t - \frac{r}{c_2} \cosh u_2\right) \cosh nu_2 \, du_2 \end{aligned} \quad (2-21)$$

where  $F^n\left(t - \frac{r}{c_1} \cosh u_1\right)$  and  $G^n\left(t - \frac{r}{c_2} \cosh u_2\right)$  represent the nth order derivative of the respective functions, n being equal to the mode number considered.

To express the velocity components of the medium at the boundary due to the outgoing waves as in equations (2-14), one differentiates equations (2-9) with respect to time and substitutes the expressions given above for the potential functions. This results in the following for the velocity coefficients

$$\begin{aligned}
 \dot{a}_{n(\text{out})} &= -\frac{(-1)^n}{c_1^{n+1}} \int_0^\infty F^{n+2}(\xi_1) \cosh u_1 \cosh nu_1 du_1 \\
 &\quad + \frac{(-1)^n}{c_2^{n+1}} \int_0^\infty G^{n+2}(\xi_2) \sinh u_2 \sinh nu_2 du_2 \\
 \dot{b}_{n(\text{out})} &= -\frac{(-1)^n}{c_1^{n+1}} \int_0^\infty F^{n+2}(\xi_1) \sinh u_1 \sinh nu_1 du_1 \\
 &\quad + \frac{(-1)^n}{c_2^{n+1}} \int_0^\infty G^{n+2}(\xi_2) \cosh u_2 \cosh nu_2 du_2
 \end{aligned} \tag{2-22}$$

where  $(\xi_1)$  and  $(\xi_2)$  represent the arguments of the respective functions. The subscript (out) refers to the outgoing wave.

The stresses in the medium due to the outgoing waves are also expressed in series form as in equations (2-18), the coefficients being found by substitution into equations (2-10)

$$\begin{aligned}
 A_{n(\text{out})} &= \frac{(-1)^n \mu}{c_1^{n+2}} \int_0^\infty F^{n+2}(\xi_1) \cosh nu_1 \left[ \frac{\lambda}{\mu} + 2 \cosh^2 u_1 \right] du_1 \\
 &\quad - \frac{(-1)^n \mu}{c_2^{n+2}} \int_0^\infty G^{n+2}(\xi_2) \sinh 2u_2 \sinh nu_2 du_2
 \end{aligned} \tag{2-23}$$

$$\begin{aligned}
B_{n(\text{out})} &= \frac{(-1)^n \mu}{c_1^{n+2}} \int_0^\infty F^{n+2}(\xi_1) \sinh 2u_1 \sinh nu_1 du_1 \\
&\quad - \frac{(-1)^n \mu}{c_2^{n+2}} \int_0^\infty G^{n+2}(\xi_2) \cosh 2u_2 \cosh nu_2 du_2 \\
C_{n(\text{out})} &= \frac{(-1)^n \mu}{c_1^{n+2}} \int_0^\infty F^{n+2}(\xi_1) \cosh nu_1 \left[ \frac{\lambda}{\mu} - 2 \sinh^2 u_1 \right] du_1 \\
&\quad + \frac{(-1)^n \mu}{c_2^{n+2}} \int_0^\infty G^{n+2}(\xi_2) \sinh 2u_2 \sinh nu_2 du_2
\end{aligned}$$

### 2.12 Shear Wave

The orientation of the incoming plane shear wave with respect to the spatial coordinates and time are shown in Fig. 2. In this case the shear stress and tangential component of displacement must be even functions of  $\theta$  while the radial stress, hoop stress, and radial component of displacement are odd functions of  $\theta$ .

The incoming wave expressed in terms of a shear potential function is

$$\psi_{\text{in}} = \sigma_s \chi_s(x + c_2 t) \quad (2-24)$$

from which the velocity of a particle behind the wave front in polar coordinates may be derived as

$$\begin{aligned}
\dot{u} &= \frac{\sigma_s}{\rho c_2} \sin \theta \\
\dot{v} &= \frac{\sigma_s}{\rho c_2} \cos \theta
\end{aligned} \quad (2-25)$$

The stresses in the medium behind the wave front are as shown in Fig. 2. In terms of polar coordinates they are

$$\begin{aligned}
 \sigma_{rr} &= \sigma_s \sin 2\theta \\
 \sigma_{r\theta} &= \sigma_s \cos 2\theta \\
 \sigma_{\theta\theta} &= -\sigma_s \sin 2\theta
 \end{aligned}
 \tag{2-26}$$

Velocities and stresses due to the incoming plane stress wave as functions of radial distance and time are expanded in terms of Fourier series in a manner similar to that of the dilatational wave, except that because of the difference in symmetry, the sine and cosine terms are interchanged. The coefficients are also found in a similar manner and are given here. The coefficients for the velocity series are

$$\dot{a}_{n(in)} = \frac{\sigma_s}{\pi \rho c_2} \times \begin{cases} \theta_1 - \frac{\sin 2\theta_1}{2} & n = 1 \\ \frac{\sin(n-1)\theta_1}{n-1} - \frac{\sin(n+1)\theta_1}{n+1} & n = 2, 3, \dots \end{cases}
 \tag{2-27}$$

$$\dot{b}_{n(in)} = \frac{\sigma_s}{\pi \rho c_2} \times \begin{cases} \sin \theta_1 & n = 0 \\ \theta_1 + \frac{\sin 2\theta_1}{2} & n = 1 \\ \frac{\sin(n-1)\theta_1}{n-1} + \frac{\sin(n+1)\theta_1}{n+1} & n = 2, 3, \dots \end{cases}$$

and the coefficients for the stress series are

$$\begin{aligned}
 A_{n(in)} &= \frac{\sigma_s}{\pi} \times \begin{cases} \theta_1 - \frac{\sin 4\theta_1}{4} & n = 2 \\ \frac{\sin(n-2)\theta_1}{n-2} - \frac{\sin(n+2)\theta_1}{n+2} & n = 1, 3, 4, 5, \dots \end{cases} \\
 B_{n(in)} &= \frac{\sigma_s}{\pi} \times \begin{cases} \frac{\sin 2\theta_1}{2} & n = 0 \\ \theta_1 + \frac{\sin 4\theta_1}{4} & n = 2 \\ \frac{\sin(n-2)\theta_1}{n-2} + \frac{\sin(n+2)\theta_1}{n+2} & n = 1, 3, 4, 5, \dots \end{cases}
 \end{aligned}
 \tag{2-28}$$

$$C_{n(in)} = -A_{n(in)}$$

$\theta_1$  is a time dependent variable similar to that for the dilatational wave except that now it is a function of the position of the incoming shear wave, which travels with velocity  $c_2$ .

The outgoing potential functions are expressed modewise as

$$\begin{aligned} \varphi_{out} &= \sum_{n=1}^{\infty} f_n(r,t) \sin n\theta \\ \psi_{out} &= \sum_{n=0}^{\infty} g_n(r,t) \cos n\theta \end{aligned} \quad (2-29)$$

where the coefficients are of the form

$$\begin{aligned} f_n &= \frac{(-1)^n}{c_1^n} \int_0^{\infty} F^n\left(t - \frac{r}{c_1} \cosh u_1\right) \cosh nu_1 du_1 \\ g_n &= \frac{(-1)^n}{c_2^n} \int_0^{\infty} G^n\left(t - \frac{r}{c_2} \cosh u_2\right) \cosh nu_2 du_2 \end{aligned} \quad (2-30)$$

The terms have the same significance as in the case of the dilatational wave. Modal coefficients are derived as before. The coefficients for the velocity terms are

$$\begin{aligned} \dot{a}_{n(out)} &= -\frac{(-1)^n}{c_1^{n+1}} \int_0^{\infty} F^{n+2}(\xi_1) \cosh u_1 \cosh nu_1 du_1 \\ &\quad - \frac{(-1)^n}{c_2^{n+1}} \int_0^{\infty} G^{n+2}(\xi_2) \sinh u_2 \sinh nu_2 du_2 \end{aligned}$$

(2-31)

$$\begin{aligned} \dot{b}_n(\text{out}) &= \frac{(-1)^n}{c_1^{n+1}} \int_0^\infty F^{n+2}(\xi_1) \sinh u_1 \sinh nu_1 du_1 \\ &\quad + \frac{(-1)^n}{c_2^{n+1}} \int_0^\infty G^{n+2}(\xi_2) \cosh u_2 \cosh nu_2 du_2 \end{aligned}$$

and the coefficients for the stress terms are

$$\begin{aligned} A_n(\text{out}) &= \frac{(-1)^n \mu}{c_1^{n+2}} \int_0^\infty F^{n+2}(\xi_1) \cosh nu_1 \left[ \frac{\lambda}{\mu} + 2 \cosh^2 u_1 \right] du_1 \\ &\quad + \frac{(-1)^n \mu}{c_2^{n+2}} \int_0^\infty G^{n+2}(\xi_2) \sinh 2u_2 \sinh nu_2 du_2 \\ B_n(\text{out}) &= - \frac{(-1)^n \mu}{c_1^{n+2}} \int_0^\infty F^{n+2}(\xi_1) \sinh 2u_1 \sinh nu_1 du_1 \\ &\quad - \frac{(-1)^n \mu}{c_2^{n+2}} \int_0^\infty G^{n+2}(\xi_2) \cosh 2u_2 \cosh nu_2 du_2 \quad (2-32) \\ C_n(\text{out}) &= \frac{(-1)^n \mu}{c_1^{n+2}} \int_0^\infty F^{n+2}(\xi_1) \cosh nu_1 \left[ \frac{\lambda}{\mu} - 2 \sinh^2 u_1 \right] du_1 \\ &\quad - \frac{(-1)^n \mu}{c_2^{n+2}} \int_0^\infty G^{n+2}(\xi_2) \sinh 2u_2 \sinh nu_2 du_2 \end{aligned}$$

## 2.2 Equations for the Shell

In the following derivations of the equations of motion for the shell, it is assumed that the thickness of the shell is small in relation to its radius. This assumption permits description of the behavior of the shell in terms of its middle surface, and effectively concentrates all of the mass in a line thickness. This should be kept in mind when interpreting the results.

The effects of shear and rotatory inertia are not considered, since they affect only the very high modes, which are not considered in this study.

The deformation of any point ( $\theta$ ) on the shell can then be described by specifying the components of displacement (Fig. 3):

$u_s$  = radial displacement, positive outwards

$v_s$  = tangential displacement, positive in the direction of increasing  $\theta$ .

The strain energy of the shell per unit length can be expressed as

$$U = \frac{\bar{E}_s I}{2} \int_0^{2\pi} (k)^2 R d\theta + \frac{\bar{E}_s A}{2} \int_0^{2\pi} (\epsilon_\theta)^2 R d\theta \quad (2-33)$$

where  $\bar{E}_s$  = "plane strain" modulus of elasticity of the shell

$I$  = moment of inertia per unit length of shell

$A$  = area of the cross section per unit length of shell

$k$  = change in curvature of the cross section

$\epsilon_\theta$  = extensional strain in the  $\theta$  direction

$R$  = radius of the cylinder

Flügge (2) gives the expressions for the curvature and extensional strain terms as

$$k = \frac{1}{R^2} \left( \frac{\partial^2 u_s}{\partial \theta^2} + u_s \right)$$

and

$$\epsilon_\theta = \frac{1}{R} \left( \frac{\partial v_s}{\partial \theta} + u_s \right)$$

correct to first order terms. The strain energy equation in terms of the components of displacement then becomes

$$U = \frac{\bar{E}_s I}{2R^3} \int_0^{2\pi} \left( \frac{\partial^2 u_s}{\partial \theta^2} + u_s \right)^2 + \frac{\bar{E}_s A}{2R} \int_0^{2\pi} \left( \frac{\partial v_s}{\partial \theta} + u_s \right)^2 d\theta \quad (2-34)$$

The kinetic energy of the shell can be expressed as

$$T = \frac{m}{2} \int_0^{2\pi} (\dot{u}_s^2 + \dot{v}_s^2) R d\theta \quad (2-35)$$

where

$m$  = mass of shell per unit surface area

### 2.21 Dilatational Wave

In view of the symmetries of the problem, the displacement components of the shell can be expanded in terms of the following Fourier series

$$u_s(\theta, t) = \sum_{n=0}^{\infty} a_{sn}(t) \cos n\theta$$

$$v_s(\theta, t) = \sum_{n=1}^{\infty} b_{sn}(t) \sin n\theta \quad (2-36)$$

Equations for the strain and kinetic energies of the shell are then expressed as the following quadratic forms in the generalized displacements and velocities

$$U = \left( \frac{\bar{E}_s I \pi}{R^3} + \frac{\bar{E}_s A \pi}{R} \right) a_{s0}^2 + \frac{\bar{E}_s I \pi}{2R^3} \sum_{n=1}^{\infty} a_{sn}^2 (1-n^2)^2 + \frac{\bar{E}_s A \pi}{2R} \sum_{n=1}^{\infty} (n b_{sn} + a_{sn})^2 \quad (2-37)$$

$$T = m \pi R a_{s0}^2 + \frac{m \pi R}{2} \sum_{n=1}^{\infty} (\dot{a}_{sn}^2 + \dot{b}_{sn}^2)$$

The Lagrangian equations of motion in terms of the generalized displacement coefficients  $a_{sn}$  and  $b_{sn}$  are

$$\frac{d}{dt} \left( \frac{\partial T}{\partial \dot{a}_{sn}} \right) + \frac{\partial U}{\partial a_{sn}} = Q_n$$

$$\frac{d}{dt} \left( \frac{\partial T}{\partial \dot{b}_{sn}} \right) + \frac{\partial U}{\partial b_{sn}} = \bar{Q}_n \quad (2-38)$$

where  $Q_n$  and  $\bar{Q}_n$  are generalized forces corresponding to the displacement terms  $a_{sn}$  and  $b_{sn}$ , respectively. The following equations of motion result

$$\begin{aligned} \ddot{a}_{s0} + \left( \frac{\bar{E}_s I}{mR^4} + \frac{\bar{E}_s A}{mR^2} \right) a_{s0} &= \frac{Q_0}{2\pi mR} & n = 0 \\ \ddot{a}_{sn} + \frac{\bar{E}_s I}{mR^4} (1-n^2)^2 a_{sn} + \frac{\bar{E}_s A}{mR^2} (a_{sn} + nb_{sn}) &= \frac{Q_n}{\pi R} & n = 1, 2, \dots \\ \dot{b}_{sn} + \frac{n\bar{E}_s A}{mR^2} (a_{sn} + nb_{sn}) &= \frac{\bar{Q}_n}{\pi R} & n = 1, 2, \dots \end{aligned} \quad (2-39)$$

Now to determine the generalized forces  $Q_n$  and  $\bar{Q}_n$ , the principle of virtual work is applied. Consider a virtual displacement corresponding to an increment  $\delta a_{sn}$  of coordinate  $a_{sn}$ .

$$\text{Virtual work, by definition} = Q_n \cdot \delta a_{sn}$$

The external forces acting on the shell are

$$\begin{aligned} \sigma_{rr} &= \sum_{n=0}^{\infty} \bar{A}_n \cos n\theta \\ \sigma_{r\theta} &= \sum_{n=1}^{\infty} \bar{B}_n \sin n\theta \end{aligned}$$

where  $\bar{A}_n$  and  $\bar{B}_n$  represent the sum of the forces on the shell due to the incoming and outgoing stress waves

$$\begin{aligned} \bar{A}_n &= A_n(\text{in}) + A_n(\text{out}) \\ \bar{B}_n &= B_n(\text{in}) + B_n(\text{out}) \end{aligned}$$

The coefficients  $A_n$  and  $B_n$  have been discussed previously. The work due to a virtual change of the generalized coordinate  $a_{sn}$  is

$$\text{Virtual Work} = \int_0^{2\pi} \bar{A}_n \cos^2 n\theta \cdot \delta a_{sn} \cdot R d\theta$$

The generalized force term is determined by equating the two expressions of work, from which we get

$$\begin{aligned} Q_0 &= 2\pi R \bar{A}_0 & n &= 0 \\ Q_n &= \pi R \bar{A}_n & n &= 1, 2, \dots \end{aligned}$$

and by a similar computation

$$\bar{Q}_n = \pi R \bar{B}_n$$

The equations of motion now become

$$\begin{aligned} \ddot{a}_{sn} + \frac{\bar{E}_s I}{mR^4} (1-n^2)^2 a_{sn} + \frac{\bar{E}_s A}{mR^2} (a_{sn} + nb_{sn}) &= \frac{\bar{A}_n}{m} \\ \ddot{b}_{sn} + \frac{n\bar{E}_s A}{mR^2} (a_{sn} + nb_{sn}) &= \frac{\bar{B}_n}{m} \end{aligned} \quad (2-40)$$

## 2.22 Shear Wave

Because of the difference in symmetry associated with the shear wave as compared to the dilatational wave, displacement components in the case of the incoming shear wave are written as

$$\begin{aligned} u_s(\theta, t) &= \sum_{n=1}^{\infty} a_{sn}(t) \sin n\theta \\ v_s(\theta, t) &= \sum_{n=0}^{\infty} b_{sn}(t) \cos n\theta \end{aligned} \quad (2-41)$$

Expressions for the strain and kinetic energies in terms of the generalized coordinates  $a_{sn}$  and  $b_{sn}$  now become

$$U = \frac{\bar{E}_s I \pi}{2R^3} \sum_{n=1}^{\infty} a_{sn}^2 (1-n^2)^2 + \frac{\bar{E}_s A \pi}{2R} \sum_{n=1}^{\infty} (-nb_{sn} + a_{sn})^2 \quad (2-42)$$

$$T = m\pi R b_{s0}^2 + \frac{m\pi R}{2} \sum_{n=1}^{\infty} (\dot{a}_{sn}^2 + \dot{b}_{sn}^2)$$

The equations of motion determined in a manner similar to that of the dilatational wave are then

$$\begin{aligned} \ddot{a}_{sn} + \frac{\bar{E}_s I}{mR^4} (1-n^2)^2 a_{sn} + \frac{\bar{E}_s A}{mR^2} (a_{sn} - nb_{sn}) &= \frac{\bar{A}_n}{m} \\ \ddot{b}_{sn} - \frac{n\bar{E}_s A}{mR^2} (a_{sn} - nb_{sn}) &= \frac{\bar{B}_n}{m} \end{aligned} \quad (2-43)$$

### 2.23 Effect of Additional Mass

The equations of motion derived thus far assumed no mass within the shell. The simplest way to consider the effect of additional mass is to assume that it is distributed within the shell symmetrically about the axis. The total quantity can be assumed equal to  $2\pi Rm'$ , with  $m'$  the magnitude of the added mass measured in terms of the surface area of the shell. If it is assumed to move with the same velocity as the mass center of the shell, its kinetic energy can be expressed as

$$T' = \frac{2\pi Rm'}{2} \frac{1}{4\pi^2} \left[ \int_0^{2\pi} (-\dot{u}_s^2 \cos^2 \theta + \dot{v}_s^2 \sin^2 \theta) d\theta \right]^2 \quad (2-44)$$

for the case of the incoming dilatational wave. If  $u_s$  and  $v_s$  are replaced by their Fourier expansions, and if the indicated integration is carried out, the kinetic energy  $T'$  due to the additional mass may be represented as

$$T' = \frac{m'\pi R}{4} (\dot{a}_{s1}^2 - 2\dot{a}_{s1}\dot{b}_{s1} + \dot{b}_{s1}^2)$$

This kinetic energy must be added to the kinetic energy of the shell which was derived earlier. Since the above expression affects only the  $n = 1$  mode,

the other modes need not be considered. With this additional kinetic energy, the equations of motion for the  $n = 1$  mode become

$$\begin{aligned}\ddot{a}_{s1} + \frac{m'}{2m} (\ddot{a}_{s1} - \ddot{b}_{s1}) + \frac{\bar{E}_s A}{mR^2} (a_{s1} + b_{s1}) &= \frac{\bar{A}_1}{m} \\ \ddot{b}_{s1} - \frac{m'}{2m} (\ddot{a}_{s1} - \ddot{b}_{s1}) + \frac{\bar{E}_s A}{mR^2} (a_{s1} + b_{s1}) &= \frac{\bar{B}_1}{m}\end{aligned}\quad (2-45)$$

If now we add the above equations, we get

$$\ddot{a}_{s1} + \ddot{b}_{s1} + \frac{2\bar{E}_s A}{mR^2} (a_{s1} + b_{s1}) = \frac{\bar{A}_1}{m} + \frac{\bar{B}_1}{m}$$

or

$$\ddot{a}_{s1} = -\ddot{b}_{s1} - \frac{2\bar{E}_s A}{mR^2} (a_{s1} + b_{s1}) + \frac{\bar{A}_1}{m} + \frac{\bar{B}_1}{m}$$

and

$$\ddot{b}_{s1} = -\ddot{a}_{s1} - \frac{2\bar{E}_s A}{mR^2} (a_{s1} + b_{s1}) + \frac{\bar{A}_1}{m} + \frac{\bar{B}_1}{m}$$

By making the appropriate substitutions for  $a_{s1}$  and  $b_{s1}$ , the equations of motion can be written as

$$\begin{aligned}\ddot{a}_{s1} + \frac{\bar{E}_s A}{mR^2} (a_{s1} + b_{s1}) &= \frac{\bar{A}_1}{m} \cdot \frac{2m+m'}{2(m+m')} + \frac{\bar{B}_1}{m} \cdot \frac{m'}{2(m+m')} \\ \ddot{b}_{s1} + \frac{\bar{E}_s A}{mR^2} (a_{s1} + b_{s1}) &= \frac{\bar{A}_1}{m} \cdot \frac{m'}{2(m+m')} + \frac{\bar{B}_1}{m} \cdot \frac{2m+m'}{2(m+m')}\end{aligned}\quad (2-46)$$

Note that these equations are similar in form to the equations derived earlier without the additional mass; the effect of the additional mass merely alters the right-hand side.

In the case of the incoming shear wave, the kinetic energy of the additional mass is

$$T' = \frac{2\pi R m'}{2} \frac{1}{4\pi^2} \left[ \int_0^{2\pi} (\dot{u}_s \sin \theta + \dot{v}_s \cos \theta) d\theta \right]^2 \quad (2-47)$$

and by a similar method, the equations of motion for the  $n = 1$  mode are written

$$\begin{aligned} \ddot{a}_{s1} + \frac{\bar{E}_s A}{mR^2} (a_{s1} - b_{s1}) &= \frac{\bar{A}_1}{m} \cdot \frac{2m+m'}{2(m+m')} - \frac{\bar{B}_1}{m} \cdot \frac{m'}{2(m+m')} \\ \ddot{b}_{s1} - \frac{\bar{E}_s A}{mR^2} (a_{s1} - b_{s1}) &= -\frac{\bar{A}_1}{m} \cdot \frac{m'}{2(m+m')} + \frac{\bar{B}_1}{m} \cdot \frac{2m+m'}{2(m+m')} \end{aligned} \quad (2-48)$$

The significance of the additional mass on the numerical results is discussed in a later chapter. Inclusion of a flexible support for the additional mass is also possible by changing the above equations; however, this problem is not treated here.

### 2.3 Boundary Conditions

It is assumed that the shell is attached to the medium permitting no differential displacements at the boundary between the two. Thus, continuity of stresses and displacements are maintained at the boundary. A convenient way of satisfying the boundary condition of equal displacements of the shell and medium is to equate the corresponding velocity components of the shell and medium. This is done modewise for both the dilatational and shear incoming waves by merely equating the coefficients of the velocity terms as follows

$$\begin{aligned} \dot{a}_{sn} &= \dot{a}_n(\text{in}) + \dot{a}_n(\text{out}) \\ \dot{b}_{sn} &= \dot{b}_n(\text{in}) + \dot{b}_n(\text{out}) \end{aligned} \quad (2-49)$$

#### 2.4 Summary of Equations in Non-Dimensionalized Form

It is convenient to express the equations derived earlier in non-dimensionalized form by introducing certain dimensionless variables and parameters. Let

$$\alpha_n = \frac{a_{sn}}{R} \cdot \frac{\bar{E}_s}{\sigma_p} \quad \tau = \frac{tc_1}{R} \quad (2-50)$$

$$\beta_n = \frac{b_{sn}}{R} \cdot \frac{\bar{E}_s}{\sigma_p}$$

be the non-dimensionalized form of the displacement and time variables.

Parameters are expressed as

$$\eta_E = \frac{\bar{E}_s}{E}$$

$$\eta_\rho = \frac{\rho_s}{\rho}$$

$$\eta_\nu = \frac{(1+\nu)(1-2\nu)}{(1-\nu)} \quad (2-51)$$

$$\eta_t = \frac{t}{R}$$

$$\eta_A = \frac{A}{R}$$

$$\eta_I = \frac{I}{R^3}$$

The last two parameters given above become unnecessary when considering an unstiffened shell since for this case A and I are given by

$$A = t \quad \text{and} \quad I = \frac{1}{12} t^3 \quad (2-52)$$

Although the equations were derived considering an unstiffened shell of uniform thickness, the response of a shell with thin, closely spaced stiffeners can also be approximated by specifying A and I separately from t. The

equations of interest in non-dimensionalized form are

$$\begin{aligned}
 \dot{\alpha}_n &= P1_n(\theta_1) + Q1_n(F,G) \\
 \dot{\beta}_n &= P2_n(\theta_1) + Q2_n(F,G) \\
 \ddot{\alpha}_n &= N1_n(\alpha_n, \beta_n) + P3_n(\theta_1) + Q3_n(F,G) \\
 \ddot{\beta}_n &= N2_n(\alpha_n, \beta_n) + P4_n(\theta_1) + Q4_n(F,G)
 \end{aligned} \tag{2-53}$$

where  $P1_n$ ,  $P2_n$ ,  $P3_n$ , and  $P4_n$  are functions whose values are determined directly from the position of the incident wave.  $Q1_n$ ,  $Q2_n$ ,  $Q3_n$ , and  $Q4_n$  are functions of the outgoing shear and dilatational waves; and  $N1_n$  and  $N2_n$  are functions of the displacements. These various functions in non-dimensionalized form are derived from equations given earlier. Given here are those for the case of the incoming dilatational stress wave.

$$\begin{aligned}
 P1_n(\theta_1) &= -\frac{\eta_v \eta_E}{\pi} \cdot \begin{cases} \sin \theta_1 & n = 0 \\ \theta_1 + \frac{\sin 2\theta_1}{2} & n = 1 \\ \frac{\sin(n-1)\theta_1}{n-1} + \frac{\sin(n+1)\theta_1}{n+1} & n = 2, 3, \dots \end{cases} \\
 P2_n(\theta_1) &= \frac{\eta_v \eta_E}{\pi} \cdot \begin{cases} \theta_1 - \frac{\sin 2\theta_1}{2} & n = 1 \\ \frac{\sin(n-1)\theta_1}{n-1} - \frac{\sin(n+1)\theta_1}{n+1} & n = 2, 3, \dots \end{cases} \tag{2-54} \\
 P3_n(\theta_1) &= -\frac{\eta_v \eta_E}{2\pi \eta_\rho \eta_t} \cdot \begin{cases} (1+\bar{v})\theta_1 + \frac{(1-\bar{v}) \sin 2\theta_1}{2} & n = 0 \\ (1-\bar{v})\theta_1 + (1+\bar{v}) \sin 2\theta_1 + \frac{(1-\bar{v}) \sin 4\theta_1}{4} & n = 2 \\ \frac{(1-\bar{v}) \sin(n-2)\theta_1}{n-2} + \frac{(1-\bar{v}) \sin(n+2)\theta_1}{n+2} \\ \quad + \frac{2(1+\bar{v}) \sin n\theta_1}{n} & n=1, 3, 4, 5, \dots \end{cases}
 \end{aligned}$$

$$P4_n(\theta_1) = \frac{\eta_v \eta_E (1-\bar{v})}{2\pi \eta_\rho \eta_t} \cdot \begin{cases} \theta_1 - \frac{\sin 4\theta_1}{4} & n = 2 \\ \frac{\sin(n-2)\theta_1}{n-2} - \frac{\sin(n+2)\theta_1}{n+2} & n = 1, 3, 4, 5, \dots \end{cases}$$

$$N1_n(\alpha_n, \beta_n) = - \frac{\eta_v \eta_E}{\eta_\rho \eta_t} \left[ \eta_A (\alpha_n + n\beta_n) + \eta_I (1-n^2)^2 \alpha_n \right]$$

$$N2_n(\alpha_n, \beta_n) = - \frac{\eta_v \eta_E}{\eta_\rho \eta_t} \left[ \eta_A (n\alpha_n + n^2 \beta_n) \right]$$

$$Q1_n(F, G) = - (-1)^n \int_0^\infty F^{n+2}(\xi_1) \cosh u_1 \cosh nu_1 du_1 \\ + (-1)^n \cdot \left(\frac{c_1}{c_2}\right)^{n+1} \int_0^\infty G^{n+2}(\xi_2) \sinh u_2 \sinh nu_2 du_2$$

$$Q2_n(F, G) = - (-1)^n \int_0^\infty F^{n+2}(\xi_1) \sinh u_1 \sinh nu_1 du_1 \\ + (-1)^n \cdot \left(\frac{c_1}{c_2}\right)^{n+1} \int_0^\infty G^{n+2}(\xi_2) \cosh u_2 \cosh nu_2 du_2$$

$$Q3_n(F, G) = \frac{(-1)^n \eta_v}{2(1+\bar{v}) \eta_\rho \eta_t} \int_0^\infty F^{n+2}(\xi_1) \cosh nu_1 \left[ \frac{\lambda}{\mu} + 2 \cosh^2 u_1 \right] du_1 \\ - \frac{(-1)^n \eta_v}{2(1+\bar{v}) \eta_\rho \eta_t} \cdot \left(\frac{c_1}{c_2}\right)^{n+2} \int_0^\infty G^{n+2}(\xi_2) \sinh 2u_2 \sinh nu_2 du_2$$

$$Q4_n(F, G) = \frac{(-1)^n \eta_v}{2(1+\bar{v}) \eta_\rho \eta_t} \int_0^\infty F^{n+2}(\xi_1) \sinh 2u_1 \sinh nu_1 du_1 \\ - \frac{(-1)^n \eta_v}{2(1+\bar{v}) \eta_\rho \eta_t} \cdot \left(\frac{c_1}{c_2}\right)^{n+2} \int_0^\infty G^{n+2}(\xi_2) \cosh 2u_2 \cosh nu_2 du_2$$

## 2.5 Other Equations of Interest

### Dilatational Wave

The hoop stress in the shell is determined from the relation

$$\sigma_{\theta\theta} = \bar{E}_s \epsilon_\theta$$

where

$$\epsilon_\theta = \frac{1}{R} \left( \frac{\partial v_s}{\partial \theta} + u_s \right)$$

By substitution of the Fourier expansion of the displacement components the hoop stress can be expressed modewise as a fraction of the absolute amplitude of the incoming stress wave, as

$$\frac{\sigma_{\theta\theta}}{|\sigma_p|} = \sum_{n=0}^{\infty} \left[ n\beta_n + \alpha_n \right] \cos n\theta \quad (2-55)$$

The bending stress is determined from the relation

$$\sigma_{sb} = \frac{\bar{E}_s d}{R^2} \left( \frac{\partial^2 u_s}{\partial \theta^2} + u_s \right)$$

which may also be expressed modewise as

$$\frac{\sigma_{sb}}{|\sigma_p|} = d \sum_{n=0}^{\infty} (n^2 - 1) \alpha_n \cos n\theta \quad (2-56)$$

where  $d$  is the distance from the neutral axis of the shell to its extreme fiber.

Stresses within the medium at any radius  $r$  may be determined by summation of modal stresses as follows

$$\frac{\sigma_{rr}}{|\sigma_p|} = \sum_{n=0}^{\infty} \frac{\bar{A}_n}{|\sigma_p|} \cos n\theta \quad (2-57)$$

$$\frac{\sigma_{r\theta}}{|\sigma_p|} = \sum_{n=1}^{\infty} \frac{\bar{B}_n}{|\sigma_p|} \sin n\theta$$

$$\frac{\sigma_{\theta\theta}}{|\sigma_p|} = \sum_{n=0}^{\infty} \frac{\bar{C}_n}{|\sigma_p|} \cos n\theta$$

where  $\bar{A}_n$ ,  $\bar{B}_n$ , and  $\bar{C}_n$  are coefficients previously described as generalized stresses of the incoming and outgoing stress waves.

### Shear Wave

The corresponding equations for the incoming shear wave are, for the shell

$$\frac{\sigma_{\theta\theta}}{|\sigma_s|} = \sum_{n=1}^{\infty} (\alpha_n - n\beta_n) \sin n\theta \quad (2-58)$$

$$\frac{\sigma_{sb}}{|\sigma_s|} = d \sum_{n=1}^{\infty} (1-n^2) \alpha_n \sin n\theta$$

and for the stresses in the medium

$$\frac{\sigma_{rr}}{|\sigma_s|} = \sum_{n=1}^{\infty} \frac{\bar{A}_n}{|\sigma_s|} \sin n\theta$$

$$\frac{\sigma_{r\theta}}{|\sigma_s|} = \sum_{n=0}^{\infty} \frac{\bar{B}_n}{|\sigma_s|} \cos n\theta \quad (2-59)$$

$$\frac{\sigma_{\theta\theta}}{|\sigma_s|} = \sum_{n=1}^{\infty} \frac{\bar{C}_n}{|\sigma_s|} \sin n\theta$$

where all terms are as defined before.

CHAPTER III  
METHOD OF SOLUTION

### 3.1 General

In this chapter are presented the numerical techniques used in solving the problem. Since the methods employed are similar in theory for both the incoming dilatational and shear waves, only the solution to the incoming dilatational (compressional) wave will be discussed in detail here. The equations (2-53) to be solved consist of two pairs of coupled integro-differential equations in the generalized coordinates of the shell and the potential functions. The integral terms in these equations contain elements of the outgoing wave potentials, both dilatational and shear, whose values must be determined through application of the boundary equations at each instant of time considered.

In the numerical solution, time is taken to be the independent variable, and is expressed in terms of the half transit time of the incoming wave across the cavity,  $\tau = tc_1/R$ . Increments of time are expressed as a fraction of the half transit time; if  $N$  is defined as the number of time steps for the wave to travel one radius, then  $i/N$  denotes the elapsed time after the  $i$ th step has been taken (Fig. 4).

The position angle,  $\theta_1$ , can be defined for any step in time as

$$\theta_1 = \arccos (1 - i/N) \quad (3-1)$$

After total envelopment, i.e., for  $i/N > 2$ ,  $\theta_1$  becomes equal to  $\pi$ .

### 3.2 Numerical Integration of the Potential Functions

Lamb (4) notes that if a point source  $f(t)dz$  is located at the point  $(x = 0, y = 0, z = z)$ , its effect at a distance  $r$  from the origin in

the xy plane can be represented by the equation

$$\varphi = \frac{1}{4\pi \sqrt{r^2+z^2}} f\left(t - \frac{\sqrt{r^2+z^2}}{c_1}\right) dz$$

which may be represented graphically as in Fig. 5. To obtain the effect of a line source of density  $F(t)$  on the z axis, spherically symmetric point sources with the same variation in time can be assumed to be situated all along the axis, and their combined effect represented as an integral over all the point sources

$$\varphi = \frac{1}{4\pi} \int_{-\infty}^{\infty} F\left(t - \frac{\sqrt{r^2+z^2}}{c_1}\right) \frac{dz}{\sqrt{r^2+z^2}} \quad (3-2)$$

The limits of minus infinity to plus infinity are shown here in order to represent the general case. It will be shown that for a disturbance beginning at some definite time, the limits of the integral may be taken as finite.

Now let

$$\begin{aligned} r^2 + z^2 &= r^2(1 + z^2/r^2) \\ &= r^2 \cosh^2 u_1 \end{aligned}$$

and the above integral can be written as

$$\varphi = \int_0^{\infty} F\left(t - \frac{r}{c_1} \cosh u_1\right) du_1 \quad (3-3)$$

from which the graphical interpretation in Fig. 6 is made.

Consider for the present the determination of the integral values at the boundary  $r = R$ . We define  $t = 0$  to be that time when the first effects of the outgoing stress waves (i.e., from the point source at  $z = 0$ ) reach the boundary. As time increases the effects of other point sources progressively further away along the z axis will reach the boundary in the xy plane. Thus it can be seen that though the limits of infinity are given in the integrals,

for finite times the limits can be represented by finite values. The maximum value of the variable  $R \cosh u_1$  in equation (3-3) that need be considered can therefore be represented as a function of time. At  $t = 0$

$$R \cosh u_{1m} = R$$

that is,  $u_{1m}$  is zero for time zero. For any time later

$$R \cosh u_{1m} = R + tc_1$$

in the case of the outgoing dilatational wave (Fig. 6).  $R \cosh u_{1m}$  locates the point farthest along the  $z$  axis whose wave front has just reached the boundary in the  $xy$  plane,  $c_1$  being the velocity of wave propagation. In non-dimensionalized form this can be written

$$\cosh u_{1m} = 1 + \tau = 1 + \frac{1}{N}$$

where the terms are as previously defined. Since the integration is over all point sources whose wave front has reached or passed the boundary in the  $xy$  plane, the integral expression of equation (3-3) can be written with new limits

$$\varphi = \int_0^{u_{1m}} F\left(t - \frac{R}{c_1} \cosh u_1\right) du_1$$

Let

$$\cosh u_1 = 1 + \zeta \tag{3-4}$$

where  $\zeta$  now becomes the variable of integration varying in value from 0 to  $\tau$ . In terms of  $\zeta$  the integral expression becomes

$$\varphi = \int_0^\tau \frac{F(-1+\tau-\zeta)d\zeta}{\sqrt{2\zeta} \sqrt{1+\zeta/2}} \tag{3-5}$$

Note that a singularity of the integrand occurs at  $\zeta = 0$ , for all values of  $\tau$ . Paul (6) has presented a numerical technique for evaluating integrals of this

general type taking into account the singular point. The method is essentially a modified trapezoidal rule in which weighting coefficients are obtained. If the range  $(0, \tau)$  of the integral is subdivided into subranges each of equal length  $\Delta\tau$ , the above integral for any time  $\tau = i\Delta\tau$  can be represented as

$$\varphi = \sum_{m=0}^{(i-1)} \int_{m\Delta\tau}^{(m+1)\Delta\tau} \frac{f(\xi)d\xi}{\sqrt{2\xi}} \quad (3-6)$$

where  $f(\xi)$  is a polynomial of first degree in  $\xi$  which approximates the quotient

$$\frac{F(-1+\tau-\xi)}{\sqrt{1+\xi/2}}$$

as a linear function over each subrange. The results of the integration of equation (3-6) are then put in the form

$$\varphi = \sum_{m=0}^{(i-1)} \left[ AM_m \cdot R_m \cdot F_{i-m} + BM_m \cdot R_{m+1} \cdot F_{i-m+1} \right] \quad (3-7)$$

where

$$AM_m = \sqrt{\frac{\Delta\tau}{2}} \left\{ 2(m+1) \left[ (m+1)^{1/2} - m^{1/2} \right] - \frac{2}{3} \left[ (m+1)^{3/2} - m^{3/2} \right] \right\}$$

$$BM_m = \sqrt{\frac{\Delta\tau}{2}} \left\{ \frac{2}{3} \left[ (m+1)^{3/2} - m^{3/2} \right] - 2m \left[ (m+1)^{1/2} - m^{1/2} \right] \right\} \quad (3-8)$$

represent a set of weighting functions which can be computed for any interval being considered. For large values of  $m$  these functions were written in a form more convenient for computational purposes by asymptotic expansion, to get the following result

$$AM_m = \sqrt{\frac{m\Delta\tau}{2}} \left[ \frac{1}{2m} - \frac{1}{12m^2} + \frac{1}{32m^3} - \frac{1}{64m^4} \right]$$

$$BM_m = \sqrt{\frac{m\Delta\tau}{2}} \left[ \frac{1}{2m} - \frac{1}{6m^2} + \frac{3}{32m^3} - \frac{1}{16m^4} \right] \quad (3-9)$$

For an illustration of the variation of AM and EM functions with  $m$ , see Fig. 10.  $R_m$  is termed the multiplying factor which for this particular integral is equal to

$$R_m = \frac{1}{\sqrt{1 + \frac{\xi_m}{2}}}$$

All of the various integral expressions for the potential functions were simplified to the form of equation (3-6) thereby permitting use of the above weighting factors for all integrals. However, the expression for the multiplying factor  $R_m$  varies for the different integrals.

The integration for the outgoing shear potential  $\psi$  is handled in a similar manner, except for a minor modification which results from the fact that the shear wave travels outward with velocity  $c_2$ .

Consider for illustrative purposes some shear potential represented as

$$\psi = \int_0^{\infty} G\left(t - \frac{R}{c_2} \cosh u_2\right) \cosh u_2 \, du_2$$

Since the incident wave strikes the shell at time  $t = 0$ , the shear wave front must also reach the boundary at this instant in order to satisfy boundary conditions. Thus at  $t = 0$

$$R \cosh u_{2m} = R$$

and for any time later

$$R \cosh u_{2m} = R + tc_2$$

using the same reasoning as for the outgoing dilatational wave. We can express the above equation in non-dimensionalized form as

$$\cosh u_{2m} = 1 + k_c \tau$$

where

$$k_c = \frac{c_2}{c_1}$$

is a constant relating the velocities.

Again since  $u_2$  is a variable of integration we can write

$$\cosh u_2 = 1 + k_c \xi$$

where  $\xi$  as in the case of the dilatational wave is the new variable of integration with limits 0 to  $\tau$ . In terms of this variable the integral is now written as

$$\psi = \int_0^\tau \frac{G\left(-\frac{1}{k_c} + \tau - \xi\right) \sqrt{k_c} (1 + k_c \xi) d\xi}{\sqrt{2\xi} \sqrt{1 + \frac{k_c \xi}{2}}} \quad (3-10)$$

Note that the shear wave starts from the  $z$  axis at time  $\tau = -1/k_c$  which is earlier than for the dilatational wave since it travels at a slower speed (with fictitious material within the shell) and must reach the boundary at time equal to zero. The numerical integration of equation (3-10) is accomplished in a similar method to that which was done for the dilatational potential. The result can be expressed as

$$\psi = \sum_{m=0}^{(i-1)} \left[ AM_m \cdot Q_m \cdot G_{i-m} + EM_m \cdot Q_{m+1} \cdot G_{i-m+1} \right] \quad (3-11)$$

where  $AM_m$  and  $EM_m$  are weighting factors identical to those derived previously, and  $Q_m$  for this particular integral is

$$Q_m = \frac{\sqrt{k_c} \cdot (1 + k_c \xi_m)}{\sqrt{1 + \frac{k_c \xi_m}{2}}}$$

The expression for  $Q_m$  is again dependent on the form of each integral considered.

For an illustration of the variation of the F and G functions with time, see Figs. 11 and 12.

### 3.3 Solution of the Basic Equations

The equations of motion for the shell are solved by an iterative procedure known as the Newmark Beta Method (5) with which values for the potential functions, and the accelerations, velocities, and displacements of the shell are determined.

In general the method consists of using a step-by-step integration technique over successive time intervals assuming a specific variation of acceleration during each interval. If we assume that at time  $\tau = (i-1)\Delta\tau$  all values of potential functions, accelerations, velocities and displacements are known, the method becomes that of determining the corresponding values at a time  $\tau = i\Delta\tau$ . For an assumed linear variation of acceleration over each interval the equations of interest are

$$\begin{aligned}\dot{\alpha}_{n,i} &= \dot{\alpha}_{n,i-1} + \frac{\Delta\tau}{2} (\ddot{\alpha}_{n,i-1} + \ddot{\alpha}_{n,i}) \\ \alpha_{n,i} &= \alpha_{n,i-1} + \Delta\tau\dot{\alpha}_{n,i-1} + \frac{\Delta\tau^2}{6} (2\ddot{\alpha}_{n,i-1} + \ddot{\alpha}_{n,i}) \\ \dot{\beta}_{n,i} &= \dot{\beta}_{n,i-1} + \frac{\Delta\tau}{2} (\ddot{\beta}_{n,i-1} + \ddot{\beta}_{n,i}) \\ \beta_{n,i} &= \beta_{n,i-1} + \Delta\tau\dot{\beta}_{n,i-1} + \frac{\Delta\tau^2}{6} (2\ddot{\beta}_{n,i-1} + \ddot{\beta}_{n,i})\end{aligned}\tag{3-12}$$

where  $n$  denotes the mode and  $i$  the time. Note that in the above equations the velocities and displacements are expressed in terms of  $\ddot{\alpha}_{n,i-1}$  and  $\ddot{\beta}_{n,i-1}$ , acceleration components which generally are unknown.

Values for the acceleration components at time  $\tau = i\Delta\tau$  are assumed and the velocities and displacements determined from the above equations; then by use of the boundary equations to determine the values of the potential

functions, values of the acceleration components can be computed from the equations of motion. The computed values are then compared with the assumed values and if they agree or are within an arbitrarily established tolerance, the step is completed; if not, the values of  $\ddot{\alpha}_{n,i}$  and  $\ddot{\beta}_{n,i}$  just computed are taken as new assumed values and the cycle repeated until the criterion is satisfied. A detailed discussion of the procedure follows.

The equations of continuity at the boundary at time  $\tau = i\Delta\tau$  are given in equations (2-49) and are rewritten here in the form

$$\begin{aligned}\dot{\alpha}_{n,i} &= P1_n(\theta_1) + \int_0^{i\Delta\tau} Q1_n(F_0, F_1, \dots, F_i; G_0, G_1, \dots, G_i) d\xi \\ \dot{\beta}_{n,i} &= P2_n(\theta_1) + \int_0^{i\Delta\tau} Q2_n(F_0, F_1, \dots, F_i; G_0, G_1, \dots, G_i) d\xi\end{aligned}\tag{3-13}$$

where  $P1_n$  and  $P2_n$  denote functions related to the particle velocities in the medium at the boundary due to the incoming stress wave; their values may be determined directly at any time. The integral expressions denote the contribution due to the outgoing waves. All values of  $F$  and  $G$  are known except  $F_i$  and  $G_i$  which are to be determined from the above equations. These equations are now written isolating the unknown values of  $F$  and  $G$  terms

$$\begin{aligned}\dot{\alpha}_{n,i} &= P1_n(\theta_1) + \int_{\Delta\tau}^{i\Delta\tau} Q1_n(F_0, F_1, \dots, F_{i-1}; G_0, G_1, \dots, G_{i-1}) d\xi \\ &\quad + \int_0^{\Delta\tau} Q1_n(F_{i-1}, F_i; G_{i-1}, G_i) d\xi \\ \dot{\beta}_{n,i} &= P2_n(\theta_1) + \int_{\Delta\tau}^{i\Delta\tau} Q2_n(F_0, F_1, \dots, F_{i-1}; G_0, G_1, \dots, G_{i-1}) d\xi \\ &\quad + \int_0^{\Delta\tau} Q2_n(F_{i-1}, F_i; G_{i-1}, G_i) d\xi\end{aligned}\tag{3-14}$$

The integrals with limits  $\Delta\tau$  to  $i\Delta\tau$  are evaluated using the numerical technique described in a previous section.

The next step is to assume values for  $\ddot{\alpha}_{n,i}$  and  $\ddot{\beta}_{n,i}$ , the radial and tangential components of acceleration of the shell, from which velocity and displacement components are determined using equations (3-12). With these values known, equations (3-14) become effectively two equations with the two unknowns,  $F_1$  and  $G_1$ , which can then be determined.

The equations of motion are given in equations (2-53) and are here written in the form

$$\ddot{\alpha}_{n,i} = N1(\alpha_{n,i}; \beta_{n,i}) + P3_n(\theta_1) + \int_0^{i\Delta\tau} Q3_n(F_0, F_1, \dots, F_i; G_0, G_1, \dots, G_i) d\zeta \quad (3-15)$$

$$\ddot{\beta}_{n,i} = N2(\alpha_{n,i}; \beta_{n,i}) + P4_n(\theta_1) + \int_0^{i\Delta\tau} Q4_n(F_0, F_1, \dots, F_i; G_0, G_1, \dots, G_i) d\zeta$$

from which the acceleration components  $\ddot{\alpha}_{n,i}$  and  $\ddot{\beta}_{n,i}$  are now computed. If the computed values agree or are within an arbitrarily established limit of the assumed values, the step is completed; otherwise the computed values are used as the assumed values for the next cycle of iteration.

The procedure described above requires that all parameters at  $\tau = 0$  be known, including the initial values  $F_0$  and  $G_0$ . Initial values of velocity and displacement of the shell are specified to be zero. From the short-time approximation presented in Section 3.7 initial values of acceleration and  $G_0$  were determined to also be zero, and the values of  $F_0$  to be the following

$$F_0 = \frac{\eta_v \eta_E}{\pi} \cdot \begin{cases} -1 & n = 0 \\ 2(-1)^{n+1} & n = 1, 2, \dots \end{cases} \quad (3-16)$$

The short-time approximation also indicated that the radial acceleration components near  $\tau = 0$  varied as  $\tau^{1/2}$  and the tangential components as  $\tau^{3/2}$ ;

thus to improve the accuracy of the calculations, equations (3-12) for the first step in time were modified to

$$\begin{aligned}\dot{\alpha}_{n,1} &= \frac{2}{3} \ddot{\alpha}_{n,1} & \dot{\beta}_{n,1} &= \frac{2}{5} \ddot{\beta}_{n,1} \\ \alpha_{n,1} &= \frac{2}{5} \dot{\alpha}_{n,1} & \beta_{n,1} &= \frac{2}{7} \dot{\beta}_{n,1}\end{aligned}\quad (3-17)$$

Without this modification, the results for the first step cannot be brought into acceptable agreement with the short-time approximation.

The  $n = 0$  mode is simplified somewhat because it has no tangential component of displacement, and contains only the dilatational component of the potential functions.

#### 3.4 Stresses of the Shell and Medium

Solution of the equations of motion yields modal values of the functions  $F$  and  $G$ , and the modal acceleration, velocity and displacement components of the shell. The stresses in the shell are determined directly from the displacements using equations (2-55) and (2-56).

Stresses in the medium at any radius and time are determined using equations (2-57). They are here written in the form

$$\frac{\sigma(r, i\Delta\tau)}{\sigma_p} = \sum_{n=0}^{\infty} \left[ S_n(\theta_1) + \int_0^{\infty} T_n(F) d\xi + \int_0^{\infty} W_n(G) d\xi \right] \quad (3-18)$$

where  $S_n(\theta_1)$  represents the stress due to the incoming wave and the integral terms that due to the outgoing waves. All are functions of both radius and time. Consider the stresses in the medium for any radius equal to  $r$  at time  $\tau = i\Delta\tau = 1/N$ .

$\theta_1$  (Fig. 7) is now determined from the equation

$$\theta_1 = \arccos \frac{R}{r} (1 - 1/N) \quad (3-19)$$

and takes on values from

$$\theta_1 = \frac{R}{r} \quad \text{for } \tau = 0$$

to

$$\theta_1 = \pi \quad \text{for } \tau \geq \left(1 + \frac{r}{R}\right)$$

The integral terms must be recomputed for each radius and time considered.

As an example consider the integral

$$\varphi = \int_0^{\infty} F\left(t - \frac{r}{c_1} \cosh u_1\right) du_1$$

and let  $\tau = \frac{1}{k_r} - 1$ , where  $k_r = R/r$ , represent the nondimensionalized time after  $\tau = 0$  required for the outgoing dilatational wave front to reach the radius  $r$  being considered. Then for  $\tau < \tau_r$  the integral is equal to zero, and for  $\tau > \tau_r$  the maximum value of  $(r \cosh u_1)$  can be written

$$r \cosh u_{1m} = r + t' c_1$$

or

$$\cosh u_{1m} = 1 + k_r \tau'$$

where  $\tau' = \tau - \tau_r$  represents the time after the wave front has reached the radius  $r$ . We express  $\cosh u_1$  as

$$\cosh u_1 = 1 + k_r \xi$$

where  $\xi$  is the same variable of integration as was used previously. The integral is then expressed in terms of  $\xi$  as

$$\varphi = \int_0^{\tau'} \frac{F(-1 + \tau' - \xi) \sqrt{k_r} d\xi}{\sqrt{2\xi} \sqrt{1 + \frac{k_r \xi}{2}}} \quad (3-20)$$

The numerical method of integration used is identical to that described

earlier for the integral at the boundary, with the result that the same weighting factors  $AM_m$  and  $EM_m$  are applicable. Note, however, that the limits of the integral are now 0 to  $\tau'$ ; also the multiplying factor  $R_m$  for this particular integral becomes

$$R_m = \frac{\sqrt{k_r}}{\sqrt{1 + \frac{k_r \zeta_m}{2}}}$$

By a similar analysis, the integral of the shear potential

$$\psi = \int_0^{\infty} G\left(t - \frac{r}{c_2} \cosh u_2\right) \cosh u_2 \, du_2$$

can be put in the form

$$\psi = \int_0^{\tau'} \frac{G\left(-\frac{1}{k_c} + \tau' - \zeta\right) \sqrt{k_r k_c} (1 + k_r k_c \zeta) d\zeta}{\sqrt{2\zeta} \sqrt{1 + \frac{k_r k_c \zeta}{2}}} \quad (3-21)$$

where

$$\tau' = \tau - \tau_{rs}$$

For the potential  $\psi$

$$\tau_{rs} = \frac{1}{k_c} \left(\frac{1}{k_r} - 1\right)$$

The weighting factors  $AM_m$  and  $EM_m$  remain the same but the multiplying factor  $Q_m$  for this particular integral becomes

$$Q_m = \frac{\sqrt{k_r k_c} (1 + k_r k_c \zeta_m)}{\sqrt{1 + \frac{k_r k_c \zeta_m}{2}}}$$

### 3.5 Time Dependent Stress Wave

The problem considered thus far has dealt with an incoming stress wave with a step distribution in time. The results obtained for the step wave can be used through the application of Duhamel's integral to find values for the response of a shell and medium to incoming waves with any time variation. As an example, a stress wave which decays exponentially with time (Fig. 8) according to the following equation is considered

$$\sigma_p(\tau) = \sigma_{po} \left(1 - \frac{\tau}{\tau_0}\right) e^{-k \frac{\tau}{\tau_0}} \quad (3-22)$$

$\tau_0$  represents the time at which the stress wave decays to zero and  $k$  is a parameter which is related to the shape of the curve. Stresses at any time equal to  $i\Delta\tau$  can be found by the application of Duhamel's integral, here written in the form

$$\sigma(i\Delta\tau) = \sigma_{st}(i\Delta\tau) + \int_0^{i\Delta\tau} \frac{d\sigma_p(\tau)}{d\tau} \cdot \sigma_{st}(i\Delta\tau - \tau) d\tau \quad (3-23)$$

$\sigma_{st}$  is defined to be that stress resulting from an incoming step wave of amplitude  $\sigma_{po}$  in equation (3-22). In the numerical analysis, the time dependent wave is approximated by a series of rectangular sections as illustrated in Fig. 8.

### 3.6 Description of the Computer Program

The problem was programmed modewise for a high speed digital computer (CDC 1604) using Fortran language, and considering only the first three modes. Input data consist of the following parameters:

- (1) The time intervals at which computations are to be performed, expressed as the number of intervals required for the incoming wave to travel

one radius (one-half transit time). The degree of accuracy achieved is dependent on this parameter, the smaller the interval the more accurate the results. However, the machine time required for a given number of transits of the incoming wave varies inversely as the square of the interval size approximately, thus some sacrifice in accuracy is necessary to reduce the time of computations required.

(2) The total time over which the computations are to be performed, expressed as the total number of time intervals to be considered. Generally speaking, all values seemed to have reached their asymptotic (static) values within ten transit times of the incoming wave across the cavity.

(3) The ratio of the moduli of elasticity,  $\bar{E}_s/E$ , where  $\bar{E}_s$  is the "plane strain" modulus for the shell and  $E$  the modulus of elasticity of the medium.

(4) The mass ratio,  $\rho_s/\rho$ , where  $\rho_s$  is the mass of the shell and  $\rho$  the mass of the medium per unit volume.

(5) Poisson's ratio of the medium.

(6) The ratio of the thickness of the shell to its radius. When considering a shell whose area,  $A$ , and moment of inertia,  $I$ , are not directly related to the thickness,  $A$  and  $I$  must be specified separately.

(7) The amount of additional mass within the shell expressed as a fraction of the mass per unit surface area of the shell.

(8) The number of radii to which stresses in the medium are desired.

(9) The time intervals at which output data are desired.

(10) The angular increment at which output data is to be computed.

Because of symmetry only values between 0 and 180 degrees need be considered.

Additional input quantities in the case of the exponentially decaying stress wave are  $\tau_0$  and  $k$ , parameters which define the duration and shape of the stress pulse, respectively.

Output data consist of the acceleration, velocity, displacement, and stress components of the shell for specified angles and times; and the stresses in the medium for specified radii, angles and times.

### 3.7 Short-Time Approximation

As a check on the accuracy of the machine solution for short times, the boundary equations and the equations of motion were solved approximately by making a series expansion of all pertinent functions in terms of time as the independent variable. Although the following discussion is limited to the case of the incoming dilatational wave, the basic principles are the same for either of the types of wave considered.

The expressions for the velocities and stresses in the medium around the boundary due to the incident wave all have been written thus far in terms of  $\theta_1$ , the position angle of the wave. In terms of nondimensionalized time  $\tau$ , all functions of  $\theta_1$  can be written in terms of  $\tau$  using the following relations

$$\begin{aligned}\cos \theta_1 &= 1 - \tau \\ \sin \theta_1 &= \sqrt{2\tau} \left[ 1 - \frac{1}{4} \tau - \frac{1}{32} \tau^2 - \dots \right] \\ \theta_1 &= \sqrt{2\tau} \left[ 1 + \frac{1}{12} \tau + \frac{3}{160} \tau^2 + \dots \right]\end{aligned}\tag{3-24}$$

The integral values representing the effects of the outgoing waves are also expressed as functions of  $\tau$ . The following example will illustrate the technique used to accomplish this. For example, consider the transformation of the integral

$$\varphi = \int_0^{\infty} F\left(t - \frac{R}{c_1} \cosh u_1\right) du_1$$

As was shown in Section 3.2,  $\cosh u_1$  in the integral varies in value for any given time  $\tau$  from 1 to  $1 + \tau$ . It is convenient for purposes of analyzing the integral to represent the variable  $\cosh u_1$  as follows

$$\cosh u_1 = 1 + \omega\tau \quad (3-25)$$

where  $\tau$  is now a fixed value in the integration and  $\omega$  is defined as the variable of integration whose value ranges from 0 to 1. The function

$$F\left(t - \frac{R}{c_1} \cosh u_1\right) = F(-1 + \tau(1-\omega))$$

is expanded in terms of a power series as

$$F(-1 + \tau(1-\omega)) = F_0 + \sum_{i=1}^{\infty} \gamma_i \tau^i (1-\omega)^i \quad (3-26)$$

where  $\gamma_i$  are unknown coefficients of the series. Since

$$du_1 = \frac{\sqrt{2\tau}}{2\sqrt{\omega}} \left[ 1 - \frac{\omega\tau}{4} + \frac{3}{32} (\omega\tau)^2 + \dots \right] d\omega$$

the integral can now be written as

$$\varphi = \frac{\sqrt{\tau}}{\sqrt{2}} \int_0^1 \frac{1}{\sqrt{\omega}} \left[ F_0 + \gamma_1 \tau(1-\omega) + \dots \right] \left[ 1 - \frac{\omega\tau}{4} + \dots \right] d\omega$$

from which after performing the indicated integration

$$\varphi = \sqrt{2\tau} \left[ F_0 + \tau \left( \frac{4}{3} \gamma_1 - \frac{1}{6} F_0 \right) + \tau^2 (\dots) \right] \quad (3-27)$$

The integrals which represent the effects of the outgoing shear wave can also be transformed in somewhat similar manner. Consider for example the integral

$$\psi = \int_0^{\infty} G\left(t - \frac{R}{c_2} \cosh u_2\right) \cosh u_2 \, du_2$$

In this case  $\cosh u_2$  varies from 1 to  $1 + k_c \tau$  where  $k_c = \frac{c_2}{c_1}$  and  $\tau = \frac{tc_1}{R}$ .

Therefore we write

$$\cosh u_2 = 1 + \omega k_c \tau \quad (3-28)$$

where  $\omega$  is now the variable of integration ranging in value from 0 to 1 in the integral. The function

$$G\left(t - \frac{R}{c_2} \cosh u_2\right) = G\left(-\frac{1}{k_c} + \tau(1-\omega)\right)$$

is expanded in terms of a power series as

$$G\left(-\frac{1}{k_c} + \tau(1-\omega)\right) = G_0 + \sum_{i=1}^{\infty} \epsilon_1 \tau^i (1-\omega)^i$$

where  $\epsilon_1$  are unknown coefficients of the series. From equation (3-28)

$$du_2 = \frac{\sqrt{2k_c \tau}}{2\sqrt{\omega}} \left[ 1 - \frac{\omega k_c \tau}{4} + \frac{3}{32} (\omega k_c \tau)^2 - \dots \right] d\omega$$

The integral written in terms of the variable  $\omega$  is now

$$\psi = \frac{\sqrt{k_c \tau}}{\sqrt{2}} \int_0^1 \frac{1}{\sqrt{\omega}} \left[ G_0 + \epsilon_1 \tau(1-\omega) + \dots \right] \left[ 1 + \frac{k_c \omega \tau}{4} + \dots \right] \left[ 1 + \omega k_c \tau \right] d\omega$$

and performing the integration

$$\psi = \sqrt{2k_c \tau} \left[ \tau \left( \frac{2}{3} G_0 \right) + \tau^2 \left( \frac{4}{15} \epsilon_1 + \frac{1}{10} k_c G_0 \right) + \tau^3 (\dots) \right] \quad (3-29)$$

The same basic technique is applied to all the integrals so that now the effects of both the incoming and outgoing waves can be written in terms of  $\tau$ . Substitution into the continuity equations and the equations of motion yield the following for any mode

$$\begin{aligned}\dot{\alpha} &= \sum_{i=1}^{\infty} f1_i(F,G)\tau^{i-\frac{1}{2}} \\ \dot{\beta} &= \sum_{i=1}^{\infty} f2_i(F,G)\tau^{i-\frac{1}{2}} \\ \ddot{\alpha} + l1_i(\alpha,\beta) &= \sum_{i=1}^{\infty} f3_i(F,G)\tau^{i-\frac{1}{2}} \\ \ddot{\beta} + l2_i(\alpha,\beta) &= \sum_{i=1}^{\infty} f4_i(F,G)\tau^{i-\frac{1}{2}}\end{aligned}\tag{3-30}$$

where  $f1_i$ ,  $f2_i$ ,  $f3_i$ , and  $f4_i$  are coefficients which contain certain elements  $F_0$ ,  $G_0$ ,  $\gamma_1$  and  $\epsilon_1$  of the potential functions;  $l1$  and  $l2$  are known functions of the displacements.

To solve the above equations, the displacement components of the shell are expressed as Frobenius (8) type series

$$\begin{aligned}\alpha &= \sum_{i=1}^{\infty} p_i \tau^{c+i} \\ \beta &= \sum_{i=1}^{\infty} q_i \tau^{c+i}\end{aligned}\tag{3-31}$$

where  $p_i$ ,  $q_i$ , and  $c$  are unknown coefficients. Substitution into equations (3-30) results in the following set of equations

$$\begin{aligned}\sum_{i=1}^{\infty} p_i \cdot (c+i) \cdot \tau^{c+i-1} &= \sum_{i=1}^{\infty} f1_i(F,G)\tau^{i-\frac{1}{2}} \\ \sum_{i=1}^{\infty} q_i \cdot (c+i) \cdot \tau^{c+i-1} &= \sum_{i=1}^{\infty} f2_i(F,G)\tau^{i-\frac{1}{2}}\end{aligned}\tag{3-32}$$

$$\sum_{i=1}^{\infty} p_i \cdot (c+1) \cdot (c+i-1) \cdot \tau^{c+i-2} + \sum_{i=1}^{\infty} l1(p_i, q_i) \tau^{c+i} = \sum_{i=1}^{\infty} f3_1(F, G) \tau^{i - \frac{1}{2}}$$

$$\sum_{i=1}^{\infty} q_i \cdot (c+1) \cdot (c+i-1) \cdot \tau^{c+i-2} + \sum_{i=1}^{\infty} l2(p_i, q_i) \tau^{c+i} = \sum_{i=1}^{\infty} f4_1(F, G) \tau^{i - \frac{1}{2}}$$

The coefficient  $c$  is now determined by inspection. Then through a step by step process which involves the equating of coefficients of like powers of  $\tau$ , values of  $p_i$ ,  $q_i$ ,  $\gamma_i$ , and  $\epsilon_i$  are determined. The following equations are then used to find values of the potential functions, and the displacement components of the shell.

$$F(\tau) = F_0 + \sum_{i=1}^{\infty} \gamma_i \tau^i$$

$$G(\tau) = G_0 + \sum_{i=1}^{\infty} \epsilon_i \tau^i$$

$$\alpha(\tau) = \sum_{i=1}^{\infty} p_i \tau^{c+i}$$

$$\beta(\tau) = \sum_{i=1}^{\infty} q_i \tau^{c+i}$$

(3-33)

Velocity and acceleration components may be determined by differentiation of the above expressions for the displacements.

## CHAPTER IV

## DISCUSSION OF RESULTS

4.1 General

Results of computations performed to determine the effect of the various parameters are discussed in this chapter.

Although equations presented throughout the study have been written to include an infinite number of modes, the greater part of the actual calculations performed and presented here are the results obtained considering only the modes  $n = 0, 1,$  and  $2$ . It is important to note that during envelopment of the shell by the plane stress wave, a Fourier series representation of the incoming wave is objectionable in that the series at this stage is slowly convergent, thus necessitating a large number of modes to accurately represent the plane wave. However, after passage of the wave across the cavity, the Fourier expansion of the incoming stresses around the boundary results in coefficients of all modes except  $n = 0$  and  $2$  becoming identically equal to zero for the plane dilatational wave, and coefficients of all modes except  $n = 2$  becoming identically equal to zero for the plane shear wave. Therefore, stresses due to the outgoing waves in modes corresponding to those of the incoming wave whose coefficients become zero must also eventually vanish at long times. The limited study conducted for modes greater than  $n = 2$  indicated that the maximum effect of the higher modes occurs within one transit time of the incident wave and rapidly decays, thus contributing relatively little to the maximum response of the shell which occurs after several transit times. However, for determining the early time response of the shell and medium, the higher modes are significant and should be considered in further extension of this work.

In the tables and figures to be discussed, quantities given in non-dimensionalized units are defined by equations (2-36) and (2-50). Stresses are given in units of the absolute value of the amplitude ( $|\sigma_p|$  or  $|\sigma_s|$ ) of the incident wave; a negative stress means a compressive response to an incoming compressional (Fig. 1) or a positive shear wave (Fig. 2). The physical properties of the shell relative to those of the medium, as well as the nature of the incoming wave are indicated on the graphs. Unless otherwise stated, the shell is considered to be an unstiffened one so that its cross sectional area and moment of inertia are related to the thickness as given by equations (2-52). Except where indicated, there is assumed to be no additional mass within the shell. Numeral subscripts denote the mode number.

The shell and medium have been assumed to exhibit linearly elastic behavior throughout their stress histories, which for the practical problem does not permit evaluation of any spalling or non-elastic effects.

Values of stresses given are in addition to those which exist prior to the arrival of the incident wave. For the elastic case, the effect of prior stresses such as those resulting from the overburden may be taken into account by merely adding them to stresses caused by the incident wave.

For clarity of presentation and because of the impracticability of including solutions for all possible permutations of the parameters involved, the discussion in this chapter is limited to a few representative cases.

#### 4.2 Modal Response of the Shell and Medium

Figures 11 and 12 illustrate the shape of the modal components of the dilatational and shear potentials obtained in the solution to a typical problem. It appears that a singularity occurs at one transit time in the case of the F functions resulting in the slight irregularity of the curves at

this point. Since computed values of stresses were determined to be rather insensitive to relatively large variations in values of the F and G functions, the effect of the irregularity would seem to be slight.

Figures 13 through 20 show modal acceleration, velocity, displacement and stress components for the shell and stress components for the medium at the boundary, as they vary with time. Static values shown were computed using the method given in Appendix B.

The high accelerations computed near the beginning are not truly representative of the actual case, since they are the result of assumptions made earlier in deriving the equations for the shell. The shell was represented by a line describing its middle surface which permits no variation in accelerations, velocities, and displacements of particles through the actual thickness. Also, no provision was made for refraction of the incident wave through the shell lining. These limitations restrict the applicability of the solutions to a shell whose thickness is small relative to its radius.

The  $n = 1$  mode is primarily a translational one which accounts for the rigid body translation of the shell after it has been enveloped by the incident wave. Thus, it can be seen that the velocity components for this mode approach constant values equal to the velocity of the medium behind the incident wave front, and displacements grow without bound reaching a straight line variation with time. Note that the stresses contributed by this mode reach their peak values within one transit time and quickly damp out, approaching zero asymptotically. For the incident shear wave, the  $n = 0$  mode is also a rigid body movement which accounts for rigid body rotation, and contributes little to the stresses.

Modal quantities obtained are coefficients of Fourier series; therefore, the total response or effect is determined by adding the coefficients

multiplied by the appropriate sine and cosine terms for any desired angle. Figures 21 through 24 show the time variation of stresses in the shell and medium for various angles when the first three modes are summed. The maximum stress in the shell for any angle may be determined by adding the bending stress to the hoop stress. This is indicated in Figs. 21 and 24 by the dotted line above the hoop stress.

Figure 25 is given to illustrate the relative magnitudes of the hoop stresses in the shell and medium for several thicknesses of shell. This also shows the effect of varying the relative thickness of the shell on the hoop stress in the medium. The dotted line indicating the hoop stress in the medium for an unlined cavity was obtained from the report by Paul (6).

Figures 26 and 27 show how the relative thickness of the shell affects the radial and shear stresses in the medium.

As was discussed earlier, stresses in the medium for any radius can be determined by reevaluating the integral terms which represent the effects of the outgoing waves, and adding them to the Fourier expansion of the incident wave. Figure 28 shows the modal and total radial, hoop, and shear stresses which were computed for a time equal to 10 transit times. These values are compared later with the static stresses, but on this figure the static stresses do not differ by more than the thickness of the lines, and therefore are not shown. The time variation of the radial and hoop stresses in the medium for various radii are shown in Fig. 29 for the incident dilatational wave, and in Fig. 30 for the incident shear wave.

#### 4.3 Short-Time and Asymptotic Comparisons

A method for obtaining a solution to the problem which is accurate for very short times ( $\tau \ll 1$ ) was presented in Section 3.7. This was desirable

to validate the machine solution and to determine the effect of the size of time interval selected. The results for a representative problem are shown in Figs. 31 through 33 for the incident dilatational wave, and in Figs. 34 through 36 for the incident shear wave. Four terms of the series representing the F and G functions, and three terms for other quantities were used in the short-time solution.

As can be seen from the graphs, good agreement was obtained for very small values of time, somewhat shorter time being obtained for the shear wave as compared to the dilatational wave. The shorter time results from the nature of the forcing functions (Eqs. 2-19 and 2-32) which indicate a more rapid rise in the incoming stresses for the incident shear wave.

Within the range of time for which the short-time solution is valid, decreasing the size of time interval for each step of the machine solution resulted in closer agreement between the two methods, as is to be expected. It also indicated that the stresses and displacements are not as sensitive to variations in the interval size as are the F and G functions.

At the other end of the time scale, i.e., at a relatively long time after passage of the incident wave front across the cavity, another check on the accuracy of the machine solution is afforded by the asymptotic approach of all values to the static results. Figures presented thus far have shown that the static condition is approached well within ten transit times.

The time interval used in the machine solution affects the stability of the results for long times. This is indicated in Fig. 37 which shows the variations in computed values of the displacement components for mode  $n = 2$  at relatively long times, for different time intervals.  $N$  represents the number of time steps required for the incident wave to travel a distance equal to the radius of the opening, and  $l/N$  defines the interval size. Note the

smaller graph which shows the percentage difference between the computed values at ten transit times and the static values.

As the interval is decreased the machine solution at long time approaches the static solution more closely. Below a certain size of time interval, there is little difference in the results, which indicates asymptotic convergence to the correct solution. For this particular problem,  $N \approx 30$  seems to be "critical" in that for  $N < 30$ , wide variations in computed values occur. As the mode number increases, the "critical" value of  $N$  increases rapidly, and the requirements of computer storage and calculation time become decisive factors which make impractical the study for long times of modes much larger than 2. The interval size selected for all problems solved (exclusive of the study to determine the effect of the interval size) was set equal to  $1/40$  ( $N = 40$ ) of the half transit time of the incident wave.

For the static case, only the modes  $n = 0$  and 2 yield values other than zero. Table 1 compares values of shell stresses and displacement components in these modes obtained from the computer solution to a particular problem at a time equal to 10 transit times, with the static solution. Most pairs of values differ by less than one percent. Comparable agreement of stresses in the medium at various radii are shown in Table 2. Values in Tables 1 and 2 were obtained from the solution to a problem whose parameters were:  $\eta_E = 4.0$ ,  $\eta_\rho = 3.0$ ,  $\eta_t = .05$ , and  $\nu = .25$ .

Although the figures and tables presented above were for a particular problem, the discussion given is applicable to all problems which were solved. Changing the physical characteristics of the shell and medium within the range of values studied had hardly any effect on the degree to which the long time machine solution and the static solution agreed. Also, the absolute value of all quantities which should asymptotically approach zero became less than .00005 in each case well before ten transit times.

#### 4.4 Effect of Parameters

Studies were conducted to determine the effect of each of the following parameters:

$$\eta_E = \frac{\bar{E}_s}{E} \quad \eta_\rho = \frac{\rho_s}{\rho}$$

$$\eta_t = \frac{t}{R} \quad \nu = \nu \text{ (medium)}$$

for an unstiffened shell without additional mass. Since it was impractical to take into account all permutations of the above parameters, a basic shell where

$$\eta_E = 4.0 \quad \eta_\rho = 3.0$$

$$\eta_t = .05 \quad \nu = .25$$

was considered from which each parameter was separately varied to determine its effect on the resulting stresses and displacements. Calculations performed were only for the case of the incident dilatational (P) wave.

Of particular interest was the determination of the maximum dynamic stresses and displacements (not including rigid body translation) due to the incident stress wave. Tables 3 through 6 compare the maximum values obtained in the machine solution with the static solution. "DLF," termed the dynamic load factor, is defined as the factor by which the displacement or stress produced by  $\sigma_p$  applied as a static load should be multiplied in order to obtain the maximum dynamic value. Figures 38 through 41 are given to graphically illustrate the variations in stresses and displacements, both static and dynamic, in the range of parameters considered. Stresses are given in units of  $|\sigma_p|$  and displacements in non-dimensionalized units defined by equations (2-36) and (2-50).

Table 3 and Fig. 38 illustrate the effect of increasing the relative thickness of the shell. The range of values selected for  $\eta_t$  is probably much greater than is practical or justified by the assumptions of the analysis, and was considered only to determine the trend of the results. As  $\eta_t$  is increased, displacements and hoop stresses of both the shell and medium decrease; however, the bending stress of the shell and the radial and shear stresses in the medium at the boundary increase. Figure 25 shows the time variation of the hoop stress in the shell and medium for various thicknesses of shell, including the case of the unlined cavity.

Increasing  $\eta_E$  results in a rapid increase in the displacements and stresses of the shell and a much lower rate of attenuation of the hoop stress in the medium. See Fig. 39 and Table 4.

Table 5 and Fig. 40 show that the parameter  $\eta_p$  has no effect on the static results but does affect the dynamic response. Increasing  $\eta_p$  increased the maximum response in both the medium and shell.

Figure 41 and Table 6 show that within the range of Poisson's ratio for the medium considered, as  $\nu$  increases displacements and stresses in the shell decrease, with very little additional reduction of the medium hoop stress.

Additional mass within the shell was shown to contribute relatively little to the overall response. This is mainly due to the simplifying assumptions which were made in deriving the equations of motion to account for the additional mass. Figure 42 shows the effect of the presence of additional mass equal to  $40\pi$  times the mass of the shell on the dynamic response of a particular shell. Additional mass decreases the displacements and increases the dynamic stresses in mode  $n = 1$ .

#### 4.5 Response to Time Varying Incident Wave

The results obtained from a solution to an incident wave with a step variation in time was shown to be useful by application of Duhamel's integral in determining the response to any time varying stress wave. The case of the exponentially decaying wave was considered, the results of which are illustrated in Fig. 43. Substantial reductions in the maximum stresses can be expected as the duration becomes smaller. In Fig. 44 is shown the effect of a linear rise in the amplitude of the incident wave. Note that for a wave with a linear rise followed by a step variation in time, very little decrease in maximum stresses occurred.

#### 4.6 Comparison with Previous Work

Baron (1), using a different method of analysis, investigated the dynamic response of two shells with different physical characteristics subjected to an incident plane dilatational wave. Figures 45 through 49 compare his results for the modal values of stresses and displacements of the thin shell, with results obtained by the method of solution given in this study. Similar results were obtained considering his so-called stiff shell. Although the shape of the response curves can be considered similar in the two reports, the magnitude of the dynamic response in Ref. (1) seems consistently higher than in the present report, and the long time results asymptotically approach values higher than the static solution. The following table compares the maximum modal stresses, for Poisson's ratio of 0.25, obtained in the two reports, and also shows values for the static case. Stresses are given in units of  $|\sigma_p|$ . The bending stresses for the stiffened shell cannot be compared directly since  $d$ , the distance from the neutral axis of the shell to its extreme fiber, is not stated in Ref. (1).

| Quant.                  | Mode | Thin Shell              |                 |        | Stiff Shell             |                 |        |
|-------------------------|------|-------------------------|-----------------|--------|-------------------------|-----------------|--------|
|                         |      | <u>Maximum Stresses</u> |                 | Static | <u>Maximum Stresses</u> |                 | Static |
|                         |      | Ref.<br>(1)             | Current<br>Work |        | Ref.<br>(1)             | Current<br>Work |        |
| $\sigma_{\theta\theta}$ | 0    | -4.79                   | -4.56           | -4.10  | -4.79                   | -4.08           | -3.67  |
| $\sigma_{\theta\theta}$ | 2    | 4.69                    | 4.11            | 3.67   | 3.42                    | 3.20            | 2.95   |
| $\sigma_{sb}$           | 0    | 0.043                   | 0.043           | 0.039  | 0.55                    | 4.08d           | 3.67d  |
| $\sigma_{sb}$           | 2    | 0.140                   | 0.137           | 0.122  | 1.70                    | 13.29d          | 11.89d |

#### 4.7 Conclusions

Conclusions drawn from the results of the analysis are:

(1) The method which has been presented is practical for effective computation of the dynamic response of a cylindrical shell embedded in an elastic medium when subjected to plane dilatational or shear waves. The solution presented herein is believed correct since it was checked by independent methods at short and long times.

(2) Peak stresses and displacements in both the medium and shell occur sometime after the transit of the incident wave across the cavity; of the problems solved, both the average and mean time at which the peak values occurred was equal to 3 transit times. The dynamic effect measured in terms of the ratio of the maximum stresses and displacements to the static values varied within a relatively small range. The average value of this ratio was 1.12 and the mean, 1.11. Thus, for the cases considered at least, the maximum stresses and displacements to be expected for a particular situation can be roughly approximated by determining the static values and by multiplying them by a factor of 1.1.

(3) The largest stresses in the shell occurred for a relatively thin liner in a medium with a low modulus of elasticity, low mass density, and low Poisson's ratio. The greatest reduction of the hoop stress in the medium as compared to the unlined cavity results from a relatively thick liner in a medium with low modulus of elasticity and high mass density. Additional mass within the shell has relatively small effect on the dynamic stresses.

(4) The practical value of tunnel linings to reduce the maximum stresses in the medium depends on the several conditions mentioned above, and on the magnitude of the incident stress wave. Under favorable conditions, reduction of stresses on the order of 30 percent or more is possible. However, for materials such as granite, smaller reductions can be expected for steel liners of practical size.

(5) Certain assumptions made concerning the behavior of the shell have limited the applicability of the analysis to relatively thin liners. Future studies of the behavior of thick shells would indicate the effect of the approximations used herein. The analysis has also been based on the assumption that the behavior of both the liner and medium is linearly elastic at all times. Perhaps a more desirable condition would be one in which some inelastic behavior is permitted to take place in the medium surrounding the shell or in the shell, or one in which some inelastic energy absorbing medium such as cinders or foamed plastic surrounds the shell. As a subject of future study, it is recommended that the behavior of thick shells, and thin shells surrounded by some energy absorbing layer, be considered.

## BIBLIOGRAPHY

1. Baron, M. L., and Parnes, R., Diffraction of a Pressure Wave by an Elastically Lined Cylindrical Cavity in an Elastic Medium, The Mitre Corporation, Bedford, Mass., December 1961.
2. Flugge, W., Stresses in Shells, Springer-Verlag, Germany, 1960, pp. 478.
3. Kolsky, H., Stress Waves in Solids, Oxford: Clarendon Press, 1953.
4. Lamb, H., Hydrodynamics, Dover Publications, New York, 1945, pp. 296-301, 503-505, 524-527.
5. Newmark, N. M., A Method of Computation for Structural Dynamics, Journal of the Engineering Mechanics Division, Proceedings of the American Society of Civil Engineers, Vol. 85, No. EM3, July 1959.
6. Paul, S. L., Interaction of Plane Elastic Waves With a Cylindrical Cavity, Ph.D. Dissertation, University of Illinois, 1963.
7. Robinson, A. R., Structural Effects of a Shock Wave Incident on a Cylindrical Shell, M.S. Thesis, University of Illinois, 1953.
8. Spiegel, M. R., Applied Differential Equations, Prentice-Hall, Inc., Englewood Cliffs, New Jersey, 1958, pp. 263-270.
9. Timoshenko, S., and Goodier, J. N., Theory of Elasticity, McGraw-Hill Book Company, Inc., New York, New York, 1951, pp. 58-80.

## APPENDIX A

## DERIVATION OF THE EXPRESSIONS INVOLVING THE POTENTIAL FUNCTIONS

A.1 General Form of the Potential Function

The dilatational potential function must satisfy the wave equation

$$\frac{\partial^2 \varphi}{\partial r^2} + \frac{1}{r} \frac{\partial \varphi}{\partial r} + \frac{1}{r^2} \frac{\partial^2 \varphi}{\partial \theta^2} = \frac{1}{c_1^2} \frac{\partial^2 \varphi}{\partial t^2} \quad (\text{A-1})$$

$\varphi$  in the case of the incoming dilatational wave is an even function of  $\theta$  and thus can be expressed as a cosine Fourier series

$$\varphi = \sum_{n=0}^{\infty} f_n(r, t) \cos n\theta \quad (\text{A-2})$$

where  $f_n$  is a function of  $r$  and  $t$  representing the modal coefficient of the potential function. By substitution of the above expression into equation (A-1) we obtain the equation that must be satisfied by  $f_n$ .

$$\frac{\partial^2 f_n}{\partial r^2} + \frac{1}{r} \frac{\partial f_n}{\partial r} - \frac{n^2}{r^2} f_n = \frac{1}{c_1^2} \frac{\partial^2 f_n}{\partial t^2} \quad (\text{A-3})$$

The general solution of  $f_n$  is assumed to be of the form

$$f_n = r^n R_n(r, t) \quad (\text{A-4})$$

Then  $R_n$  is some function of  $r$  and  $t$  satisfying

$$\frac{\partial^2 R_n}{\partial t^2} = c_1^2 \left[ \frac{\partial^2 R_n}{\partial r^2} + \frac{(2n+1)}{r} \frac{\partial R_n}{\partial r} \right] \quad (\text{A-5})$$

If  $R_n$  is a solution it can be shown that the corresponding equation for  $R_{n+1}$  is satisfied by

$$R_{n+1} = \frac{1}{r} \frac{\partial R_n}{\partial r} \quad (\text{A-6})$$

By repeated application of this result it can be shown that equation (A-5) is satisfied by

$$R_n = \left(\frac{1}{r} \frac{\partial}{\partial r}\right)^n R_0 \quad (\text{A-7})$$

where  $R_0$  is the solution of

$$\frac{\partial^2 R_0}{\partial t^2} = c_1^2 \left[ \frac{\partial^2 R_0}{\partial r^2} + \frac{1}{r} \frac{\partial R_0}{\partial r} \right] \quad (\text{A-8})$$

The solution to this equation for the case of a wave diverging from a center is

$$R_0 = \int_0^\infty F\left(t - \frac{r}{c_1} \cosh u_1\right) du_1 \quad (\text{A-9})$$

For the proof of this, see Lamb (4). Therefore, the coefficient  $f_n$  of the potential function is written as

$$f_n = r^n \left(\frac{1}{r} \frac{\partial}{\partial r}\right)^n \int_0^\infty F\left(t - \frac{r}{c_1} \cosh u_1\right) du_1 \quad (\text{A-10})$$

For modes 0, 1, and 2, this can be written

$$f_0 = \int_0^\infty F(\xi_1) du_1$$

$$f_1 = -\frac{1}{c_1} \int_0^\infty F'(\xi_1) \cosh u_1 du_1$$

$$f_2 = \frac{1}{c_1^2} \int_0^\infty F''(\xi_1) \cosh^2 u_1 du_1 + \frac{1}{rc_1} \int_0^\infty F'(\xi_1) \cosh u_1 du_1$$

where primes indicate the derivative of the function  $F$  with respect to its argument. Note that the expression for the  $n = 2$  mode contains derivatives of two different orders. It is convenient to express the function  $f_n$  in terms of derivatives of a single order which may be done through integration

by parts. For the  $n = 2$  mode we then wish to change the second integral to an integral involving the second derivative of the function  $F$ . Integrating by parts gives

$$\int_0^{u_{1m}} \xi d\eta = \xi \cdot \eta \Big|_0^{u_{1m}} - \int_0^{u_{1m}} \eta \cdot d\xi$$

where

$$\begin{aligned} \xi &= F'(\xi_1) & \eta &= \sinh u_1 \\ d\xi &= -\frac{r}{c_1} F''(\xi_1) \sinh u_1 du_1 & d\eta &= \cosh u_1 du_1 \end{aligned}$$

Thus

$$\int_0^\infty F'(\xi_1) \cosh u_1 du_1 = \frac{r}{c_1} \int_0^\infty F''(\xi_1) \sinh^2 u_1 du_1 + \left[ F'(\xi_1) \sinh u_1 \right]_0^{u_{1m}}$$

The second term can be shown to equal zero since for its lower limit  $\sinh u_1 = 0$ ; and for its upper limit,  $F'$  is the integral of the function  $F''$  at the wave front which under the assumed initial conditions, does not exist. Therefore, the coefficient of the potential function for the  $n = 2$  mode can be written as

$$f_2 = \frac{1}{c_1^2} \int_0^\infty F''\left(t - \frac{r}{c_1} \cosh u_1\right) \cosh 2u_1 du_1 \quad (\text{A-11})$$

By a similar process the coefficients of the potential function for any other mode can be reduced to the form

$$f_n = \frac{(-1)^n}{c_1^n} \int_0^\infty F^n\left(t - \frac{r}{c_1} \cosh u_1\right) \cosh nu_1 du_1 \quad (\text{A-12})$$

The shear potential function must satisfy the wave equation

$$\frac{\partial^2 \psi}{\partial r^2} + \frac{1}{r} \frac{\partial \psi}{\partial r} + \frac{1}{r^2} \frac{\partial^2 \psi}{\partial \theta^2} = \frac{1}{c_2^2} \frac{\partial^2 \psi}{\partial t^2} \quad (\text{A-13})$$

$\psi$  in the case of the incoming dilatational wave must be an odd function of  $\theta$  and can be represented as

$$\psi = \sum_{n=1}^{\infty} g_n(r,t) \sin n\theta$$

and proceeding exactly as in the case of the dilatational potential the general expression for the coefficient  $g_n$  is found to be

$$g_n = \frac{(-1)^n}{c_2^n} \int_0^{\infty} G^n\left(t - \frac{r}{c_2} \cosh u_2\right) \cosh nu_2 du_2 \quad (\text{A-14})$$

## A.2 Velocity Terms

The equations for the velocity components of a particle on the boundary due to the outgoing waves are

$$\begin{aligned} \dot{u} &= \frac{\partial^2 \varphi}{\partial r \partial t} + \frac{1}{r} \frac{\partial^2 \varphi}{\partial \theta \partial t} \\ \dot{v} &= \frac{1}{r} \frac{\partial^2 \varphi}{\partial \theta \partial t} - \frac{\partial^2 \psi}{\partial r \partial t} \end{aligned} \quad (\text{A-15})$$

The components of velocity and the potential functions are expanded in series as

$$\begin{aligned} \dot{u} &= \sum_{n=0}^{\infty} \dot{a}_n(r,t) \cos n\theta \\ \dot{v} &= \sum_{n=1}^{\infty} \dot{b}_n(r,t) \sin n\theta \\ \varphi &= \sum_{n=0}^{\infty} f_n(r,t) \cos n\theta \\ \psi &= \sum_{n=0}^{\infty} g_n(r,t) \sin n\theta \end{aligned} \quad (\text{A-16})$$

Substitution into equations (A-15) gives

$$\begin{aligned}\dot{a}_n(\text{out}) &= \frac{\partial^2 f_n}{\partial r \partial t} + \frac{n}{r} \frac{\partial g_n}{\partial t} \\ \dot{b}_n(\text{out}) &= -\frac{n}{r} \frac{\partial f_n}{\partial t} - \frac{\partial^2 g_n}{\partial r \partial t}\end{aligned}\tag{A-17}$$

The expressions for the coefficients  $f_n$  and  $g_n$  are given in equations (A-12) and (A-14). Using these in the above equations and by the application of integration by parts we get the following velocity terms

$$\begin{aligned}\dot{a}_n(\text{out}) &= -\frac{(-1)^n}{c_1^{n+1}} \int_0^\infty F^{n+2}(\xi_1) \cosh u_1 \cosh nu_1 du_1 \\ &\quad + \frac{(-1)^n}{c_2^{n+1}} \int_0^\infty G^{n+2}(\xi_2) \sinh u_2 \sinh nu_2 du_2 \\ \dot{b}_n(\text{out}) &= -\frac{(-1)^n}{c_1^{n+1}} \int_0^\infty F^{n+2}(\xi_1) \sinh u_1 \sinh nu_1 du_1 \\ &\quad + \frac{(-1)^n}{c_2^{n+1}} \int_0^\infty G^{n+2}(\xi_2) \cosh u_2 \cosh nu_2 du_2\end{aligned}\tag{A-18}$$

### A.3 Stress Terms

Stresses in the medium due to the outgoing waves are written in series form as

$$\begin{aligned}\sigma_{rr} &= \sum_{n=0}^{\infty} A_n(r,t) \cos n\theta \\ \sigma_{r\theta} &= \sum_{n=1}^{\infty} B_n(r,t) \sin n\theta \\ \sigma_{\theta\theta} &= \sum_{n=0}^{\infty} C_n(r,t) \cos n\theta\end{aligned}\tag{A-19}$$

By substitution into equations (2-10) the coefficients  $A_n$ ,  $B_n$ , and  $C_n$  are expressed in terms of the coefficients of the potential functions,  $f_n$  and  $g_n$

$$\begin{aligned}
 A_n(\text{out}) &= (\lambda + 2\mu) \left[ \frac{\partial^2 f_n}{\partial r^2} + \frac{n}{r} \frac{\partial g_n}{\partial r} - \frac{ng_n}{r^2} \right] \\
 &\quad + \frac{\lambda}{r} \left[ \frac{\partial f_n}{\partial r} + \frac{n}{r} g_n - \frac{n^2}{r} f_n - n \frac{\partial g_n}{\partial r} \right] \\
 B_n(\text{out}) &= \mu \left[ -\frac{2n}{r} \frac{\partial f_n}{\partial r} + \frac{2n}{r^2} f_n - \frac{\partial^2 g_n}{\partial r^2} - \frac{n^2}{r^2} g_n + \frac{1}{r} \frac{\partial g_n}{\partial r} \right] \\
 C_n(\text{out}) &= \frac{\lambda+2\mu}{r} \left[ \frac{\partial f_n}{\partial r} + \frac{n}{r} g_n - \frac{n^2}{r} f_n - n \frac{\partial g_n}{\partial r} \right] \\
 &\quad + \lambda \left[ \frac{\partial^2 f_n}{\partial r^2} + \frac{n}{r} \frac{\partial g_n}{\partial r} - \frac{ng_n}{r^2} \right]
 \end{aligned} \tag{A-20}$$

Again, using the equations for  $f_n$  and  $g_n$  given earlier we can write the above coefficients finally as

$$\begin{aligned}
 A_n(\text{out}) &= \frac{(-1)^n \mu}{c_1^{n+2}} \int_0^\infty F^{n+2}(\xi_1) \cosh nu_1 \left[ \frac{\lambda}{\mu} + 2 \cosh^2 u_1 \right] du_1 \\
 &\quad - \frac{(-1)^n \mu}{c_2^{n+2}} \int_0^\infty G^{n+2}(\xi_2) \sinh 2u_2 \sinh nu_2 du_2 \\
 B_n(\text{out}) &= \frac{(-1)^n \mu}{c_1^{n+2}} \int_0^\infty F^{n+2}(\xi_1) \sinh 2u_1 \sinh nu_1 du_1 \\
 &\quad - \frac{(-1)^n \mu}{c_2^{n+2}} \int_0^\infty G^{n+2}(\xi_2) \cosh nu_2 \cosh 2u_2 du_2 \\
 C_n(\text{out}) &= \frac{(-1)^n \mu}{c_1^{n+2}} \int_0^\infty F^{n+2}(\xi_1) \cosh nu_1 \left[ \frac{\lambda}{\mu} - 2 \sinh^2 u_1 \right] du_1 \\
 &\quad + \frac{(-1)^n \mu}{c_2^{n+2}} \int_0^\infty G^{n+2}(\xi_2) \sinh 2u_2 \sinh nu_2 du_2
 \end{aligned} \tag{A-21}$$

APPENDIX B  
STATIC SOLUTION

B.1 Dilatational Wave

The static solution presented here is based on the application of the theory of stress functions presented by Timoshenko (9). Under static conditions, it can be assumed that at large distances from the boundary of the cavity the state of stress in the medium is equal to the stress field in the medium behind the front. In polar coordinates this is

$$\begin{aligned}\sigma_{rr} &= - \left(\frac{1+\bar{\nu}}{2}\right) \sigma_p - \left(\frac{1-\bar{\nu}}{2}\right) \sigma_p \cos 2\theta \\ \sigma_{r\theta} &= \left(\frac{1-\bar{\nu}}{2}\right) \sigma_p \sin 2\theta \\ \sigma_{\theta\theta} &= \left(\frac{1+\bar{\nu}}{2}\right) \sigma_p + \left(\frac{1-\bar{\nu}}{2}\right) \sigma_p \cos 2\theta\end{aligned}\tag{B-1}$$

$\sigma_p$  is the stress in the medium in the direction of wave propagation and  $\bar{\nu}\sigma_p$  is the stress parallel to the wave front.  $\bar{\nu}$ , derived from the assumption that there is no strain parallel to the wave front, is equal to

$$\bar{\nu} = \frac{\nu}{1-\nu}\tag{B-2}$$

It can be seen from equations (B-1) that the  $n = 0$  and  $2$  modes describe exactly the free field stresses. Therefore, the unknown stresses at the edge of the cavity can likewise be expressed in terms of these modes

$$\begin{aligned}\sigma_{rr} &= - P_0 - P_2 \cos 2\theta \\ \sigma_{r\theta} &= S_2 \sin 2\theta\end{aligned}\tag{B-3}$$

where  $P_0$ ,  $P_2$ , and  $S_2$  are the unknown modal components of stress acting at the boundary. These same stresses must act on the shell. Thus the boundary stresses in the medium and shell can be illustrated as shown in Fig. 9.

The equations of equilibrium in the medium under plane strain conditions are satisfied by the following expressions for the components of stress

$$\begin{aligned}\sigma_{rr} &= \frac{1}{r} \frac{\partial \Omega}{\partial r} + \frac{1}{r^2} \frac{\partial^2 \Omega}{\partial \theta^2} \\ \sigma_{r\theta} &= \frac{1}{r^2} \frac{\partial \Omega}{\partial \theta} - \frac{1}{r} \frac{\partial^2 \Omega}{\partial r \partial \theta} \\ \sigma_{\theta\theta} &= \frac{\partial^2 \Omega}{\partial r^2}\end{aligned}\tag{B-4}$$

where  $\Omega$  is the stress function in terms of  $r$  and  $\theta$ .

#### B.11 n = 0 Mode

The general solution of the stress function for the  $n = 0$  mode is given by Timoshenko as

$$\Omega = K \log r + Mr^2$$

from which can be derived the stress components

$$\begin{aligned}\sigma_{rr} &= \frac{k}{r^2} + 2M \\ \sigma_{r\theta} &= 0 \\ \sigma_{\theta\theta} &= -\frac{k}{r^2} + 2M\end{aligned}\tag{B-5}$$

The coefficients  $K$  and  $M$  are determined from the states of stress at  $r \rightarrow \infty$  and  $r = R$

$$\begin{aligned}K &= R^2 \left[ \left( \frac{1+\bar{\nu}}{2} \right) \sigma_p - P_o \right] \\ M &= - \left( \frac{1+\bar{\nu}}{4} \right) \sigma_p\end{aligned}\tag{B-6}$$

For the conditions of plane strain, the strains are

$$\begin{aligned}\epsilon_r &= \frac{1}{\bar{E}} \left[ \sigma_{rr} - \bar{\nu} \sigma_{\theta\theta} \right] \\ \epsilon_\theta &= \frac{1}{\bar{E}} \left[ \sigma_{\theta\theta} - \bar{\nu} \sigma_{rr} \right] \\ \gamma_{r\theta} &= \frac{1}{\mu} \sigma_{r\theta}\end{aligned}\tag{B-7}$$

where

$$\bar{E} = \frac{E}{1 - \nu^2} \quad \text{modulus of plane strain for the medium}$$

Displacement components are found by suitable integration of the following equations for the strains in the medium

$$\begin{aligned}\epsilon_r &= \frac{\partial u}{\partial r} \\ \epsilon_\theta &= \frac{u}{r} + \frac{1}{r} \frac{\partial v}{\partial \theta} \\ \gamma_{r\theta} &= \frac{1}{r} \frac{\partial u}{\partial \theta} + \frac{\partial v}{\partial r} - \frac{v}{r}\end{aligned}\tag{B-8}$$

Displacements in the medium for the zero mode are

$$\begin{aligned}\frac{u}{R} &= \frac{(1+\bar{\nu})}{\bar{E}} \left[ -\sigma_p + p_0 \right] \\ \frac{v}{R} &= 0\end{aligned}\tag{B-9}$$

The corresponding displacement components of the shell with an exterior compressive force  $P_0$  are found in Flugge (2) to be

$$\begin{aligned}\frac{u_s}{R} &= -\frac{P_0 R}{E_s A} \\ \frac{v_s}{R} &= 0\end{aligned}\tag{B-10}$$

where

$$\bar{E}_s = \frac{E_s}{1 - \nu_s^2} \quad \text{modulus of plane strain for the shell}$$

The unknown stress  $P_0$  is now determined by equating the radial displacement components, to get

$$P_0 = \frac{(1+\bar{\nu}) \sigma_p}{\left[ \frac{\bar{E}}{\bar{E}_s} \cdot \frac{R}{A} + 1 + \bar{\nu} \right]} \quad (\text{B-11})$$

After  $P_0$  is determined, stresses in the medium at any radius can be found using equations (B-5). Equation (B-10) gives the displacement of the shell; and the hoop and bending stresses of the shell are, respectively

$$\sigma_{\theta\theta} = \frac{P_0 R}{A} \quad (\text{B-12})$$

$$\frac{\sigma_{sB}}{|\sigma_p|} = \frac{u_s t}{2 R}$$

#### B.12 n = 2 Mode

The general solution in terms of a stress function  $\Omega$  is given as

$$\Omega = \left[ kr^2 + \frac{M}{r^2} + N \right] \cos 2\theta$$

from which the stress components in the medium become

$$\sigma_{rr} = - \left[ 2K + \frac{6M}{r^4} + \frac{4N}{r^2} \right] \cos 2\theta$$

$$\sigma_{\theta\theta} = \left[ 2K + \frac{6M}{r^4} \right] \cos 2\theta \quad (\text{B-13})$$

$$\sigma_{r\theta} = \left[ 2K - \frac{6M}{r^4} - \frac{2N}{r^2} \right] \sin 2\theta$$

Coefficients are determined as before from the states of stress at  $r \rightarrow \infty$

and  $r = R$

$$K = \left( \frac{1-\bar{\nu}}{4} \right) \sigma_p \quad (\text{B-14})$$

$$M = \frac{R^4}{6} \left[ \frac{3(1-\bar{\nu})}{2} \sigma_p - P_2 - 2S_2 \right]$$

$$N = \frac{R^2}{2} \left[ -(1-\bar{\nu}) \sigma_p + P_2 + S_2 \right]$$

The displacement components of the medium at the boundary can be expressed as

$$\frac{u}{R} = \frac{1}{E} \left[ 2(\bar{\nu}-1) + \frac{(5-\bar{\nu})}{3} P_2 + \frac{2(2-\bar{\nu})S_2}{3} \right] \cos 2\theta$$

$$\frac{v}{R} = \frac{1}{E} \left[ 2(1-\bar{\nu}) - \frac{2(2-\bar{\nu})}{3} P_2 - \frac{(5-\bar{\nu})}{3} S_2 \right] \sin 2\theta$$
(B-15)

and the corresponding components for the shell are

$$\frac{u_s}{R} = \left[ -\frac{P_2}{E_s} \frac{R^3}{9I} - \frac{S_2}{E_s} \frac{R^3}{6A} \right] \cos 2\theta$$

$$\frac{v_s}{R} = \left[ \frac{P_2}{E_s} \left( \frac{R^3}{18I} + \frac{R}{6A} \right) + \frac{S_2}{E_s} \left( \frac{R^3}{36I} + \frac{R}{3A} \right) \right] \sin 2\theta$$
(B-16)

The unknown boundary stresses  $P_2$  and  $S_2$  are determined by equating the displacement of the shell and medium at the boundary. The hoop and bending stresses in the shell are then found from the following equations

$$\sigma_{\theta\theta} = \left( \frac{P_2 R}{3A} + \frac{2S_2 R}{3A} \right) \cos 2\theta$$

$$\sigma_{SB} = \frac{tR^3}{12I} (2P_2 + S_2) \cos 2\theta$$
(B-17)

Displacements of the shell and stresses in the medium can be determined using equations given earlier in the discussion. Total static stresses and displacements are merely the sum of the modal values for any angle.

## B.2 Shear Wave

The free field shear wave stresses expressed in polar coordinates include only the  $n = 2$  mode

$$\begin{aligned}\sigma_{rr} &= \sigma_s \sin 2\theta \\ \sigma_{r\theta} &= \sigma_s \cos 2\theta \\ \sigma_{\theta\theta} &= -\sigma_s \sin 2\theta\end{aligned}\tag{B-18}$$

where  $\sigma_s$  is the amplitude of the incoming wave. The static solution is obtained exactly as in the case of the dilatational wave except for the interchange of sines and cosines resulting from the difference in geometry.

The resulting equations are

### a. Displacement components

$$\frac{u_s}{R} = \left[ \frac{P_2 R^3}{1.9 E_s I} + \frac{S_2 R^3}{18 E_s I} \right] \sin 2\theta\tag{B-19}$$

$$\frac{v_s}{R} = \left[ \frac{P_2}{6E_s} \left( \frac{R^3}{3I} + \frac{R}{A} \right) + \frac{S_2}{3E_s} \left( \frac{R^3}{12I} + \frac{R}{A} \right) \right] \cos 2\theta$$

### b. Shell Stresses

$$\begin{aligned}\sigma_{\theta\theta} &= - \left[ \frac{P_2 R}{3A} + \frac{2S_2 R}{3A} \right] \sin 2\theta \\ \sigma_{sB} &= - \frac{tR^3}{12I} (2P_2 + S_2) \sin 2\theta\end{aligned}\tag{B-20}$$

### c. Medium Stresses

$$\begin{aligned}\sigma_{rr} &= - \left( 2A + \frac{6C}{r^4} + \frac{4D}{r^2} \right) \sin 2\theta \\ \sigma_{r\theta} &= - \left( 2A - \frac{6C}{r^4} - \frac{2D}{r^2} \right) \cos 2\theta \\ \sigma_{\theta\theta} &= \left( 2A + \frac{6C}{r^4} \right) \sin 2\theta\end{aligned}\tag{B-21}$$

where

$$A = -\frac{\sigma_s}{2}$$

$$C = \frac{R^4}{6} \left[ -3\sigma_s + P_2 + 2S_2 \right]$$

$$D = \frac{R^2}{2} \left[ 2\sigma_s - P_2 - S_2 \right]$$

In the machine program, the  $n = 0$  mode is purely rotational and thus we get a static value of tangential displacement. This is calculated as follows

$$\theta_{\text{rot}} = \frac{1}{2} \gamma_{xy} = \frac{1}{2} \frac{\sigma_s}{\mu}$$

(B-22)

$$\frac{v}{R} = \theta_{\text{rot}} = \frac{1}{2} \frac{\sigma_s}{\mu}$$

## DILATATIONAL WAVE

time = 20 R/c<sub>1</sub>

| Mode | Quant.*                  | Stat. | Mach. | Dev. From Static | Mode | Quant                   | Stat. | Mach. | Dev. From Static |
|------|--------------------------|-------|-------|------------------|------|-------------------------|-------|-------|------------------|
| 0    | - $\alpha$               | 4.000 | 4.006 | .15%             | 2    | - $\alpha$              | 4.613 | 4.599 | .30%             |
| 0    | $-\sigma_{\theta\theta}$ | 4.000 | 4.006 | .15              | 2    | $\beta$                 | 3.845 | 3.856 | .29              |
| 0    | $\sigma_{\theta\theta}$  | .100  | .100  | .00              | 2    | $\sigma_{\theta\theta}$ | 3.077 | 3.114 | 1.20             |
|      |                          |       |       |                  | 2    | $\sigma_{\theta\theta}$ | .346  | .345  | .29              |

\* Stresses given in units of  $|\sigma_p|$   
 Displacements defined by Eqs. (2-50) and (2-36)

## SHEAR WAVE

time = 20 R/c<sub>2</sub>

| Mode | Quant.                   | Stat.  | Mach.  | Dev. From Static |
|------|--------------------------|--------|--------|------------------|
| 0    | $\beta$                  | 5.000  | 4.996  | .08%             |
| 2    | $\alpha$                 | 13.840 | 13.930 | .65              |
| 2    | $\beta$                  | 11.535 | 11.539 | .03              |
| 2    | $-\sigma_{\theta\theta}$ | 9.232  | 9.149  | .90              |
| 2    | $\sigma_{\theta\theta}$  | 1.038  | 1.045  | .67              |

TABLE 1

COMPARISON OF STATIC AND MACHINE VALUES FOR MODAL RESPONSE OF THE SHELL

DILATATIONAL WAVE

time = 20 R/c<sub>1</sub>

| Mode | Quant.*                   | 1.0 R |       | 2.0 R |       | 3.0 R |       | 4.0 R |       |
|------|---------------------------|-------|-------|-------|-------|-------|-------|-------|-------|
|      |                           | Stat. | Mach. | Stat. | Mach. | Stat. | Mach. | Stat. | Mach. |
| 0    | - $\sigma_{rr}$           | .200  | .200  | .550  | .551  | .615  | .616  | .638  | .639  |
| 0    | - $\sigma_{\theta\theta}$ | 1.133 | 1.135 | .783  | .785  | .718  | .720  | .696  | .697  |
| 2    | - $\sigma_{rr}$           | -.153 | -.155 | .111  | .112  | .226  | .229  | .271  | .273  |
| 2    | $\sigma_{r\theta}$        | .307  | .312  | .428  | .429  | .384  | .386  | .363  | .366  |
| 2    | $\sigma_{\theta\theta}$   | .872  | .868  | .367  | .368  | .340  | .342  | .335  | .337  |

\* Stresses given in units of  $(\sigma_r)$

SHEAR WAVE

time = 20 R/c<sub>2</sub>

| Mode | Quant.                    | 1.0 R |       | 2.0 R |       | 3.0 R |       | 4.0 R |       |
|------|---------------------------|-------|-------|-------|-------|-------|-------|-------|-------|
|      |                           | Stat. | Mach. | Stat. | Mach. | Stat. | Mach. | Stat. | Mach. |
| 2    | $\sigma_{rr}$             | -.460 | -.455 | .332  | .331  | .675  | .678  | .814  | .815  |
| 2    | $\sigma_{r\theta}$        | .921  | .913  | 1.283 | 1.286 | 1.151 | 1.154 | 1.090 | 1.092 |
| 2    | - $\sigma_{\theta\theta}$ | 2.616 | 2.636 | 1.101 | 1.104 | 1.020 | 1.022 | 1.006 | 1.009 |

TABLE 2

COMPARISON OF STATIC AND MACHINE VALUES FOR MODAL STRESSES IN THE MEDIUM

| $\eta_t$ | $\sigma_{00_s}(90^\circ)$ |        | DLP* | $t_m^\#$ | $\sigma_{00_m}(90^\circ)$ |       | DLP  | $t_m$ |
|----------|---------------------------|--------|------|----------|---------------------------|-------|------|-------|
|          | Static                    | Max.   |      |          | Static                    | Max.  |      |       |
| .01      | -9.21                     | -10.12 | 1.10 | 3.12     | -2.49                     | -2.73 | 1.09 | 3.13  |
| .05      | -7.08                     | -7.74  | 1.09 | 2.88     | -2.01                     | -2.19 | 1.09 | 2.88  |
| .10      | -5.56                     | -6.15  | 1.10 | 2.25     | -1.67                     | -1.84 | 1.11 | 2.25  |
| .15      | -4.60                     | -5.21  | 1.13 | 2.25     | -1.45                     | -1.65 | 1.13 | 2.25  |
| .20      | -3.94                     | -4.52  | 1.14 | 2.25     | -1.30                     | -1.50 | 1.15 | 2.25  |

| $\eta_t$ | $\sigma_{00_b}(90^\circ)$ |      | DLP  | $t_m$ | $\sigma_{00_m}(90^\circ)$ |      | DLP  | $t_m$ |
|----------|---------------------------|------|------|-------|---------------------------|------|------|-------|
|          | Static                    | Max. |      |       | Static                    | Max. |      |       |
| .01      | .10                       | .11  | 1.11 | 3.38  | -.09                      | -.10 | 1.10 | 3.25  |
| .05      | .45                       | .50  | 1.11 | 3.25  | -.35                      | -.39 | 1.11 | 2.88  |
| .10      | .83                       | .94  | 1.13 | 3.00  | -.55                      | -.63 | 1.14 | 2.50  |
| .15      | 1.18                      | 1.36 | 1.15 | 2.88  | -.68                      | -.79 | 1.17 | 2.50  |
| .20      | 1.50                      | 1.76 | 1.18 | 2.88  | -.75                      | -.91 | 1.21 | 2.50  |

| $\eta_t$ | $\alpha(0^\circ)$ |        | DLP  | $t_m$ | $\beta(45^\circ)$ |      | DLP  | $t_m$ |
|----------|-------------------|--------|------|-------|-------------------|------|------|-------|
|          | Static            | Max.   |      |       | Static            | Max. |      |       |
| .01      | -9.65             | -10.64 | 1.10 | 3.12  | 4.67              | 5.23 | 1.12 | 3.75  |
| .05      | -8.61             | -9.50  | 1.10 | 3.00  | 3.85              | 4.33 | 1.13 | 3.50  |
| .10      | -7.76             | -8.62  | 1.11 | 2.76  | 3.33              | 3.82 | 1.15 | 3.25  |
| .15      | -7.15             | -8.01  | 1.12 | 2.88  | 3.02              | 3.55 | 1.18 | 3.25  |
| .20      | -6.66             | -7.56  | 1.13 | 2.88  | 2.80              | 3.37 | 1.20 | 3.38  |

\* Ratio of Max. to Static # Time in transit times at which Max. occurs

TABLE 3

EFFECT OF RELATIVE THICKNESS OF SHE.

| $\eta_E$ | $\sigma_{90s}(90^\circ)$ |        | DLP* | $t_m^\dagger$ | $\sigma_{90m}(90^\circ)$ |       | DLP  | $t_m$ |
|----------|--------------------------|--------|------|---------------|--------------------------|-------|------|-------|
|          | Static                   | Max.   |      |               | Static                   | Max.  |      |       |
| 2        | -4.16                    | -4.57  | 1.10 | 2.76          | -2.27                    | -2.51 | 1.11 | 2.76  |
| 4        | -7.08                    | -7.74  | 1.09 | 2.88          | -2.01                    | -2.19 | 1.09 | 2.88  |
| 6        | -9.33                    | -10.11 | 1.08 | 2.76          | -1.81                    | -1.97 | 1.08 | 2.76  |
| 10       | -12.57                   | -13.41 | 1.07 | 2.76          | -1.55                    | -1.65 | 1.07 | 2.76  |
| 16       | -15.72                   | -16.47 | 1.05 | 2.88          | -1.31                    | -1.37 | 1.05 | 2.76  |

| $\eta_E$ | $\sigma_{sb}(90^\circ)$ |      | DLP  | $t_m$ | $\sigma_{vsm}(90^\circ)$ |      | DLP  | $t_m$ |
|----------|-------------------------|------|------|-------|--------------------------|------|------|-------|
|          | Static                  | Max. |      |       | Static                   | Max. |      |       |
| 2        | .23                     | .26  | 1.12 | 3.25  | -.21                     | -.23 | 1.13 | 3.12  |
| 4        | .45                     | .50  | 1.11 | 3.25  | -.35                     | -.39 | 1.11 | 2.88  |
| 6        | .64                     | .71  | 1.11 | 3.12  | -.47                     | -.51 | 1.10 | 2.76  |
| 10       | 1.01                    | 1.12 | 1.10 | 3.12  | -.63                     | -.68 | 1.08 | 2.62  |
| 16       | 1.53                    | 1.68 | 1.09 | 3.12  | -.78                     | -.83 | 1.06 | 2.62  |

| $\eta_E$ | $\alpha(0^\circ)$ |        | DLP  | $t_m$ | $\beta(45^\circ)$ |       | DLP  | $t_m$ |
|----------|-------------------|--------|------|-------|-------------------|-------|------|-------|
|          | Static            | Max.   |      |       | Static            | Max.  |      |       |
| 2        | -4.60             | -5.12  | 1.11 | 3.00  | 2.14              | 2.43  | 1.13 | 3.62  |
| 4        | -8.61             | -9.50  | 1.10 | 3.00  | 3.85              | 4.33  | 1.13 | 3.50  |
| 6        | -12.22            | -13.37 | 1.09 | 2.88  | 5.32              | 5.96  | 1.12 | 3.38  |
| 10       | -18.65            | -20.20 | 1.08 | 2.88  | 7.92              | 8.82  | 1.11 | 3.25  |
| 16       | -27.11            | -29.15 | 1.08 | 3.00  | 11.41             | 12.64 | 1.11 | 3.12  |

\*Ratio of Max. to Static

†Time in transit times at which Max. occurs

TABLE 4

EFFECT OF RATIO OF MODULI OF ELASTICITY

| $\eta\rho$ | $\sigma_{\theta\theta} (90^\circ)$ |       | DLF <sup>a</sup> | $t_m^{\dagger}$ | $\sigma_{\theta\theta m} (90^\circ)$ |       | DLF  | $t_m$ |
|------------|------------------------------------|-------|------------------|-----------------|--------------------------------------|-------|------|-------|
|            | Static                             | Max.  |                  |                 | Static                               | Max.  |      |       |
| 1          | -7.08                              | -7.67 | 1.08             | 3.00            | -2.01                                | -2.17 | 1.08 | 2.88  |
| 3          | "                                  | -7.74 | 1.09             | 2.88            | "                                    | -2.19 | 1.09 | 2.88  |
| 5          | "                                  | -7.97 | 1.13             | 2.50            | "                                    | -2.26 | 1.12 | 2.50  |
| 7          | "                                  | -8.30 | 1.17             | 2.61            | "                                    | -2.34 | 1.17 | 2.62  |
| 10         | "                                  | -8.70 | 1.23             | 2.88            | "                                    | -2.45 | 1.22 | 2.88  |

| $\eta\rho$ | $\sigma_{\theta\theta} (90^\circ)$ |      | DLF  | $t_m$ | $\sigma_{\theta\theta m} (90^\circ)$ |      | DLF  | $t_m$ |
|------------|------------------------------------|------|------|-------|--------------------------------------|------|------|-------|
|            | Static                             | Max. |      |       | Static                               | Max. |      |       |
| 1          | .45                                | .49  | 1.10 | 3.25  | -.35                                 | -.38 | 1.09 | 3.00  |
| 3          | "                                  | .50  | 1.11 | 3.25  | "                                    | -.39 | 1.11 | 2.88  |
| 5          | "                                  | .50  | 1.13 | 3.12  | "                                    | -.41 | 1.15 | 2.88  |
| 7          | "                                  | .51  | 1.15 | 3.25  | "                                    | -.43 | 1.21 | 3.12  |
| 10         | "                                  | .53  | 1.18 | 3.50  | "                                    | -.46 | 1.30 | 3.50  |

| $\eta\rho$ | $\alpha (0^\circ)$ |       | DLF  | $t_m$ | $\beta (45^\circ)$ |      | DLF  | $t_m$ |
|------------|--------------------|-------|------|-------|--------------------|------|------|-------|
|            | Static             | Max.  |      |       | Static             | Max. |      |       |
| 1          | -8.61              | -9.38 | 1.09 | 3.00  | 3.85               | 4.27 | 1.11 | 3.50  |
| 3          | "                  | -9.50 | 1.10 | 3.00  | "                  | 4.33 | 1.13 | 3.50  |
| 5          | "                  | -9.64 | 1.12 | 2.88  | "                  | 4.41 | 1.15 | 3.62  |
| 7          | "                  | -9.77 | 1.14 | 3.00  | "                  | 4.45 | 1.16 | 2.76  |
| 10         | "                  | -9.95 | 1.16 | 2.62  | "                  | 4.72 | 1.23 | 3.00  |

<sup>a</sup>Ratio of Max. to Static

<sup>†</sup>Time in transit times at which Max. occurs

TABLE 5  
EFFECT OF MASS RATIO

| $\nu$ | $\sigma_{\theta\theta_s}(90^\circ)$ |        | DLP* | $t_m^\dagger$ | $\sigma_{\theta\theta_m}(90^\circ)$ |       | DLP  | $t_m$ |
|-------|-------------------------------------|--------|------|---------------|-------------------------------------|-------|------|-------|
|       | Static                              | Max.   |      |               | Static                              | Max.  |      |       |
| 0     | - 8.33                              | - 9.17 | 1.10 | 3.25          | -2.08                               | -2.29 | 1.10 | 3.25  |
| .1    | - 7.96                              | - 8.69 | 1.09 | 3.12          | -2.06                               | -2.24 | 1.09 | 3.12  |
| .2    | - 7.42                              | - 8.08 | 1.09 | 3.00          | -2.02                               | -2.20 | 1.09 | 3.00  |
| .25   | - 7.08                              | - 7.74 | 1.09 | 2.88          | -2.01                               | -2.19 | 1.09 | 2.88  |
| .4    | - 5.76                              | - 6.75 | 1.17 | 3.12          | -1.91                               | -2.22 | 1.16 | 3.25  |

| $\nu$ | $\sigma_{\theta\theta_b}(90^\circ)$ |      | DLP  | $t_m$ | $\sigma_{\nu\nu_m}(90^\circ)$ |       | DLP  | $t_m$ |
|-------|-------------------------------------|------|------|-------|-------------------------------|-------|------|-------|
|       | Static                              | Max. |      |       | Static                        | Max.  |      |       |
| 0     | .61                                 | .69  | 1.14 | 3.25  | - .42                         | - .47 | 1.13 | 3.00  |
| .1    | .56                                 | .63  | 1.13 | 3.25  | - .40                         | - .44 | 1.12 | 2.88  |
| .2    | .49                                 | .55  | 1.12 | 3.25  | - .37                         | - .41 | 1.11 | 2.88  |
| .25   | .45                                 | .50  | 1.11 | 3.25  | - .35                         | - .39 | 1.11 | 2.88  |
| .4    | .27                                 | .31  | 1.14 | 3.75  | - .29                         | - .33 | 1.15 | 3.88  |

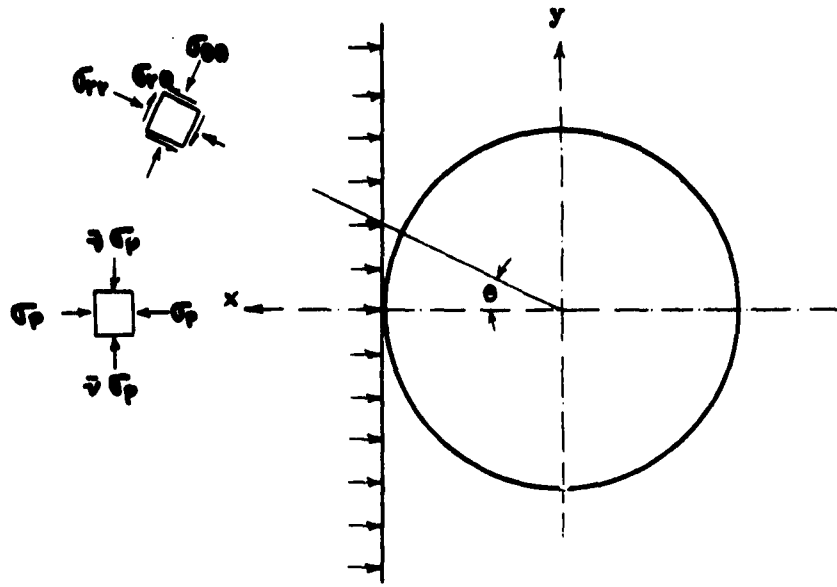
| $\nu$ | $\alpha(0^\circ)$ |        | DLP  | $t_m$ | $\beta(45^\circ)$ |      | DLP  | $t_m$ |
|-------|-------------------|--------|------|-------|-------------------|------|------|-------|
|       | Static            | Max.   |      |       | Static            | Max. |      |       |
| 0     | -10.33            | -11.48 | 1.11 | 3.25  | 6.00              | 6.94 | 1.16 | 3.38  |
| .1    | - 9.88            | -10.90 | 1.10 | 3.12  | 5.31              | 6.08 | 1.14 | 3.38  |
| .2    | - 9.12            | -10.03 | 1.10 | 3.00  | 4.40              | 4.98 | 1.13 | 3.38  |
| .25   | - 8.61            | - 9.50 | 1.10 | 3.00  | 3.85              | 4.33 | 1.13 | 3.50  |
| .4    | - 6.54            | - 7.61 | 1.16 | 3.50  | 1.77              | 1.97 | 1.11 | 4.38  |

\*Ratio of Max. to Static

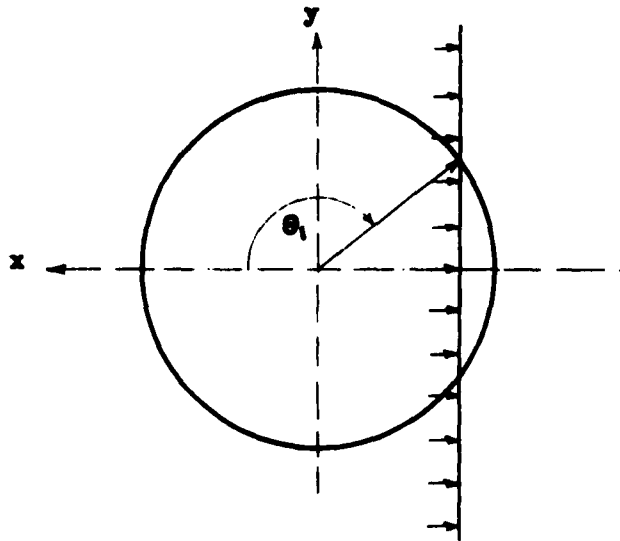
†Time in transit times at which Max. occurs

TABLE 6

EFFECT OF POISSON'S RATIO

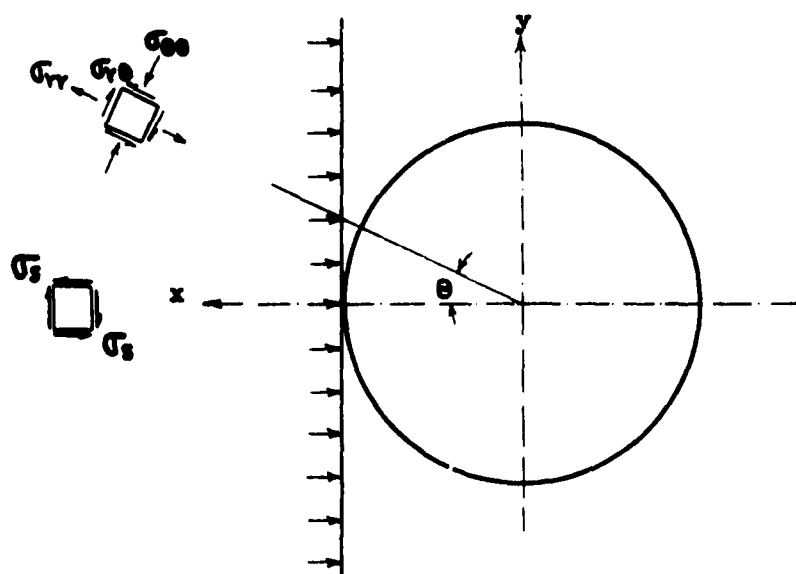


Plane Dilatational Wave Front at time  $t = 0$   
 Stresses Behind Wave Front Shown in Both Rectangular  
 and Polar Coordinates

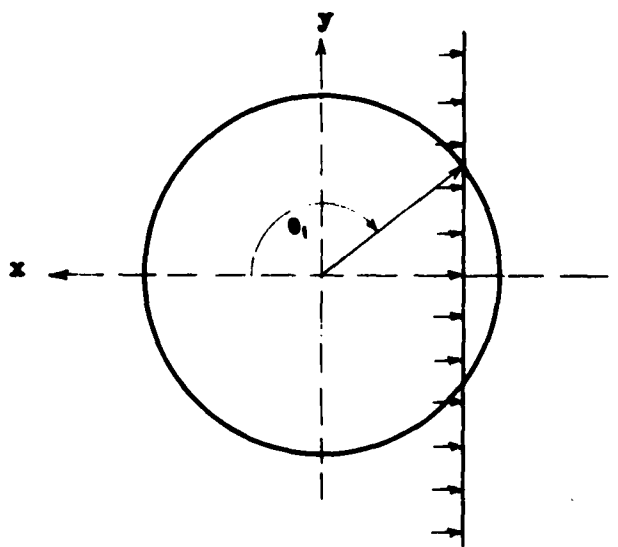


Plane Dilatational Wave Front at time  $t > 0$

FIGURE 1



Plane Shear Wave Front at time  $t = 0$   
 Stresses Behind Wave Front Shown in Both Rectangular  
 and Polar Coordinates



Plane Shear Wave Front at time  $t > 0$

FIGURE 2

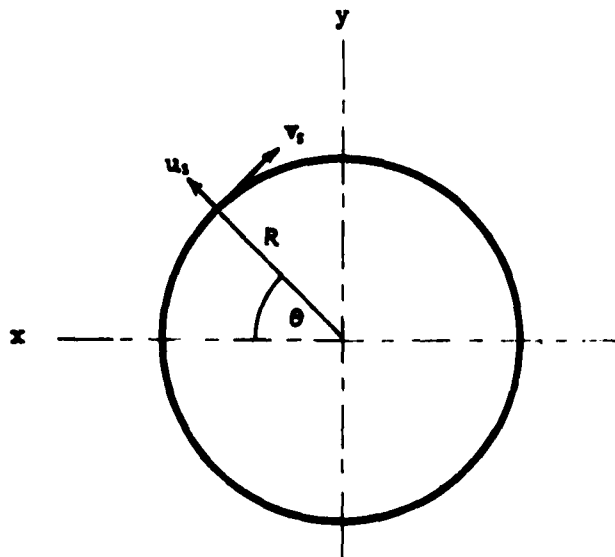


FIG. 3 DISPLACEMENT COMPONENTS OF THE SHELL

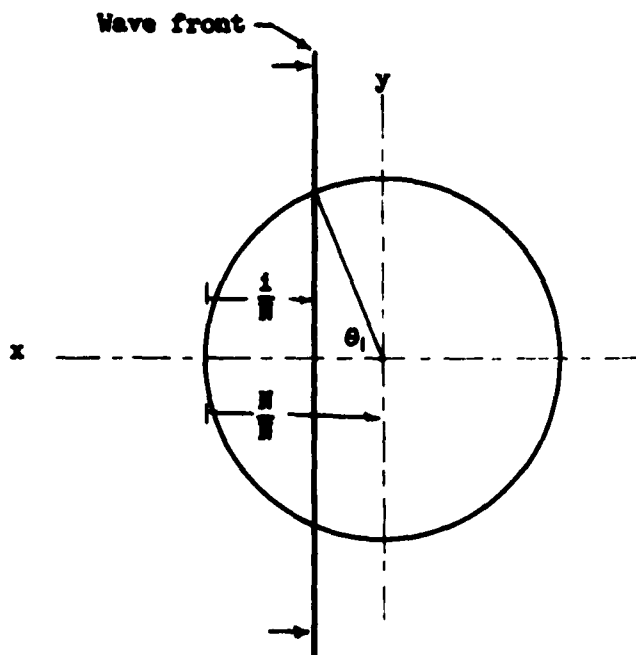


FIG. 4 DEFINITION OF POSITION ANGLE,  $\theta_1$

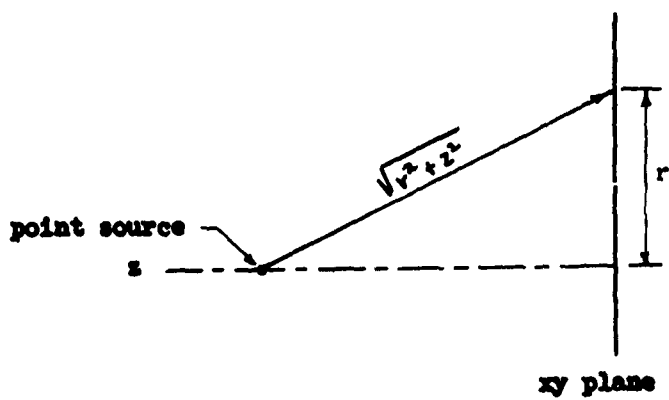


FIG. 5 GEOMETRY OF A POINT SOURCE ON THE z AXIS

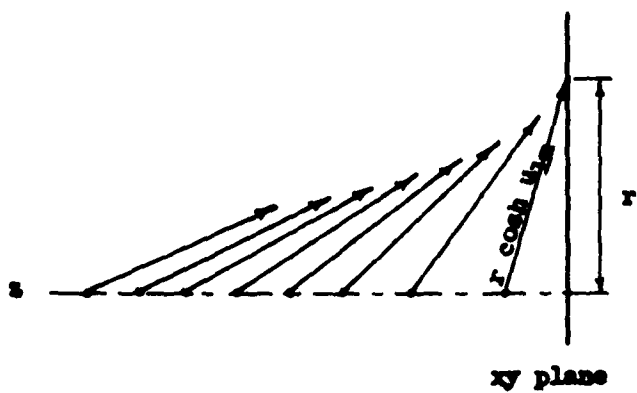


FIG. 6 GEOMETRY OF MANY POINT SOURCES

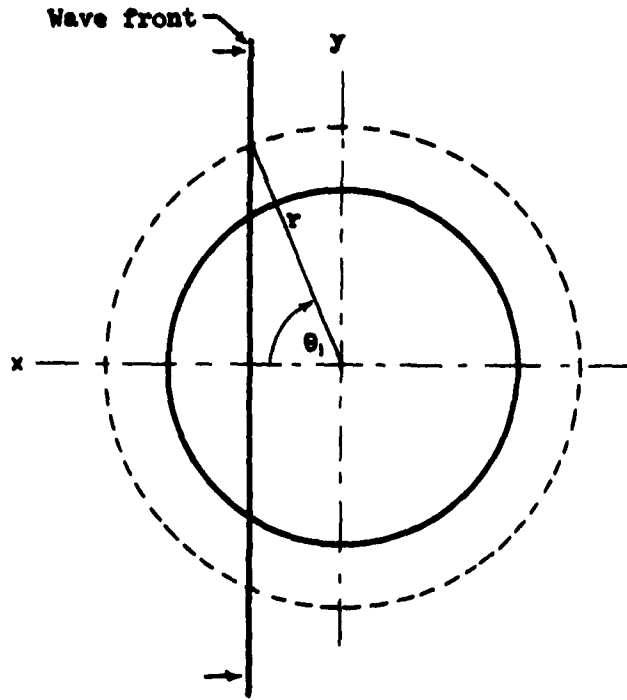


FIG. 7 POSITION ANGLE,  $\theta_1$ , FOR ANY RADIUS

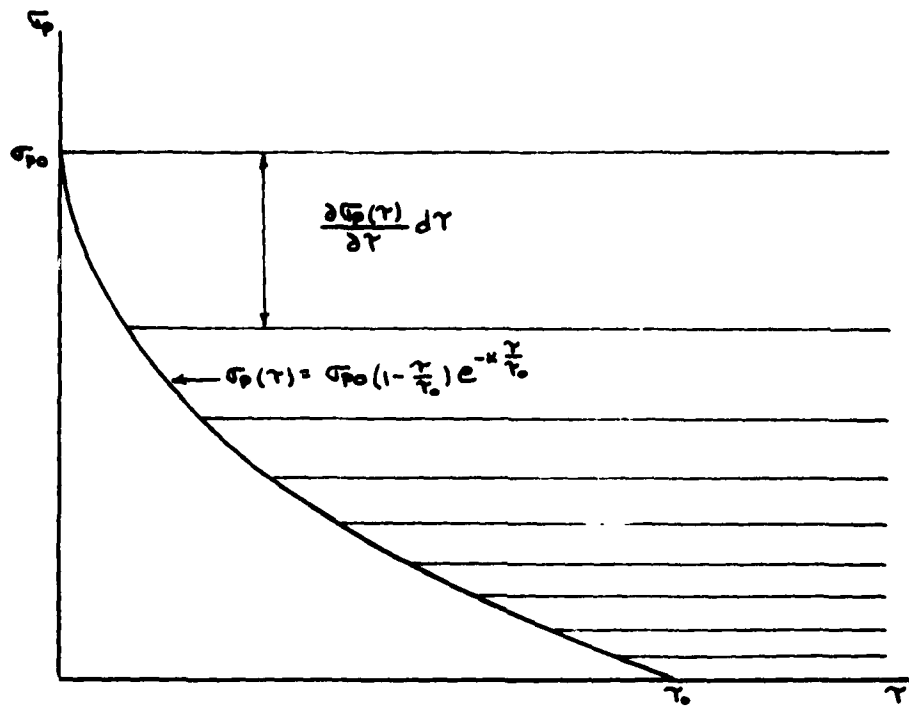


FIG. 8 TIME DEPENDENT STRESS WAVE

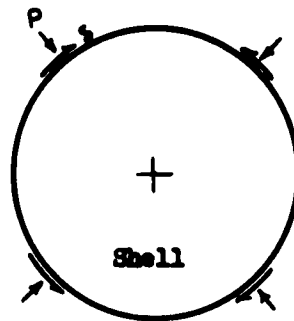
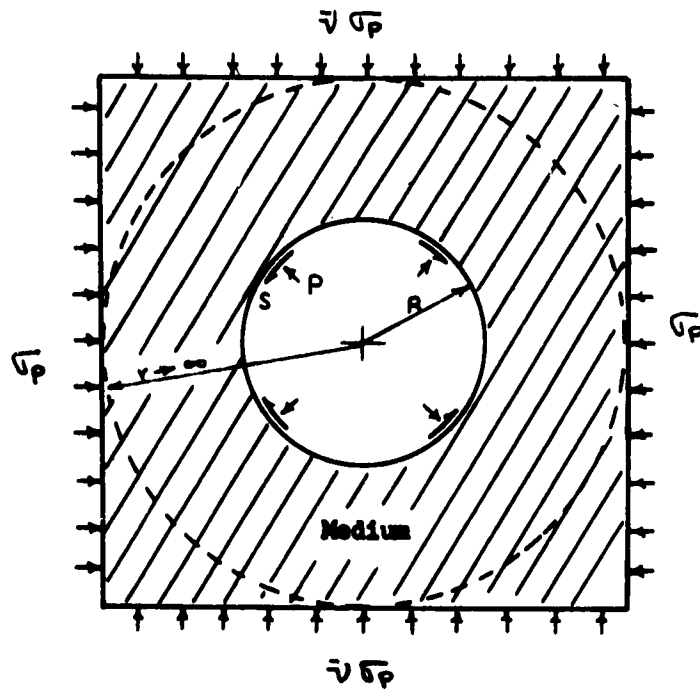


FIG. 9 STATIC STRESSES ACTING ON THE MEDIUM AND SHELL

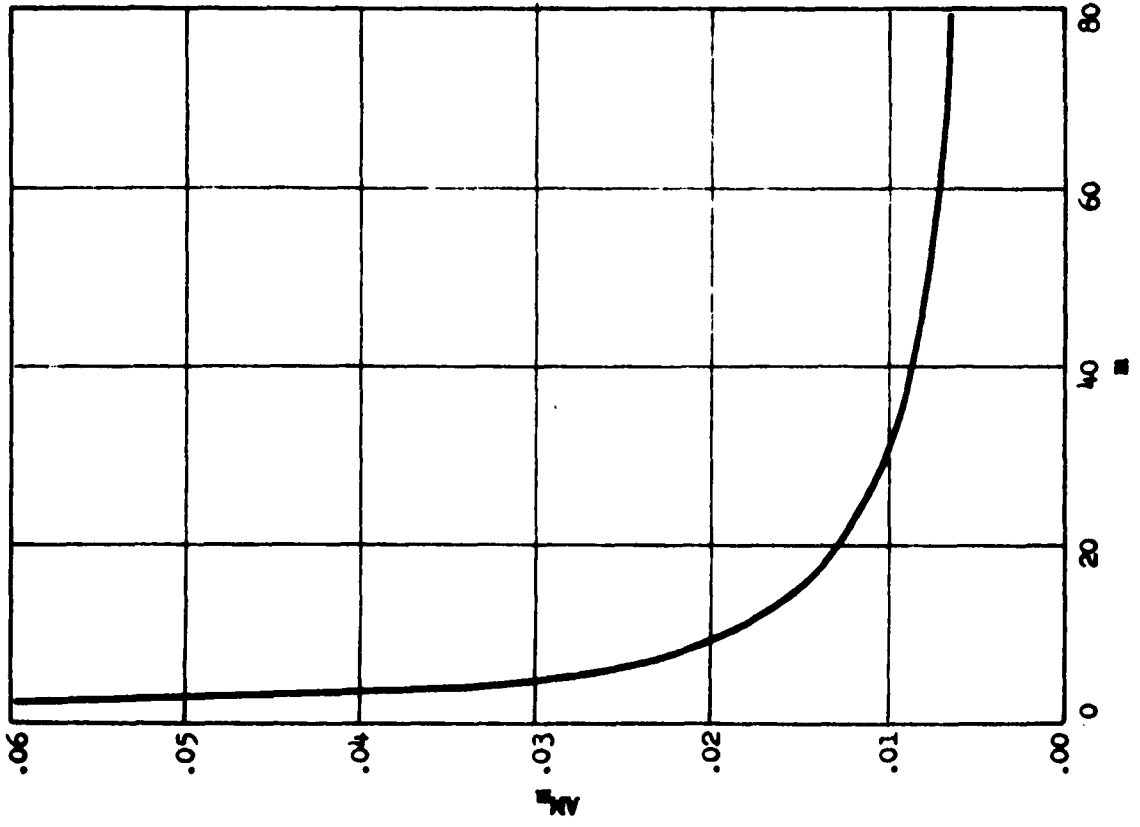
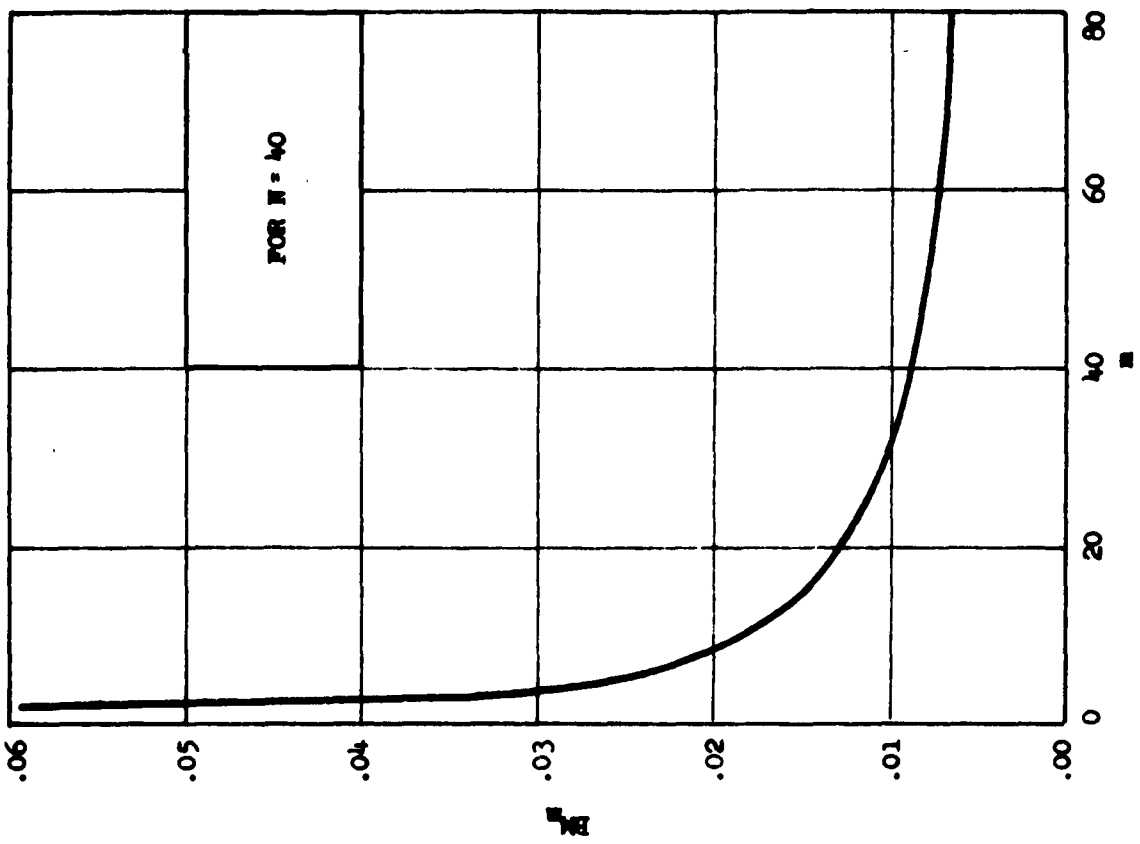
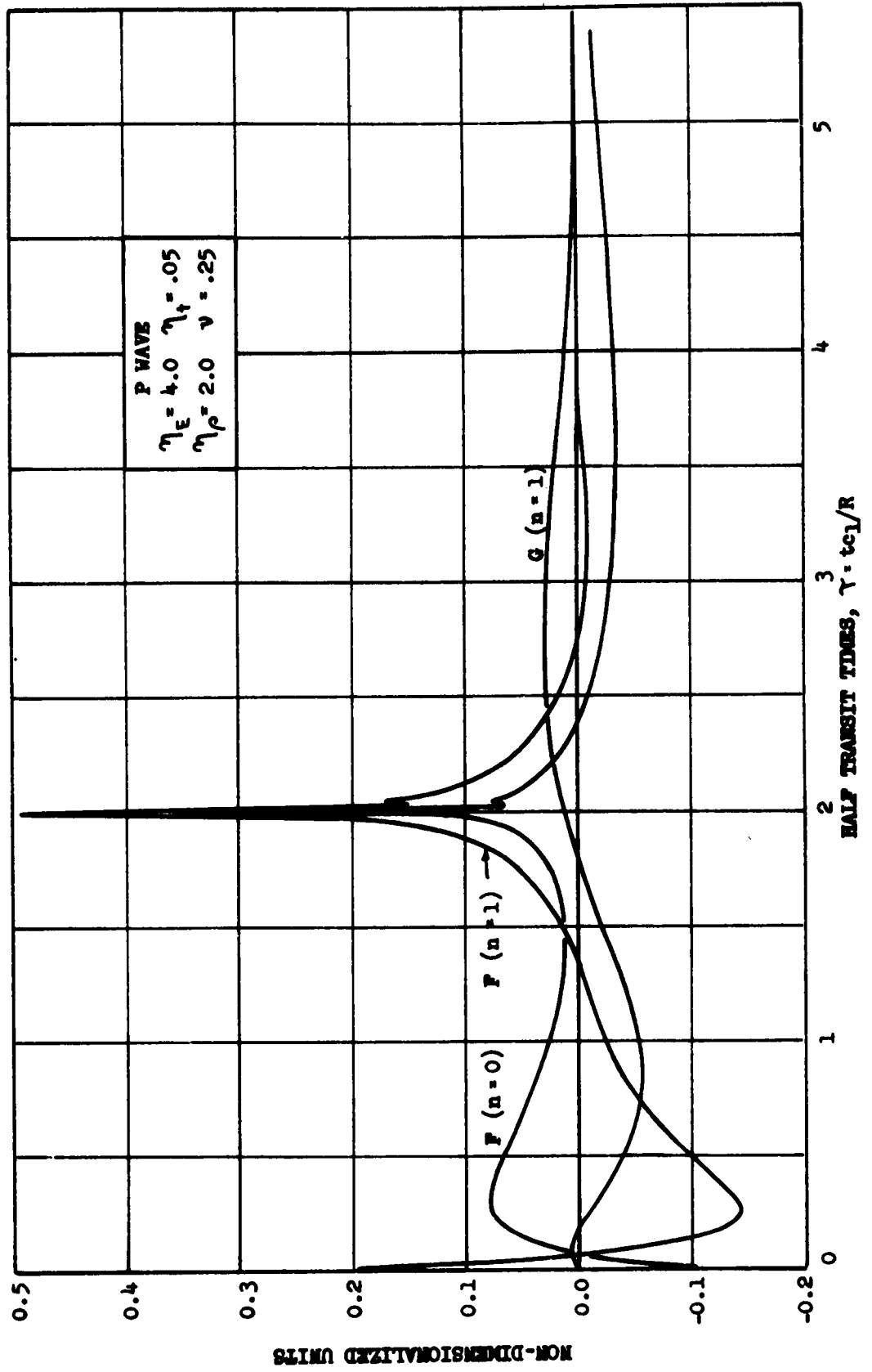


FIG. 10 WEIGHTING COEFFICIENTS  $A_M$  and  $B_M$


 FIG. 11 FUNCTIONS  $F(-1+\gamma)$  and  $G(-1/k_c+\gamma)$

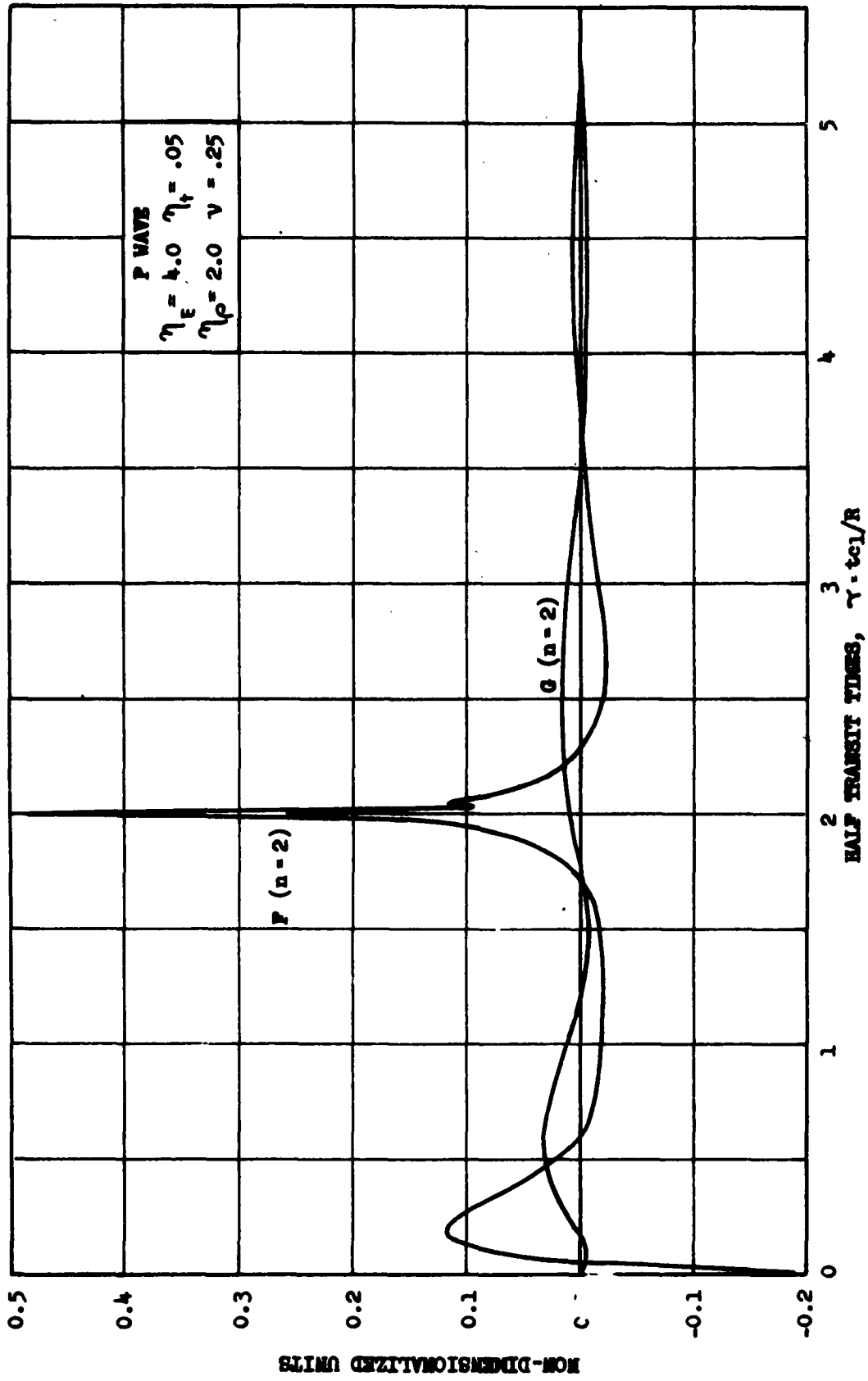


FIG. 12 FUNCTIONS  $F(-1+\tau)$  and  $G(-1/k_c+\tau)$

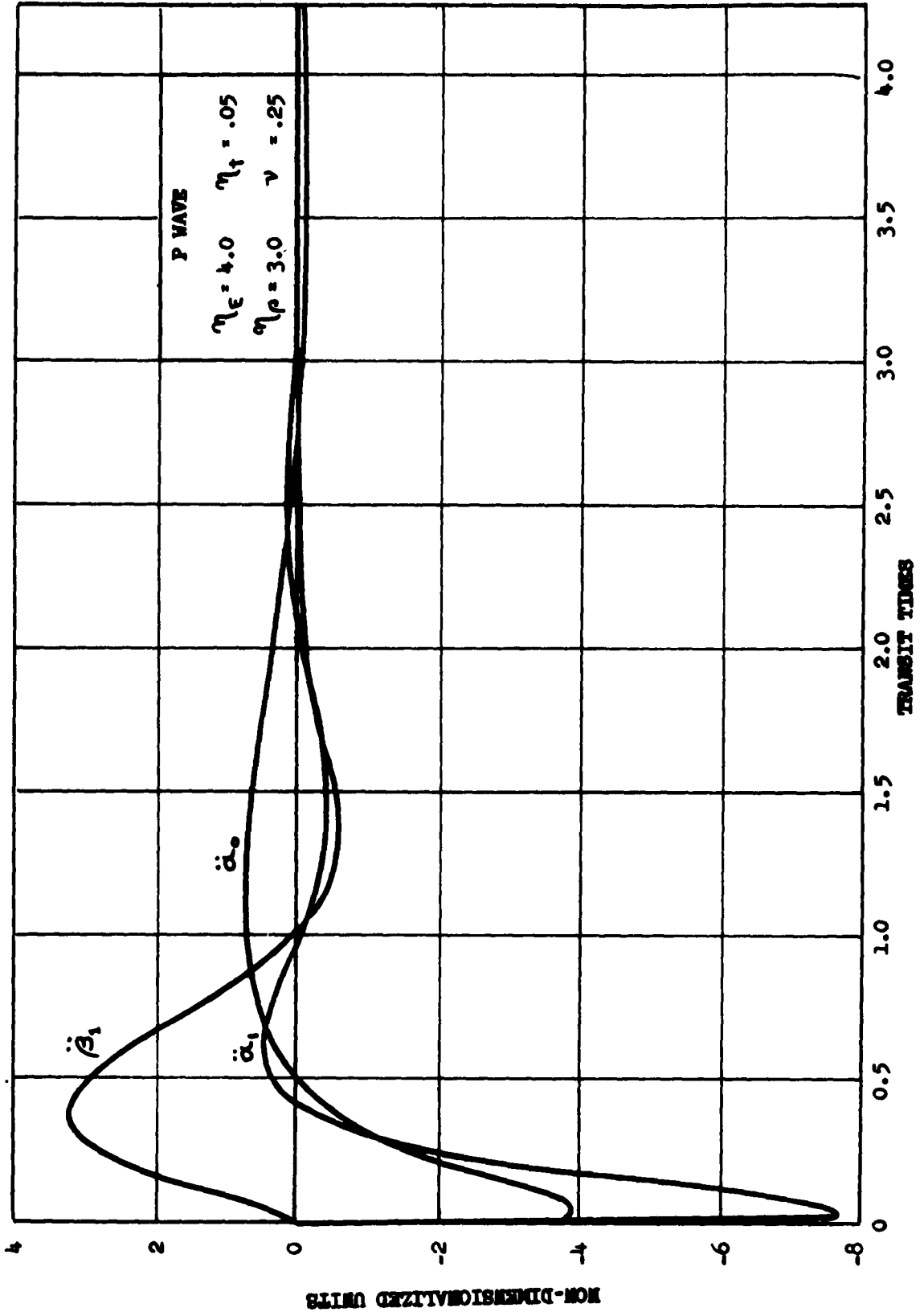


FIG. 13 COMPONENTS OF ACCELERATION FOR MODE  $n = 0$  and 1

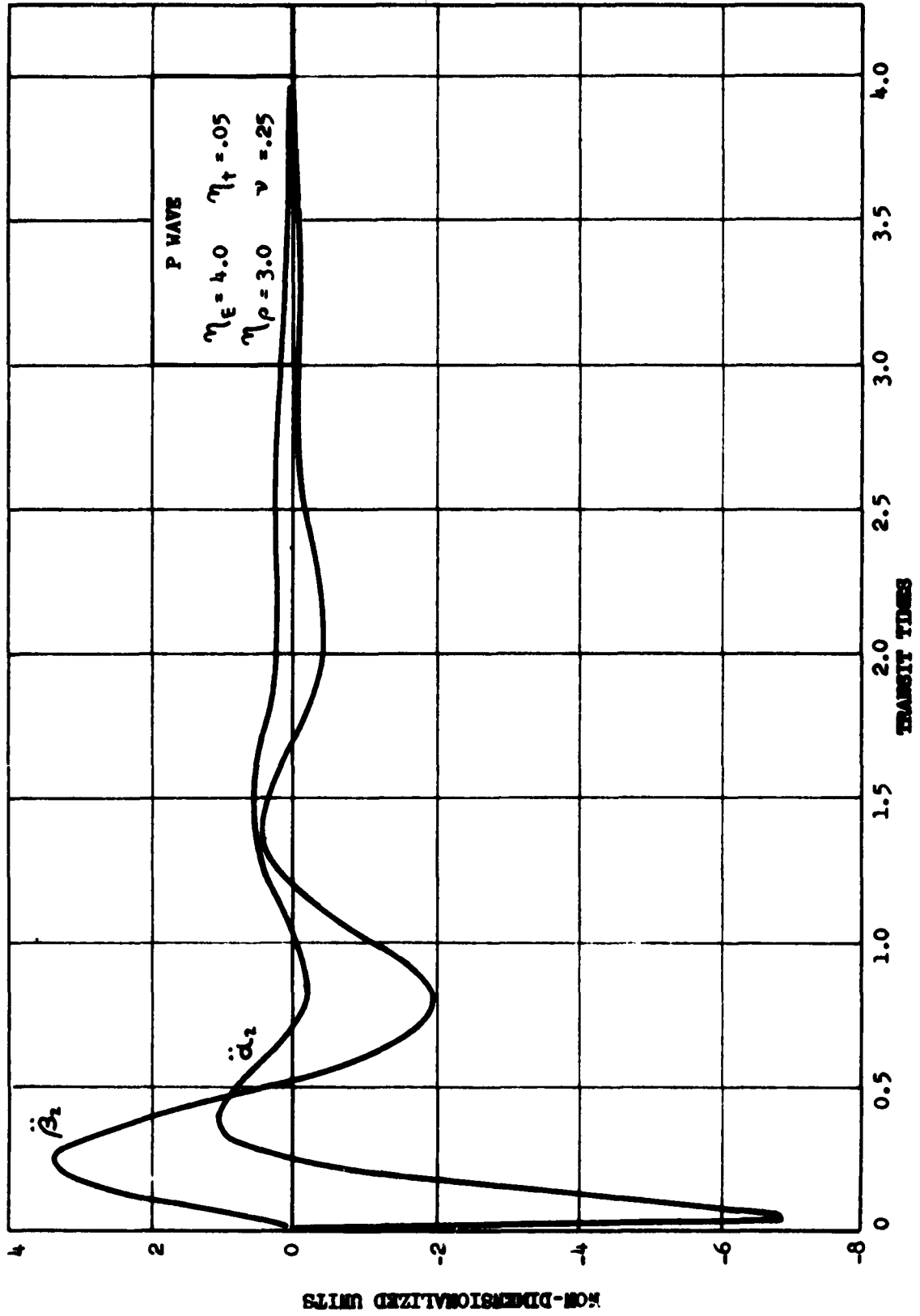


FIG. 14 COMPONENTS OF ACCELERATION FOR MODE  $n = 2$

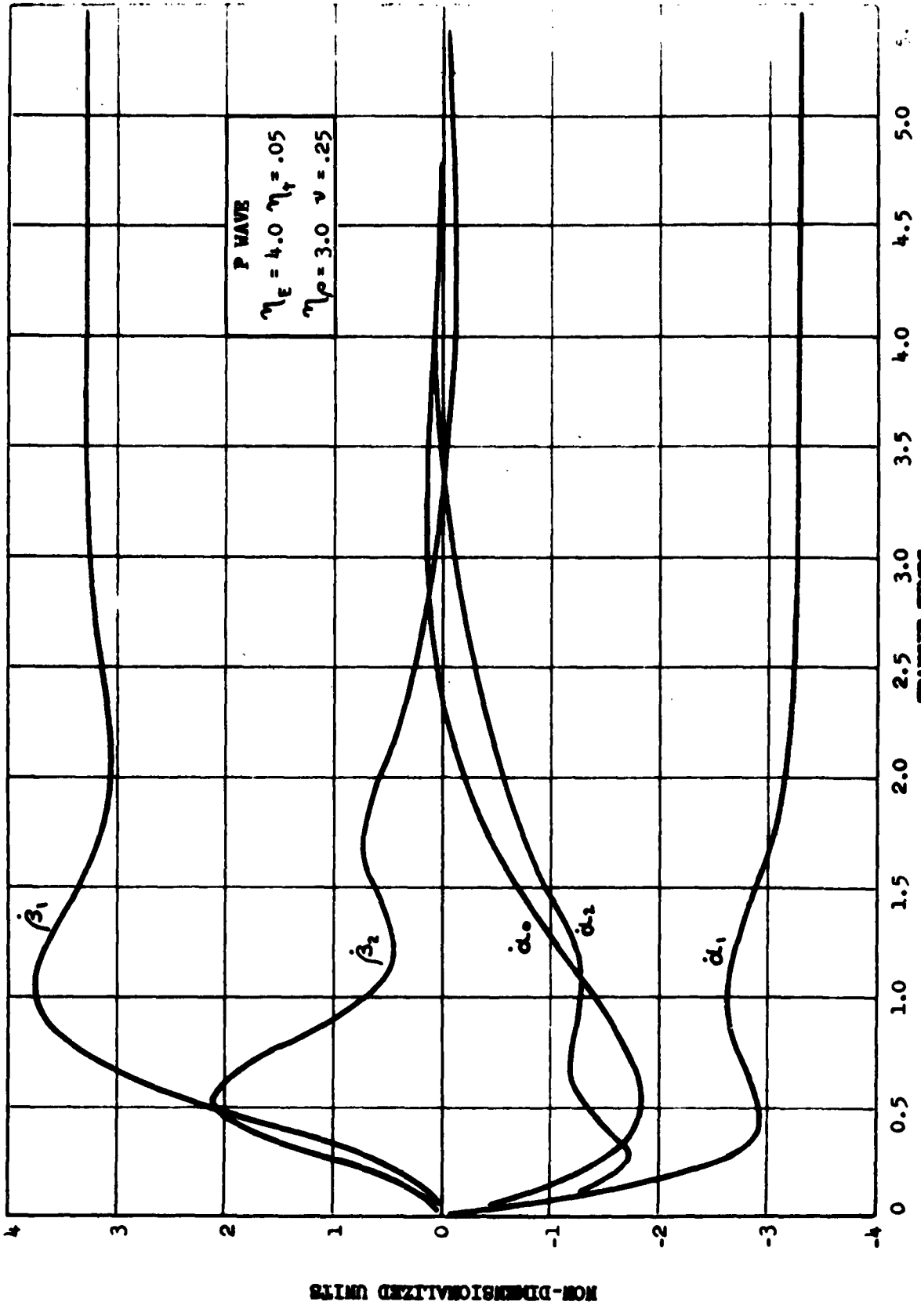


FIG. 15 MODAL VELOCITY COMPONENTS

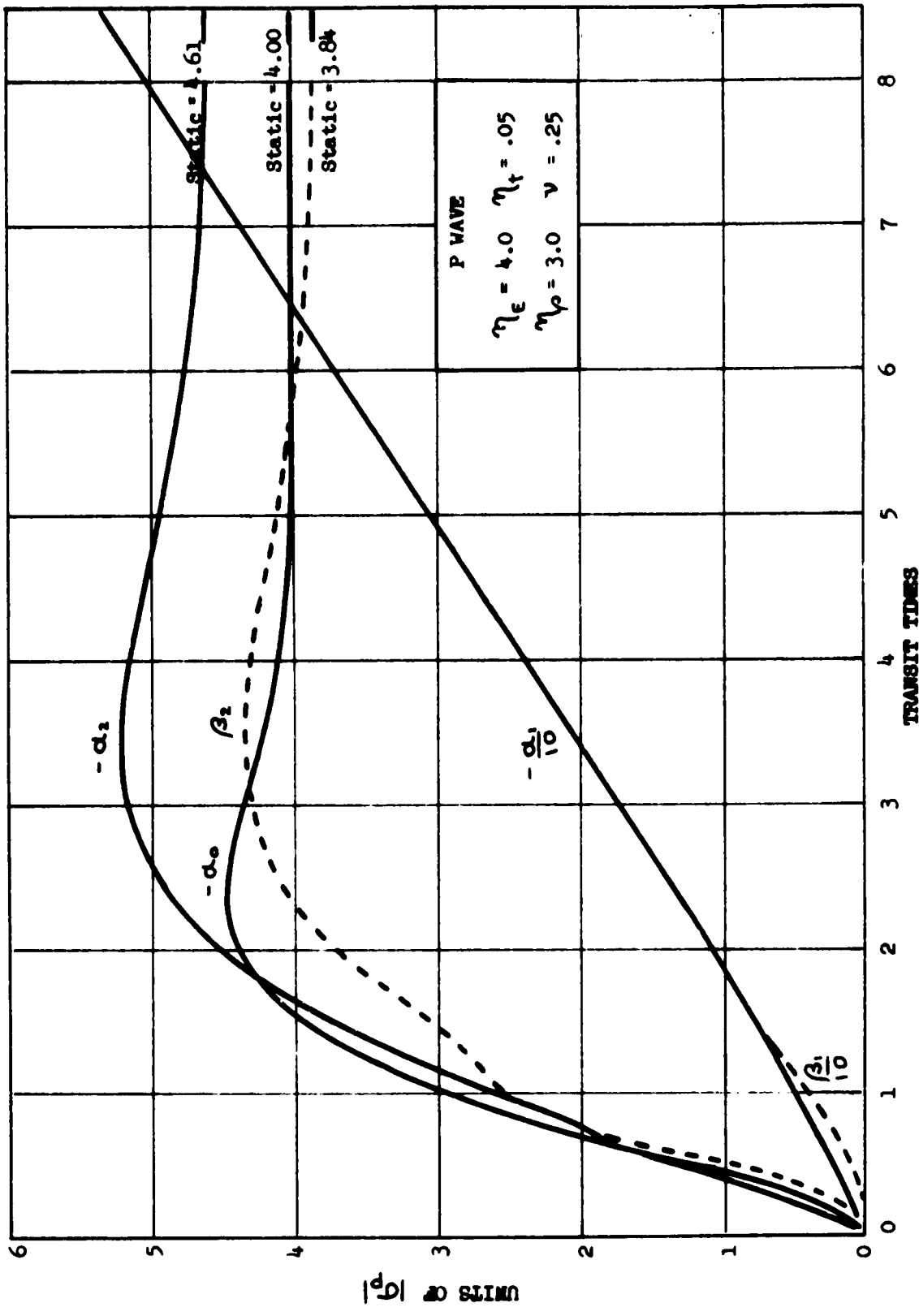


FIG. 16 MODAL DISPLACEMENT COMPONENTS

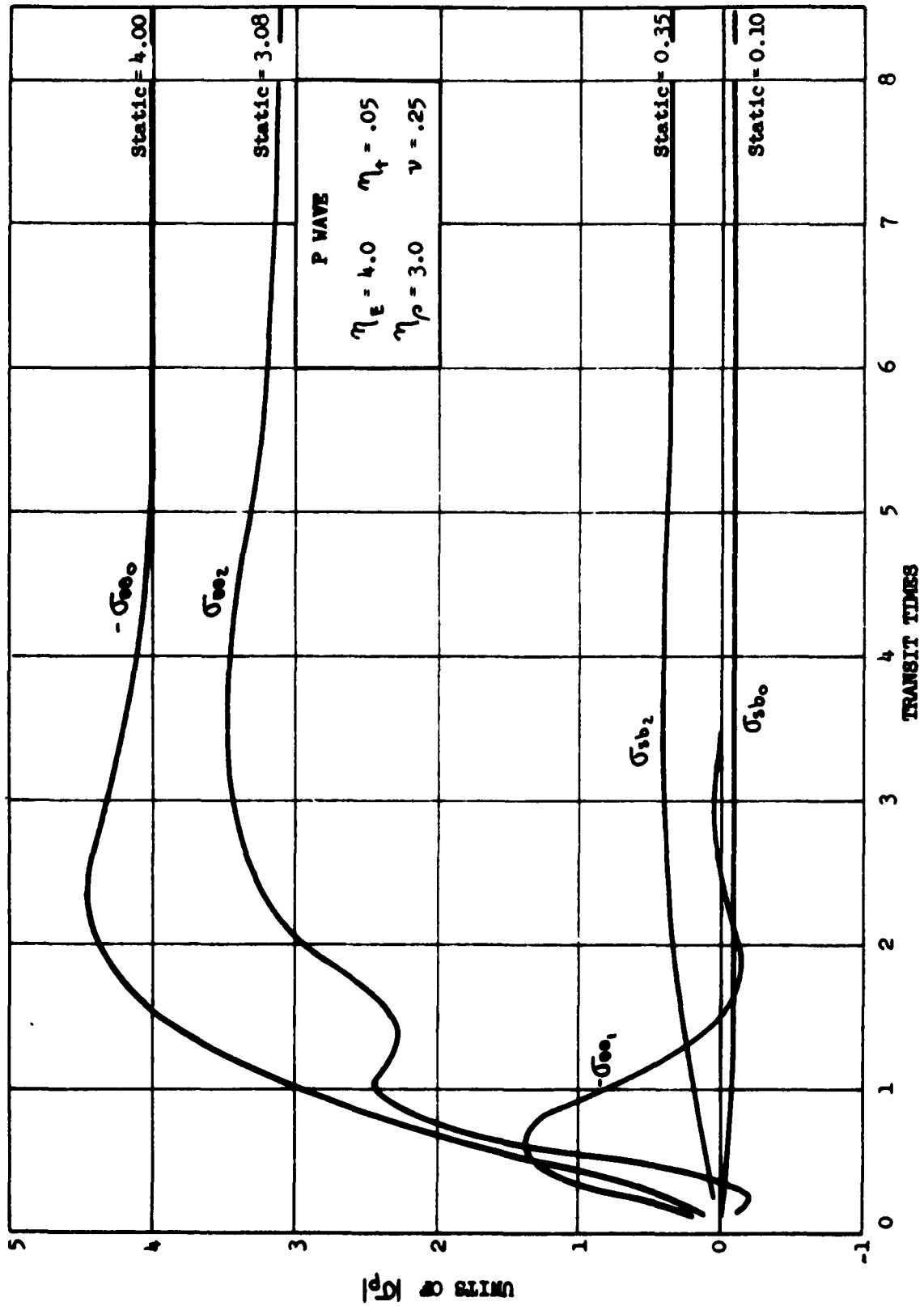


FIG. 17 MODAL COMPONENTS OF SHELL STRESSES

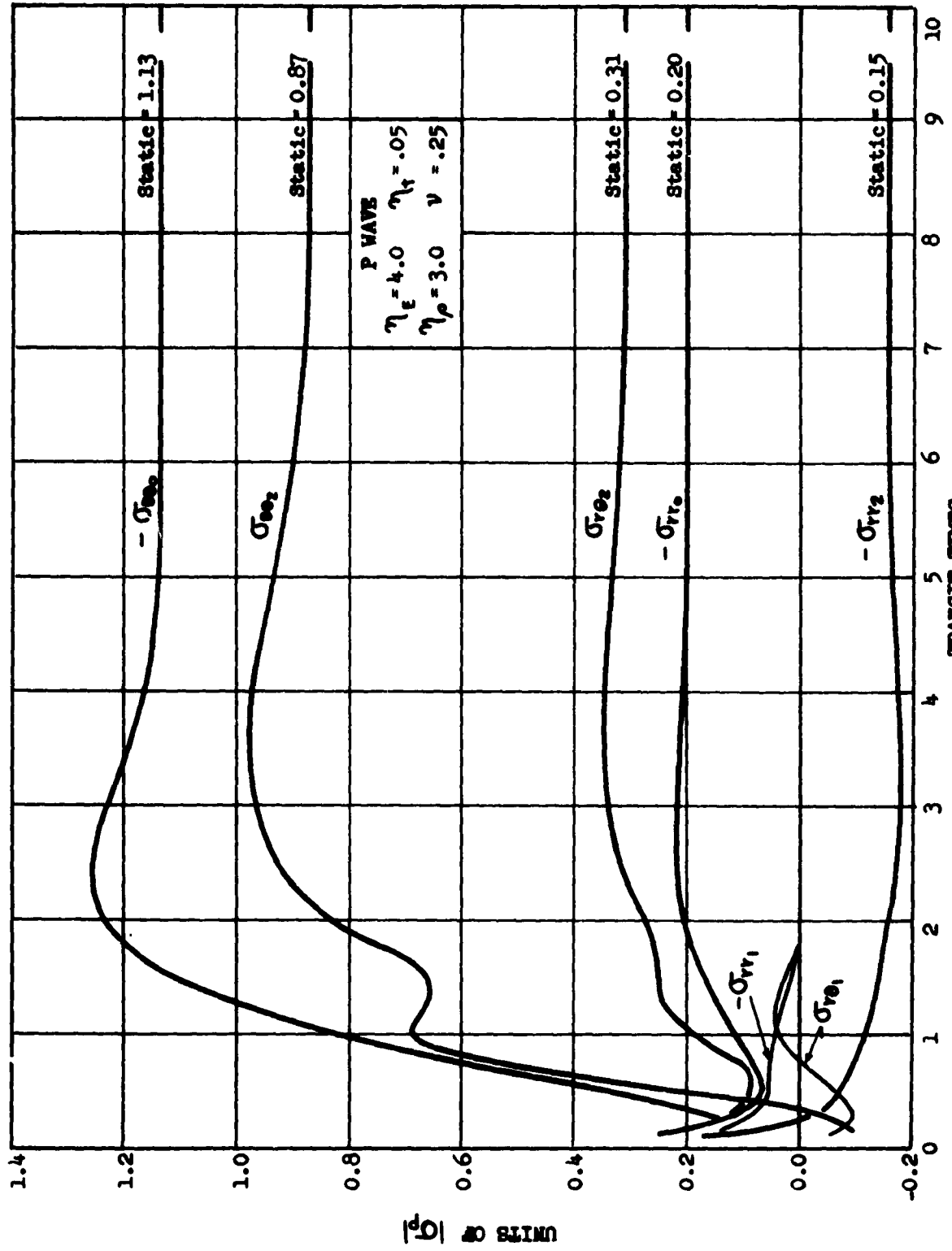


FIG. 18 MODAL COMPONENTS OF MEDIUM STRESSES

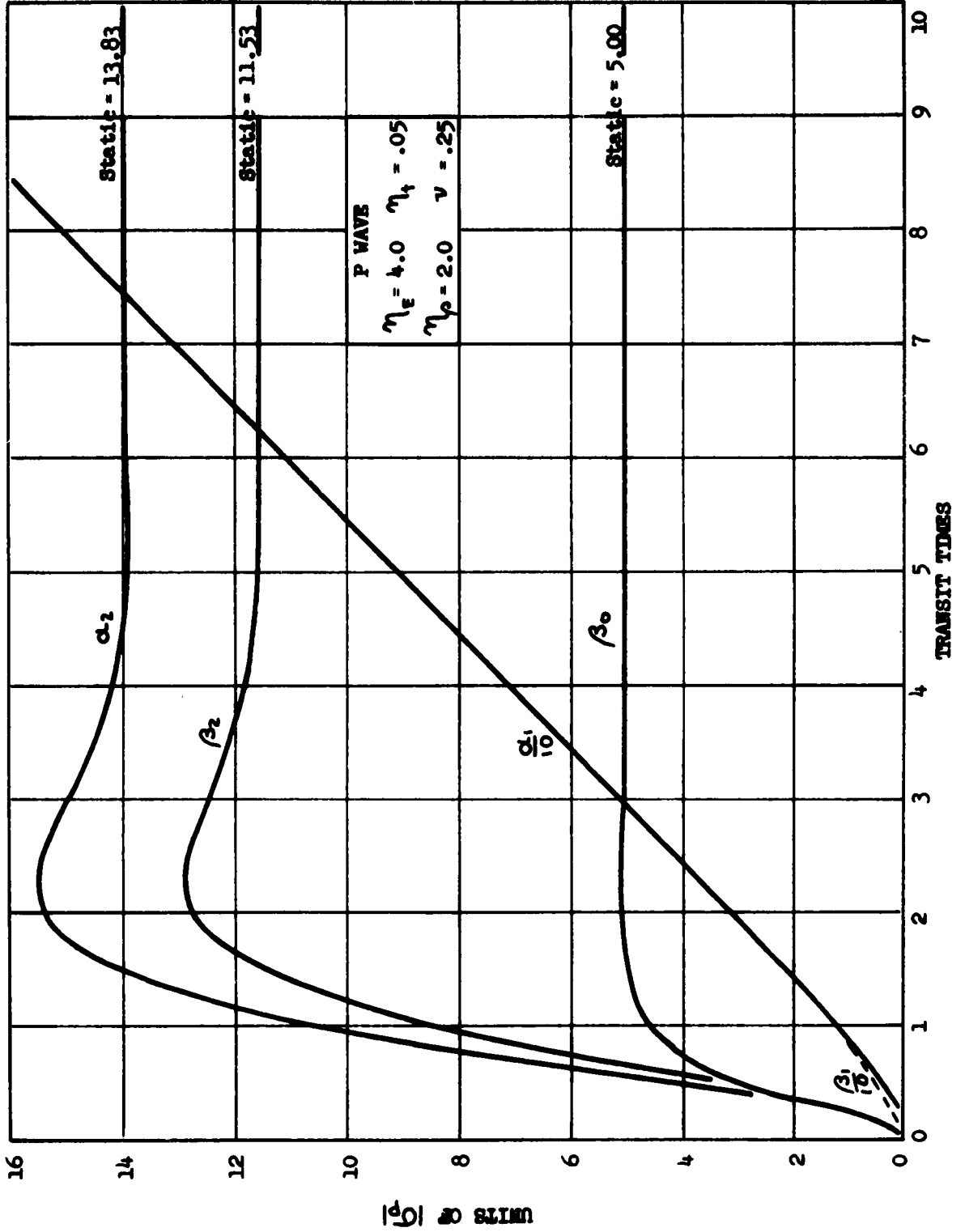


FIG. 19 MODAL DISPLACEMENT COMPONENTS FOR INCIDENT SHEAR WAVE

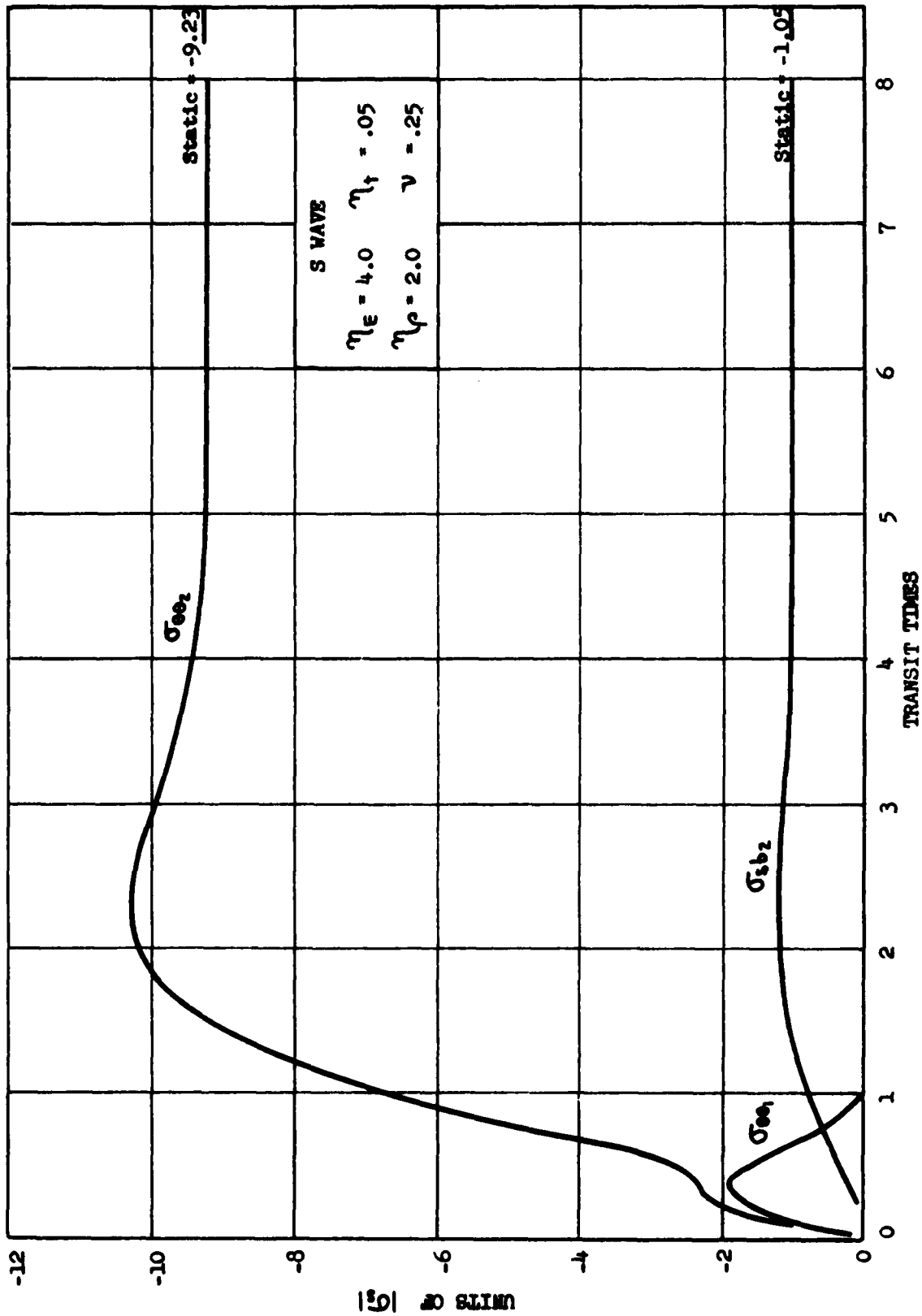


FIG. 20 MODAL SHELL STRESSES FOR INCIDENT SHEAR WAVE

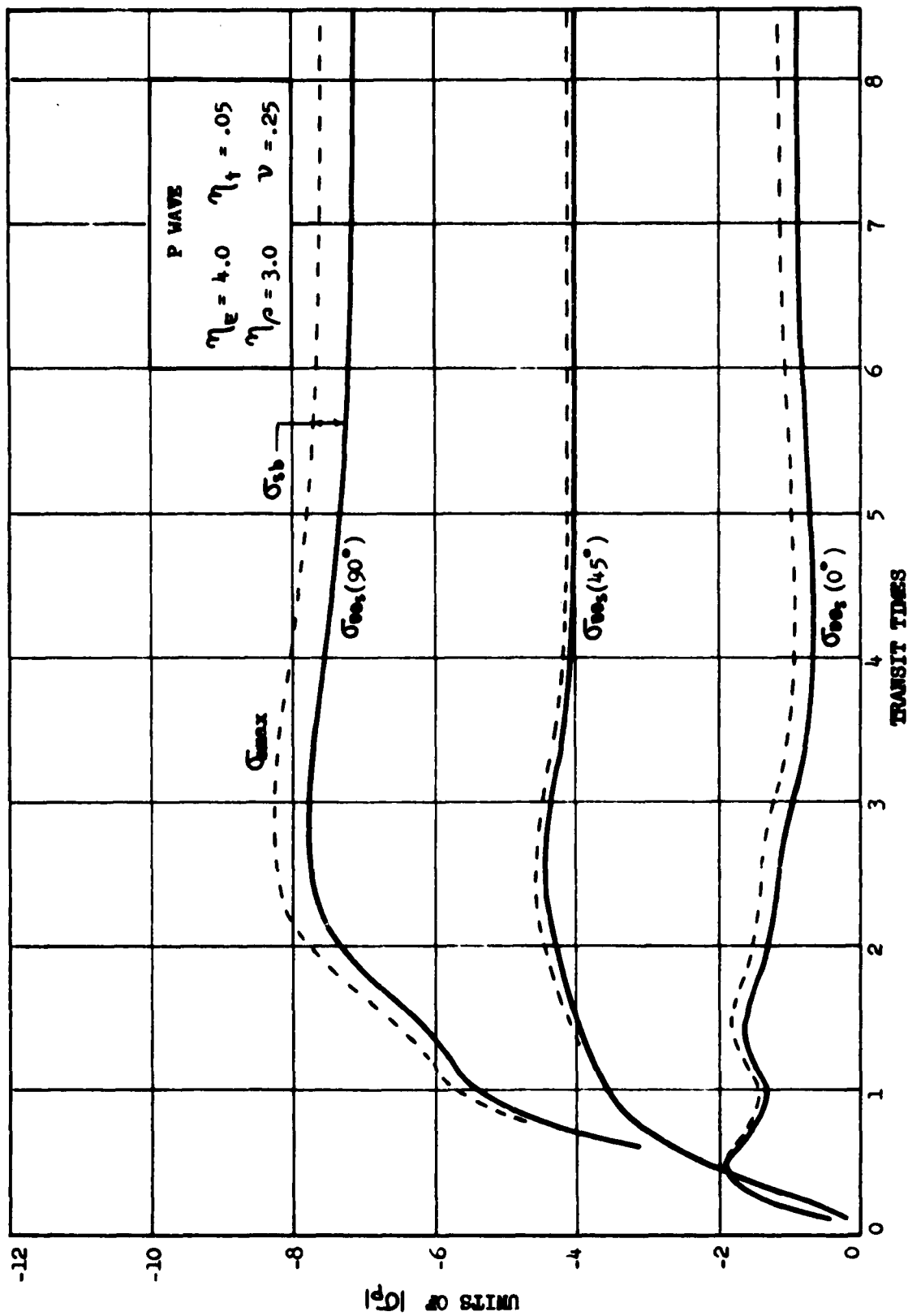


FIG. 21 HOOP AND BENDING STRESSES OF THE SHELL AT VARIOUS ANGLES

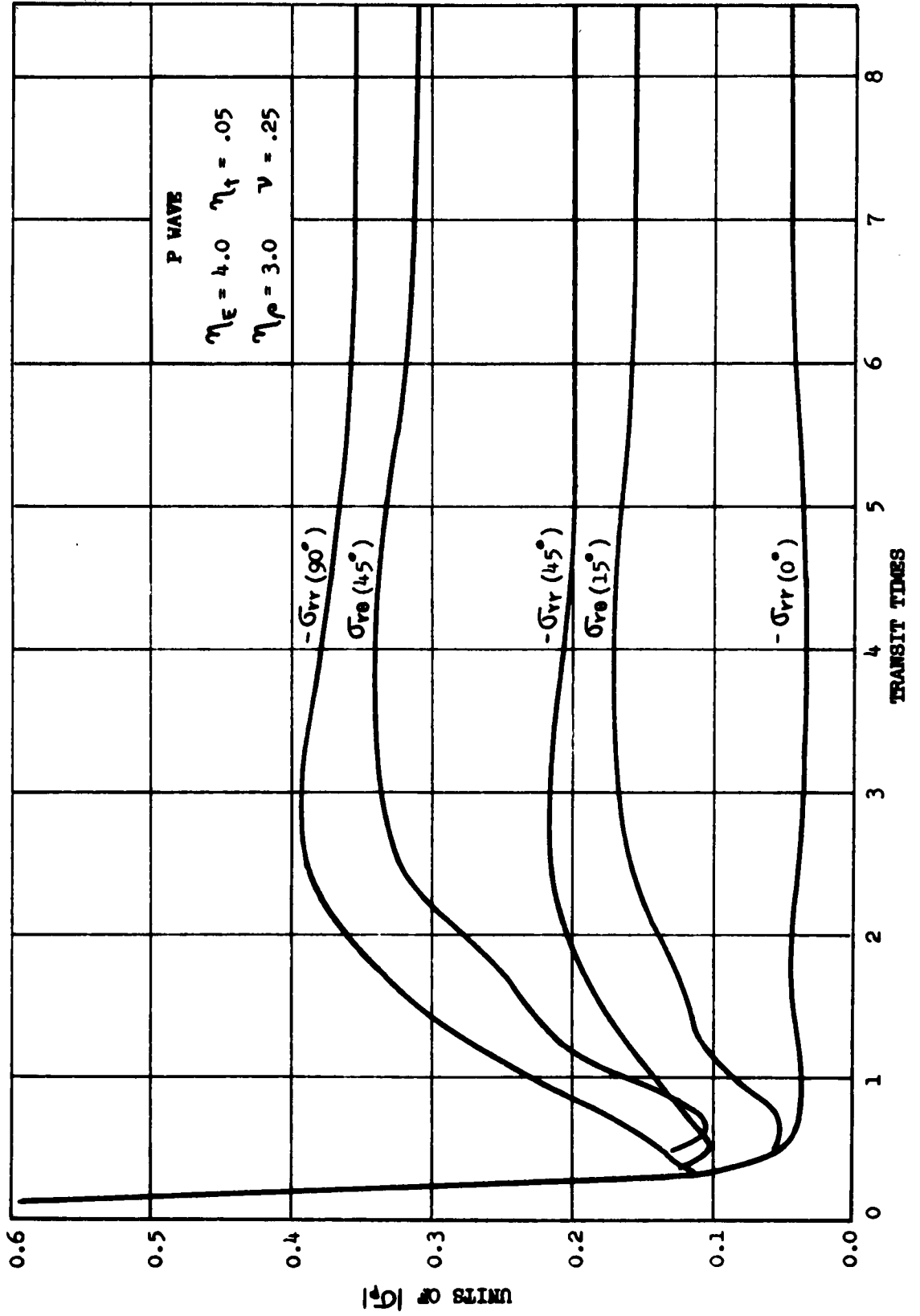


FIG. 22 RADIAL AND SHEAR STRESSES IN THE MEDIUM AT THE BOUNDARY

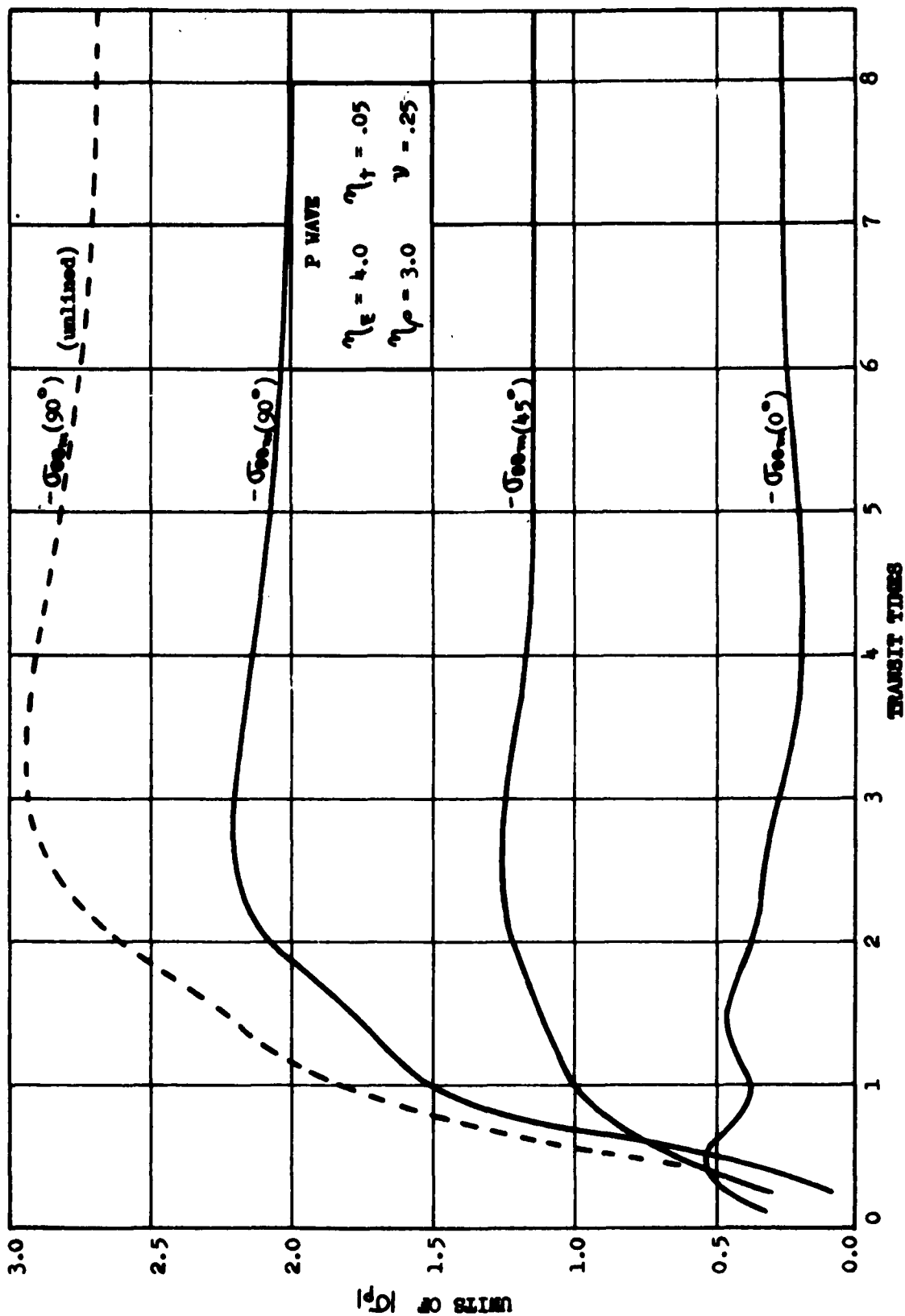


FIG. 23 HOOP STRESSES IN THE MEDIUM AT THE BOUNDARY

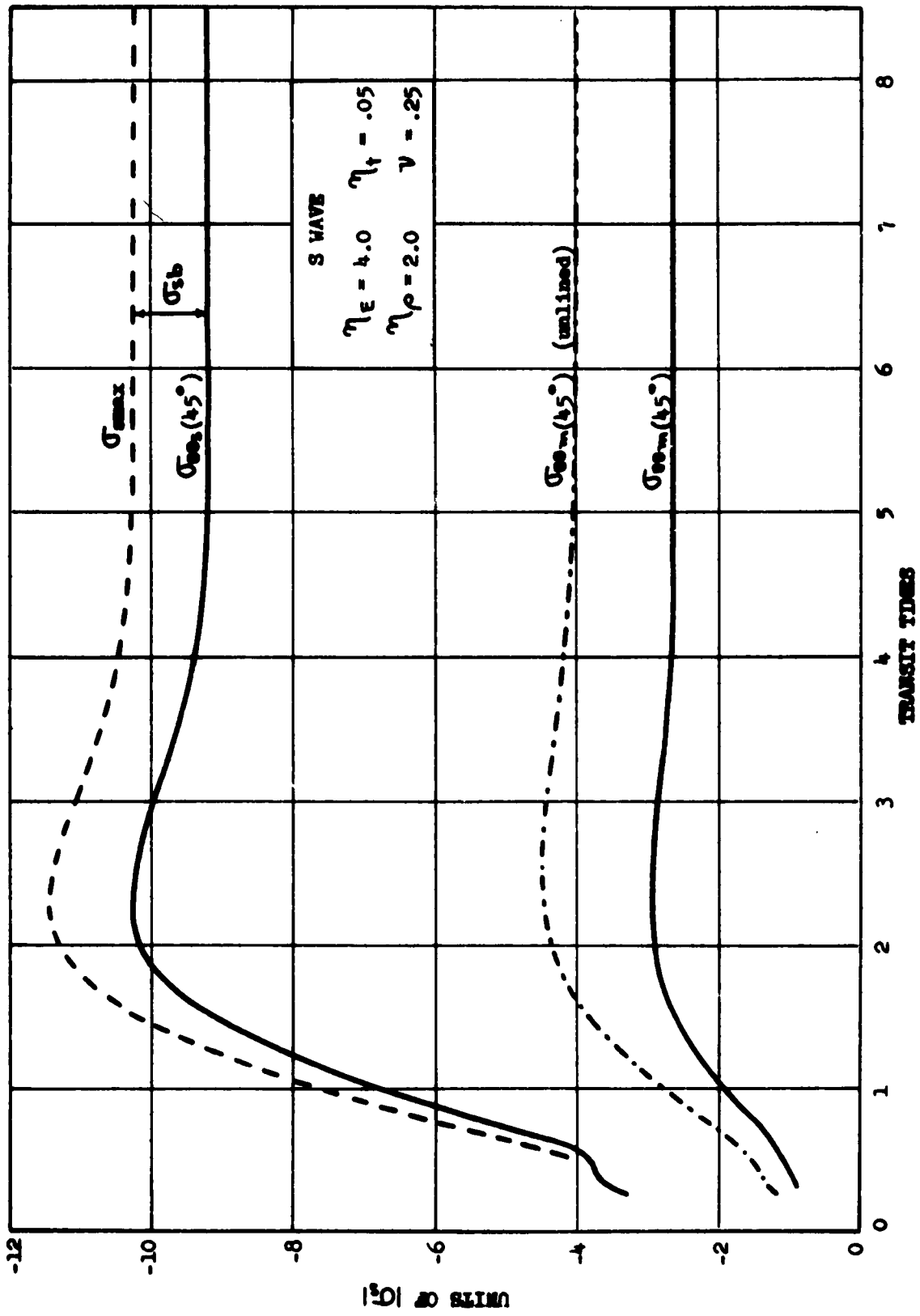


FIG. 24 STRESSES IN THE SHELL AND MEDIUM FOR INCIDENT SHEAR WAVE

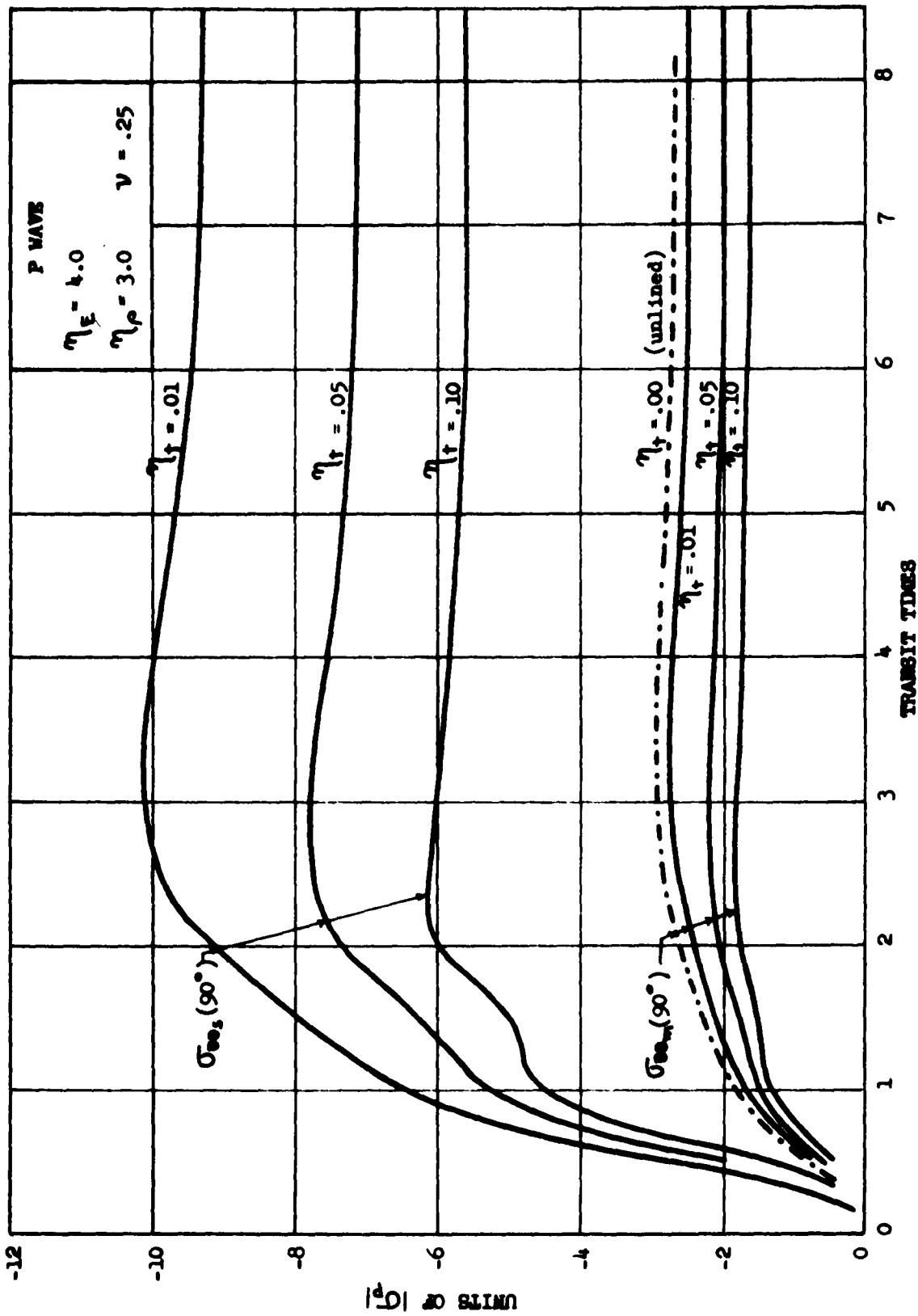


FIG. 25 HOOP STRESSES IN THE SHELL AND MEDIUM FOR VARIOUS RELATIVE THICKNESSES OF SHELL

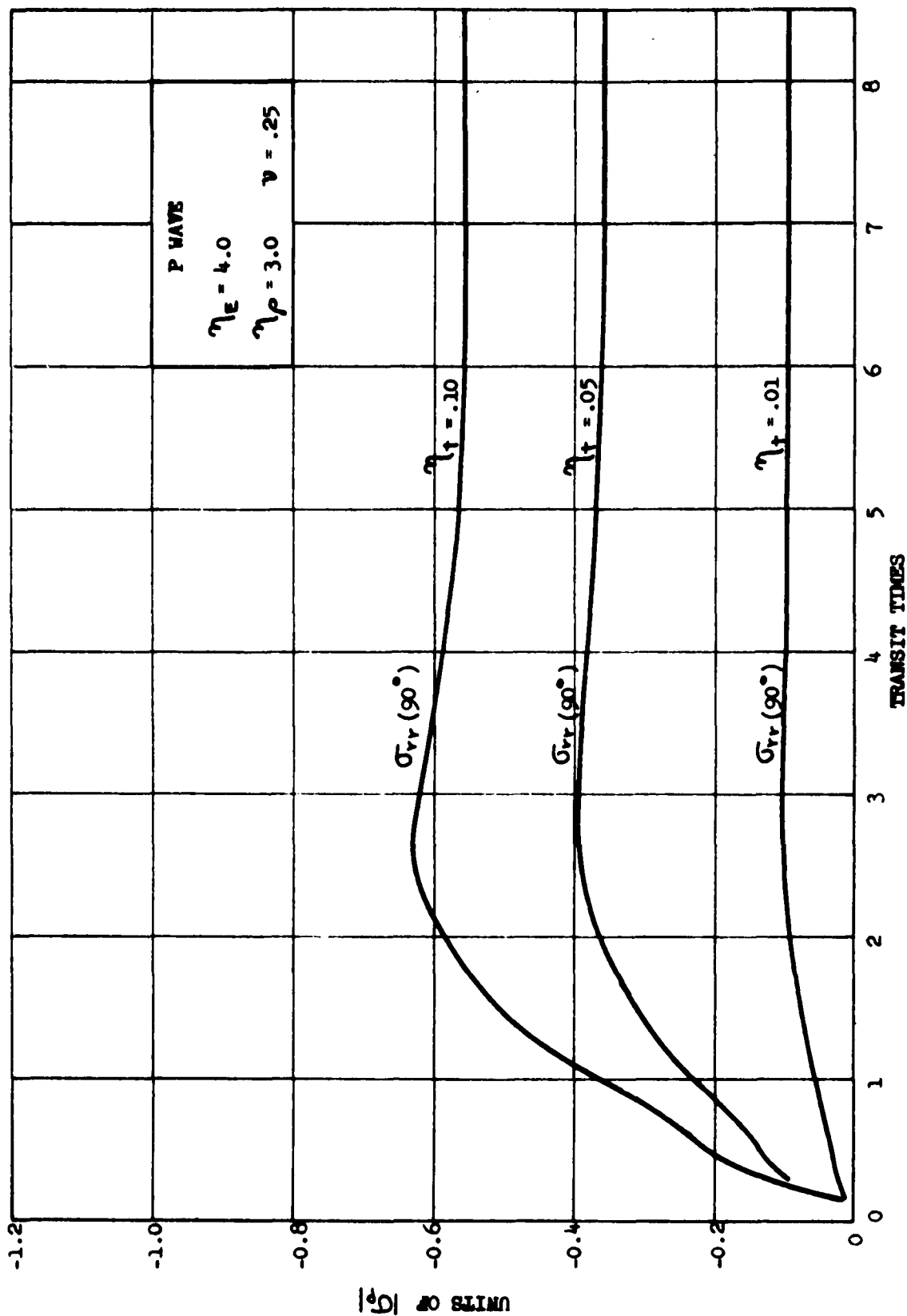


FIG. 26 RADIAL STRESS IN THE MEDIUM AT THE BOUNDARY FOR VARIOUS THICKNESSES OF SHELL

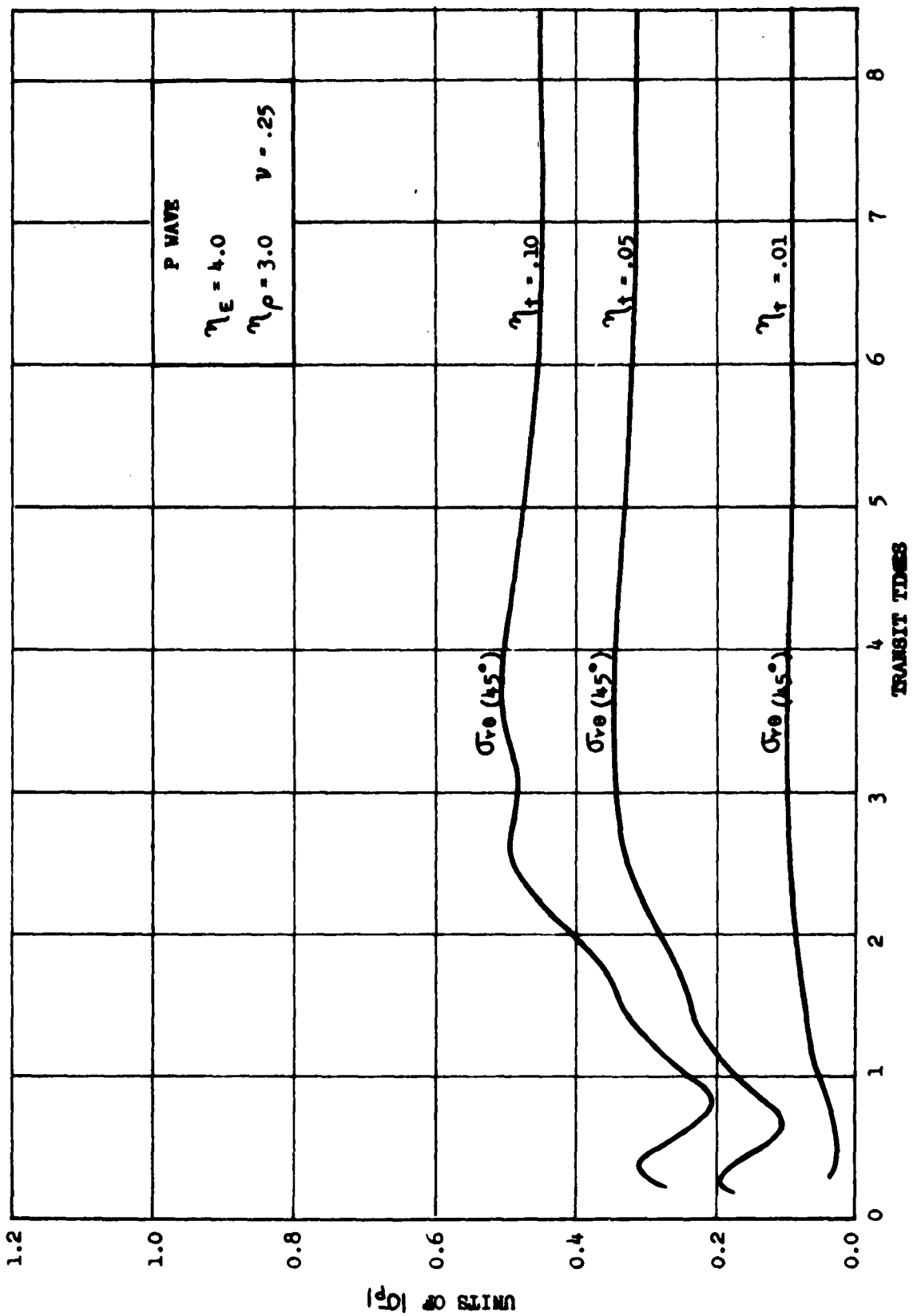


FIG. 27 SHEAR STRESS IN THE MEDIUM AT THE BOUNDARY FOR VARIOUS RELATIVE THICKNESSES OF SHELL

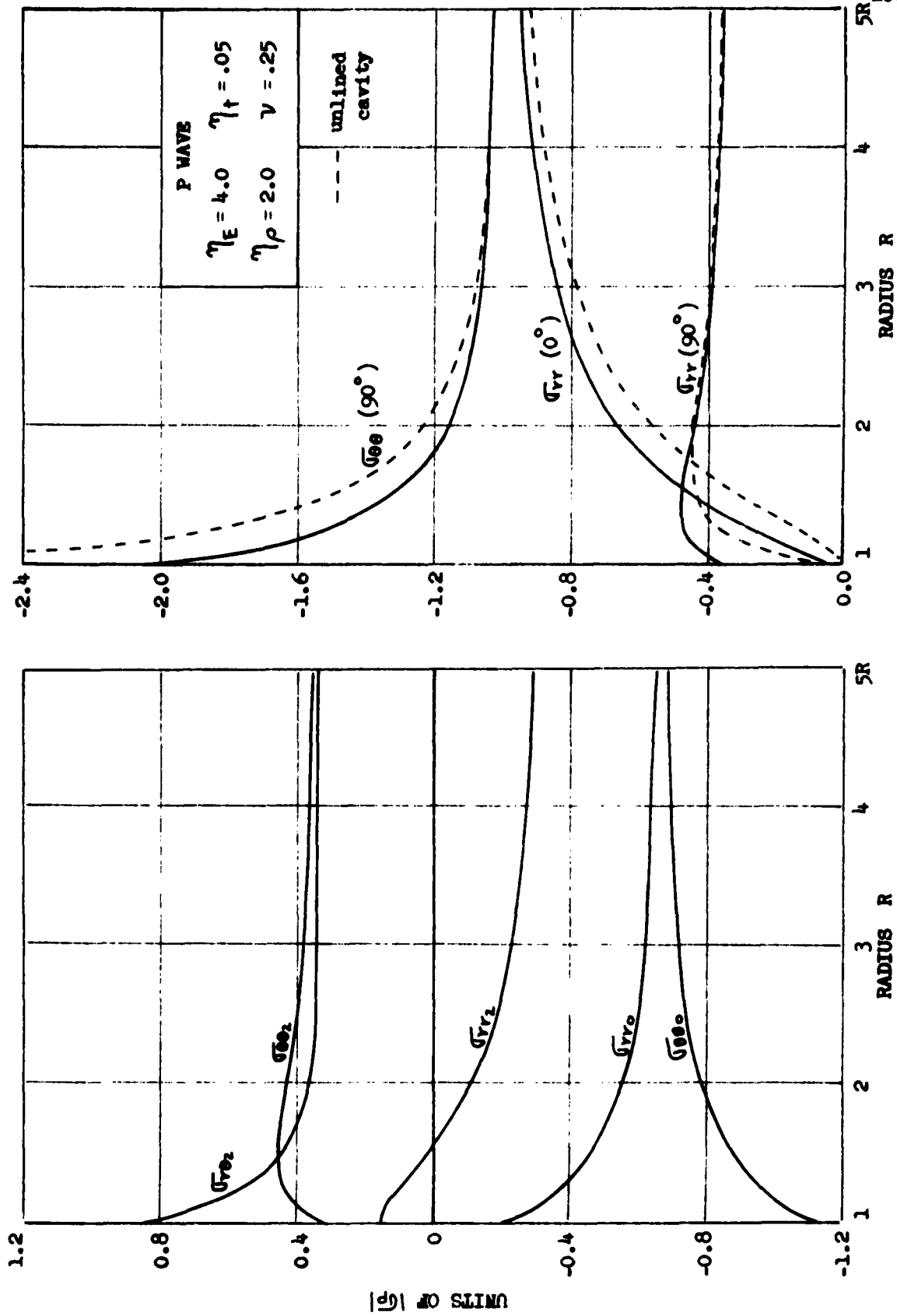
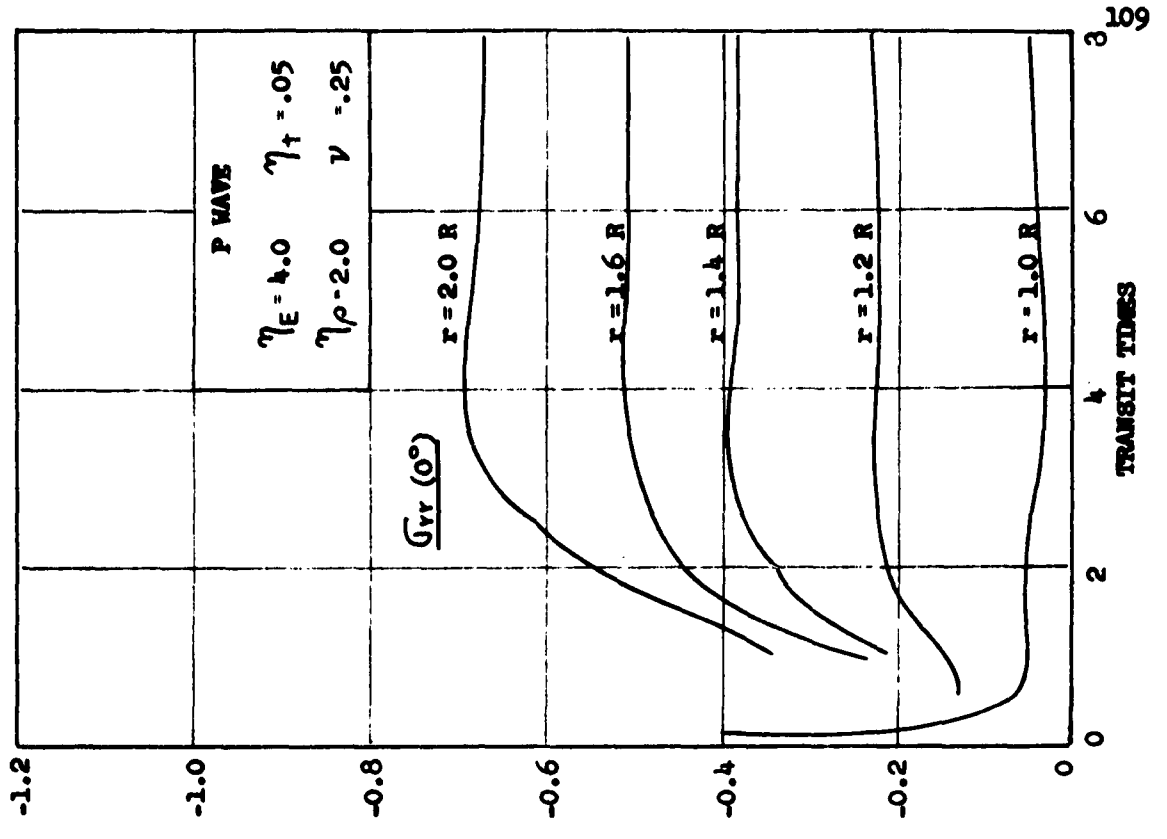
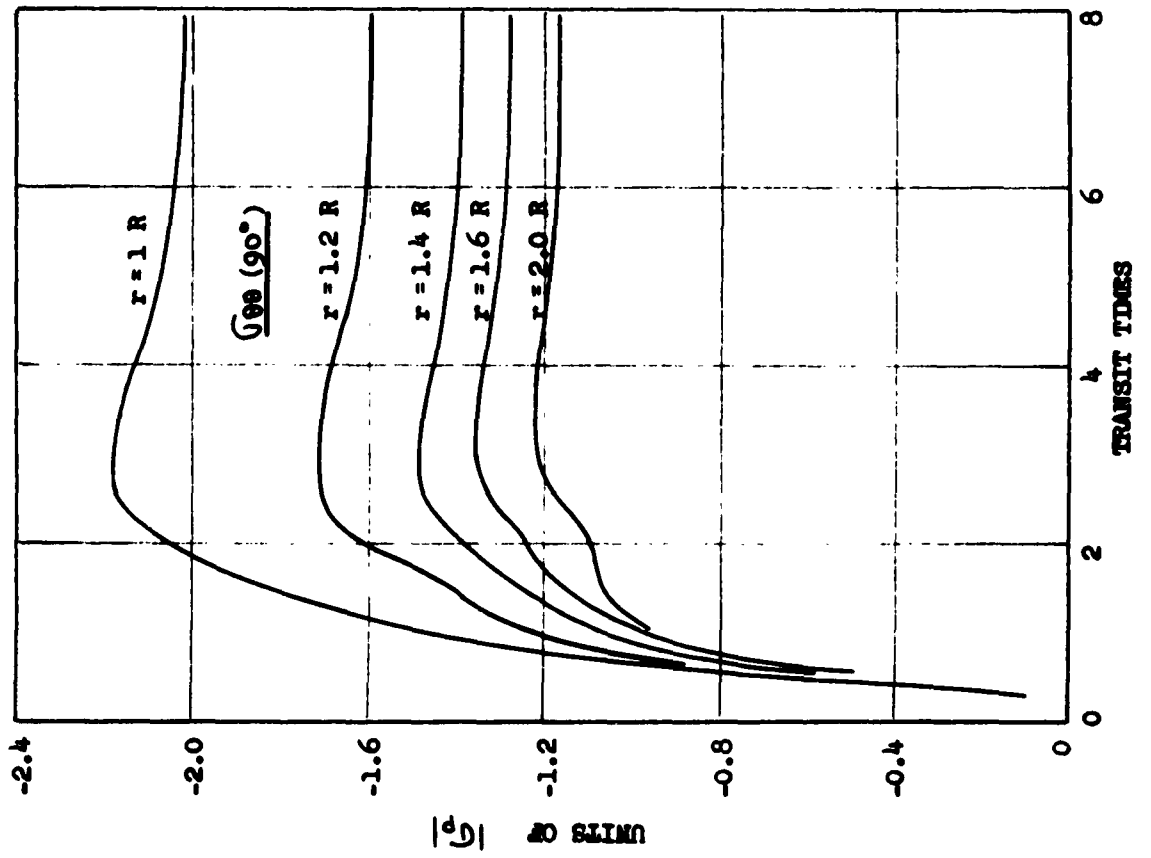


FIG. 26 STRESSES IN THE MEDIUM FOR VARIOUS RADII AT TEN TRANSIT TIME



P WAVE  
 $\eta_E = 4.0$     $\eta_T = .05$   
 $\eta_\rho = 2.0$     $\nu = .25$

FIG. 29 VARIATION OF STRESSES IN THE MEDIUM WITH RADIUS AND TIME

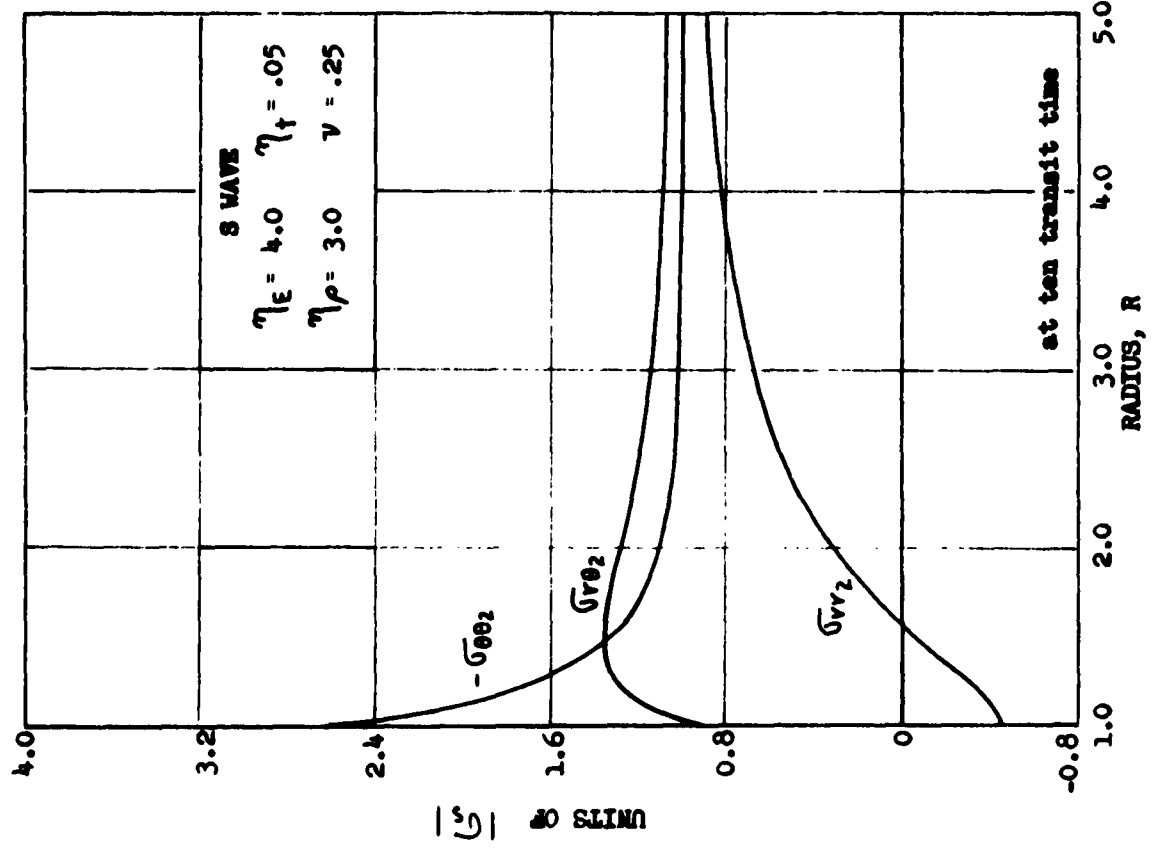
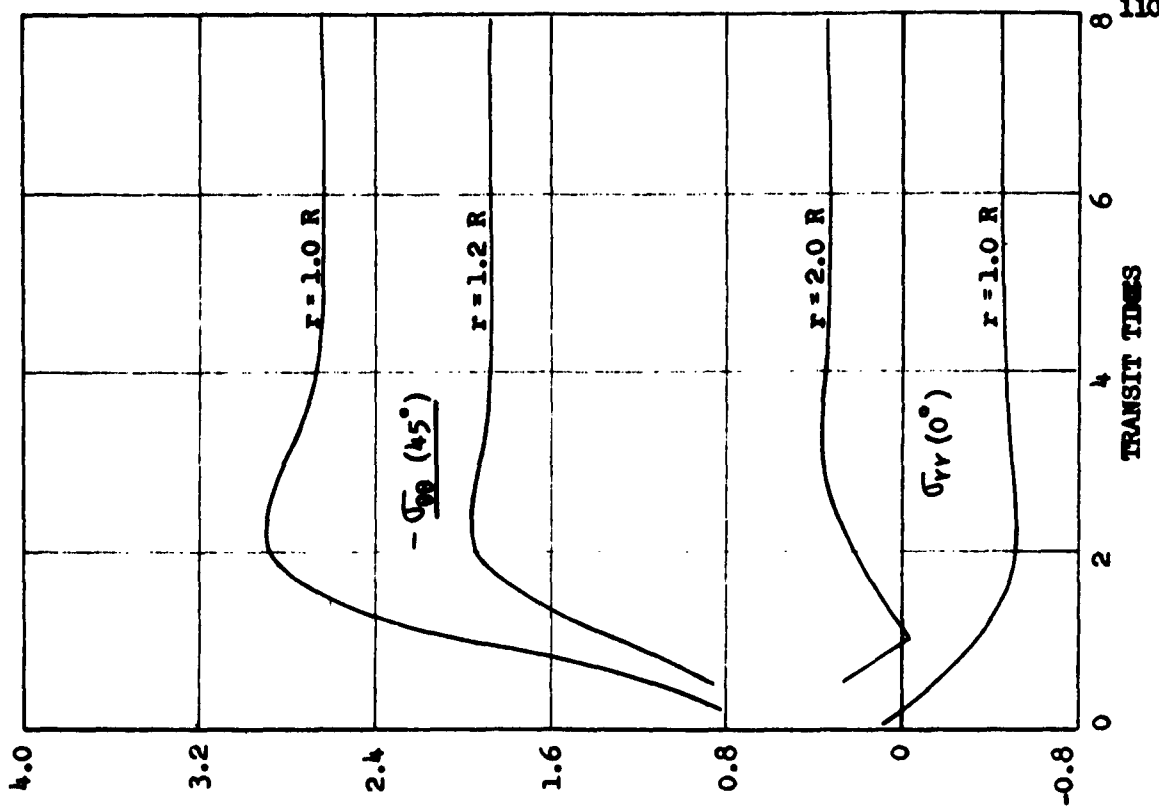


FIG. 30 STRESSES IN THE MEDIUM FOR VARIOUS RADI AND TIMES

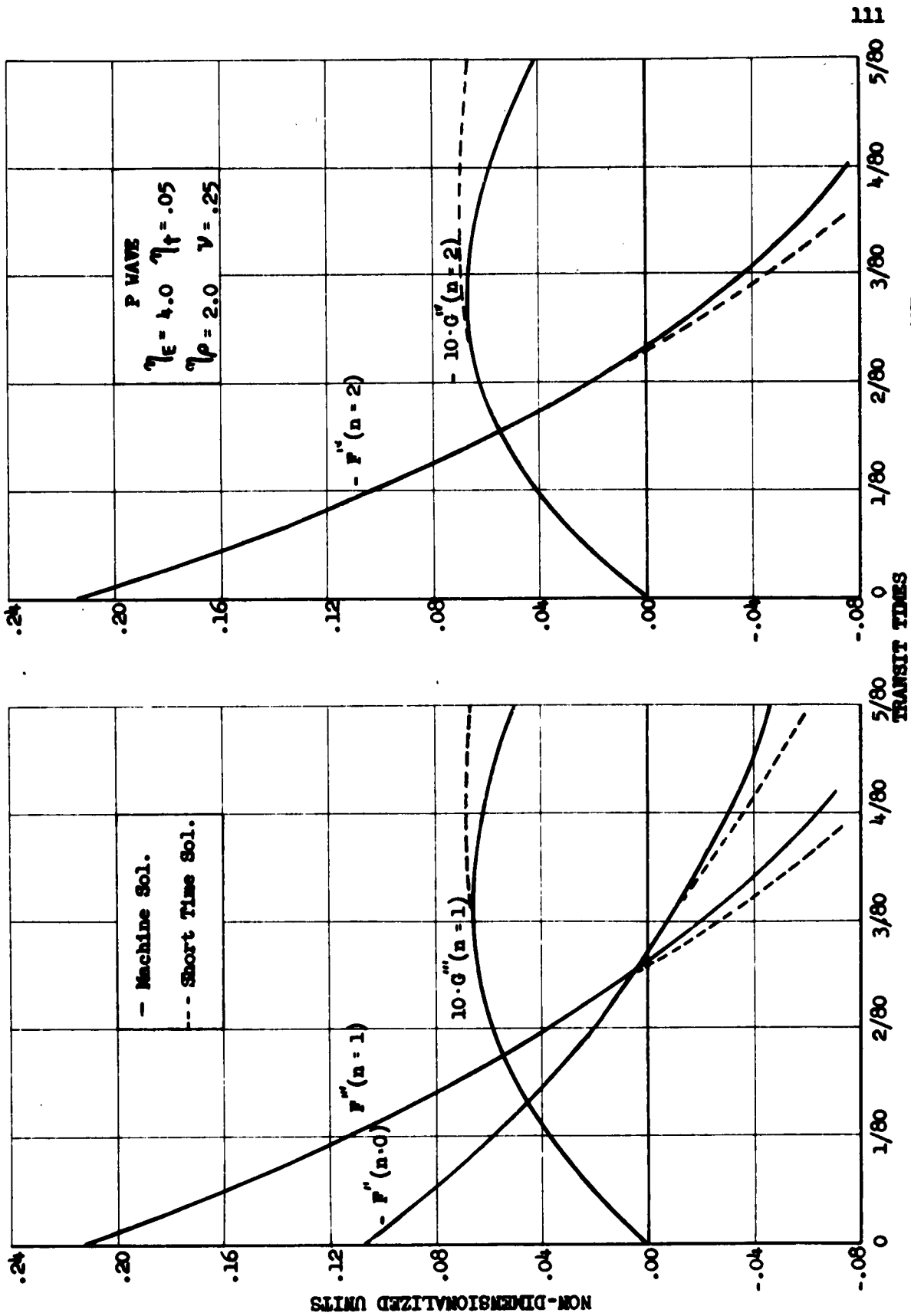


FIG. 31 COMPARISON OF SHORT-TIME RESULTS FOR INCIDENT P WAVE

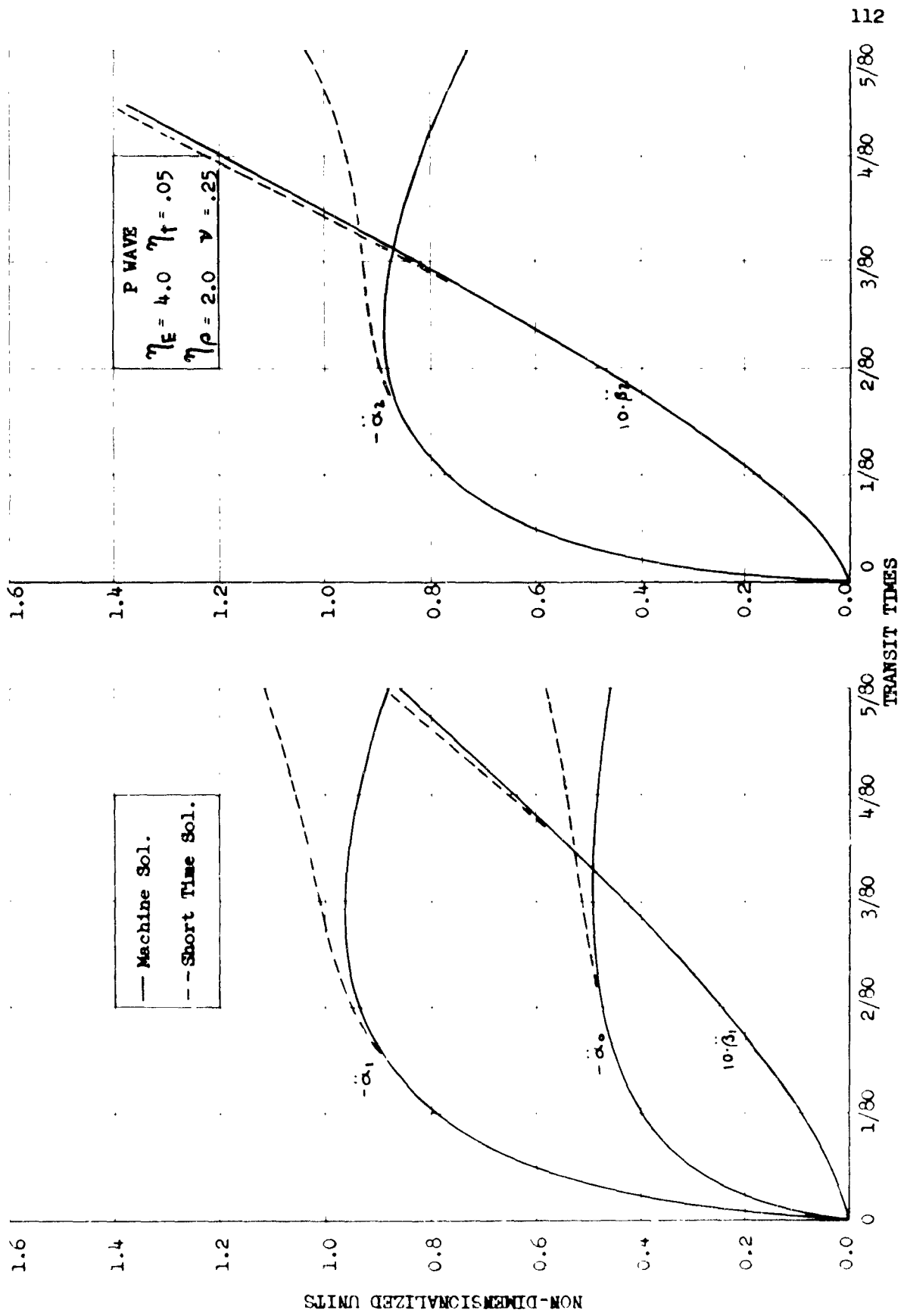


FIG. 32 COMPARISON OF SHORT-TIME RESULTS FOR INCIDENT P WAVE

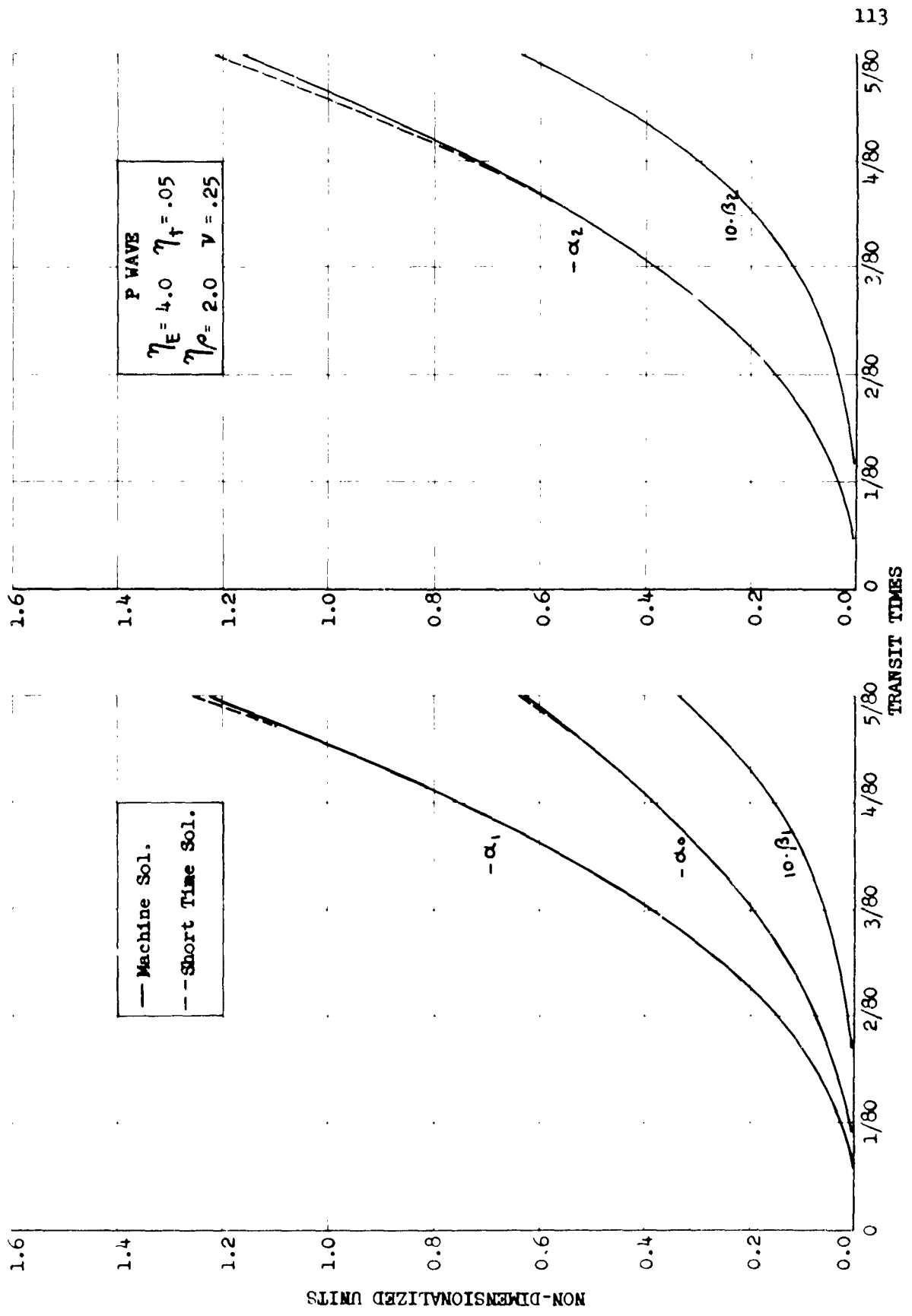


FIG. 33 COMPARISON OF SHORT-TIME RESULTS FOR INCIDENT P WAVE

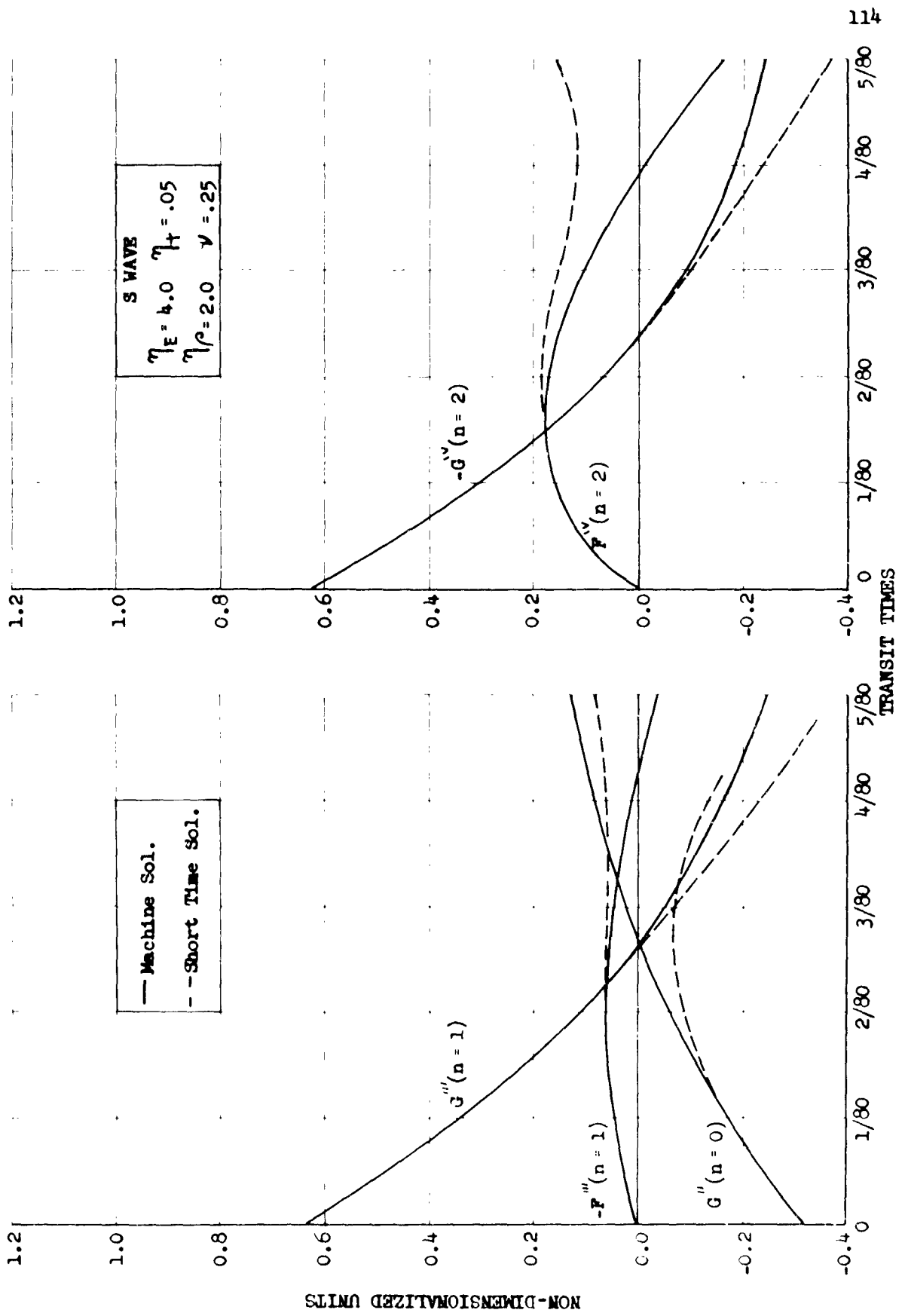


FIG. 34 COMPARISON OF SHORT-TIME RESULTS FOR INCIDENT S WAVE

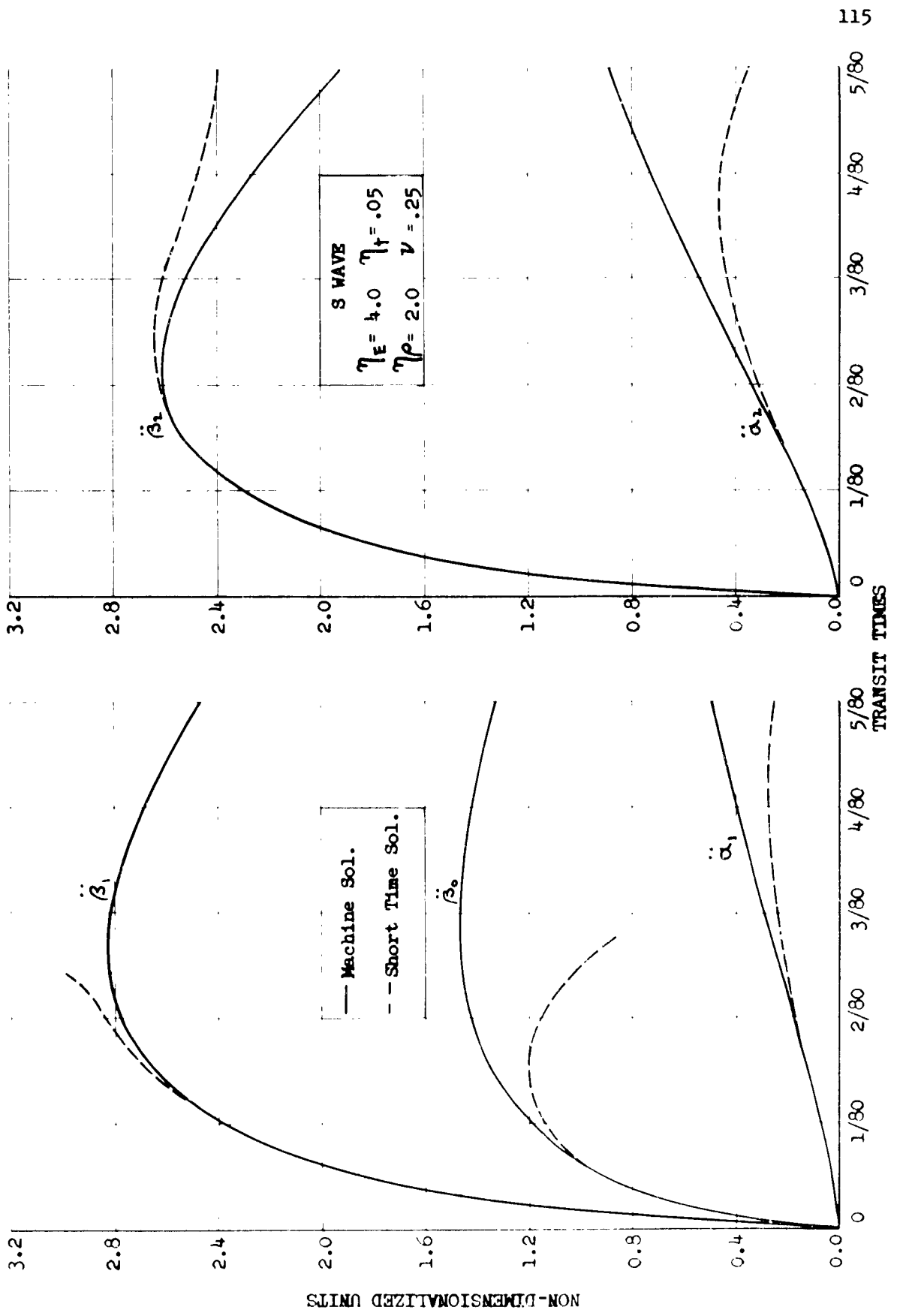


FIG. 35 COMPARISON OF SHORT-TIME RESULTS FOR INCIDENT S WAVE

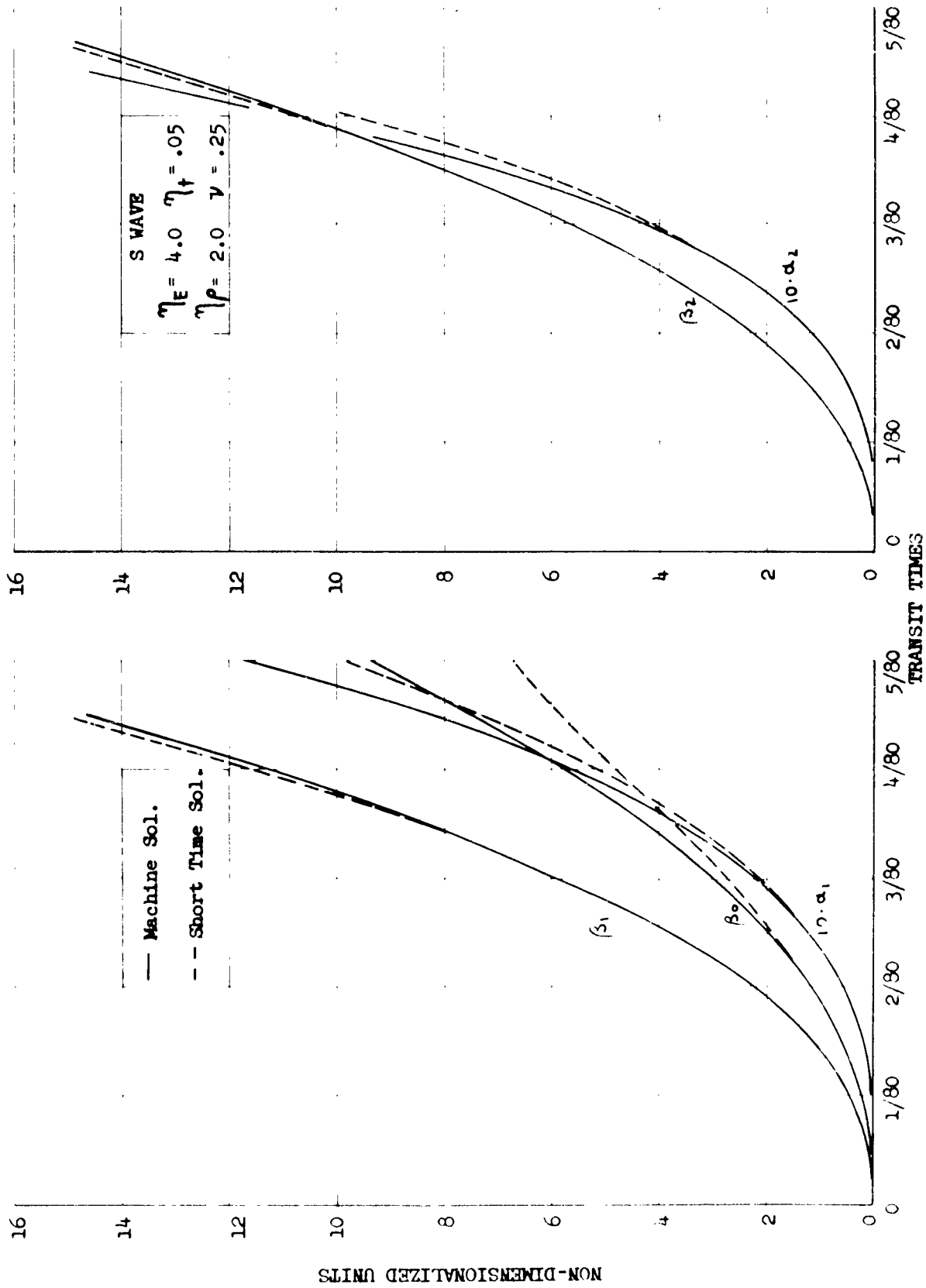


FIG. 36 COMPARISON OF SHORT-TIME RESULTS FOR INCIDENT S WAVE

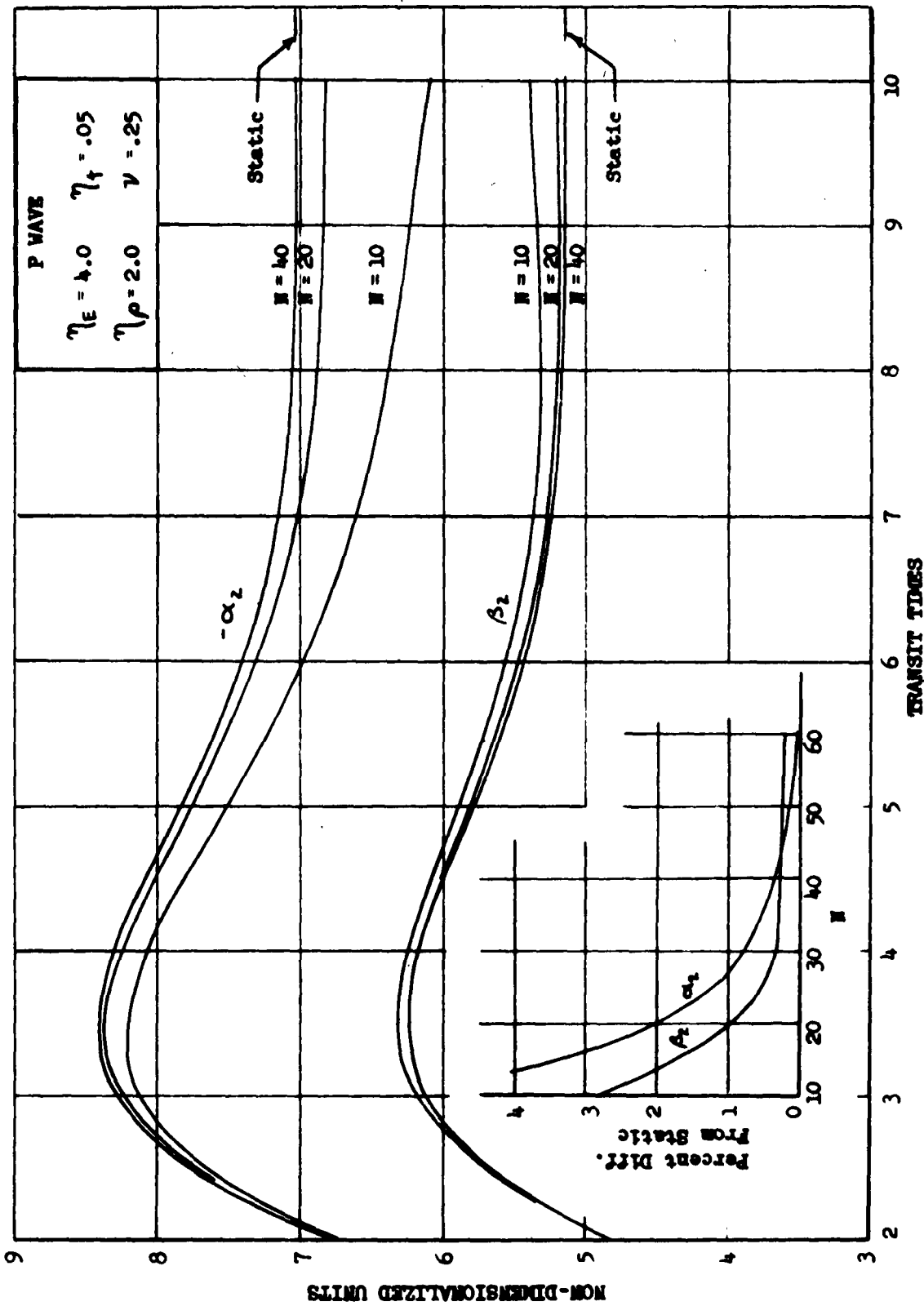


FIG. 37 EFFECT OF SIZE OF TIME INTERVAL ON LONG-TIME RESULTS

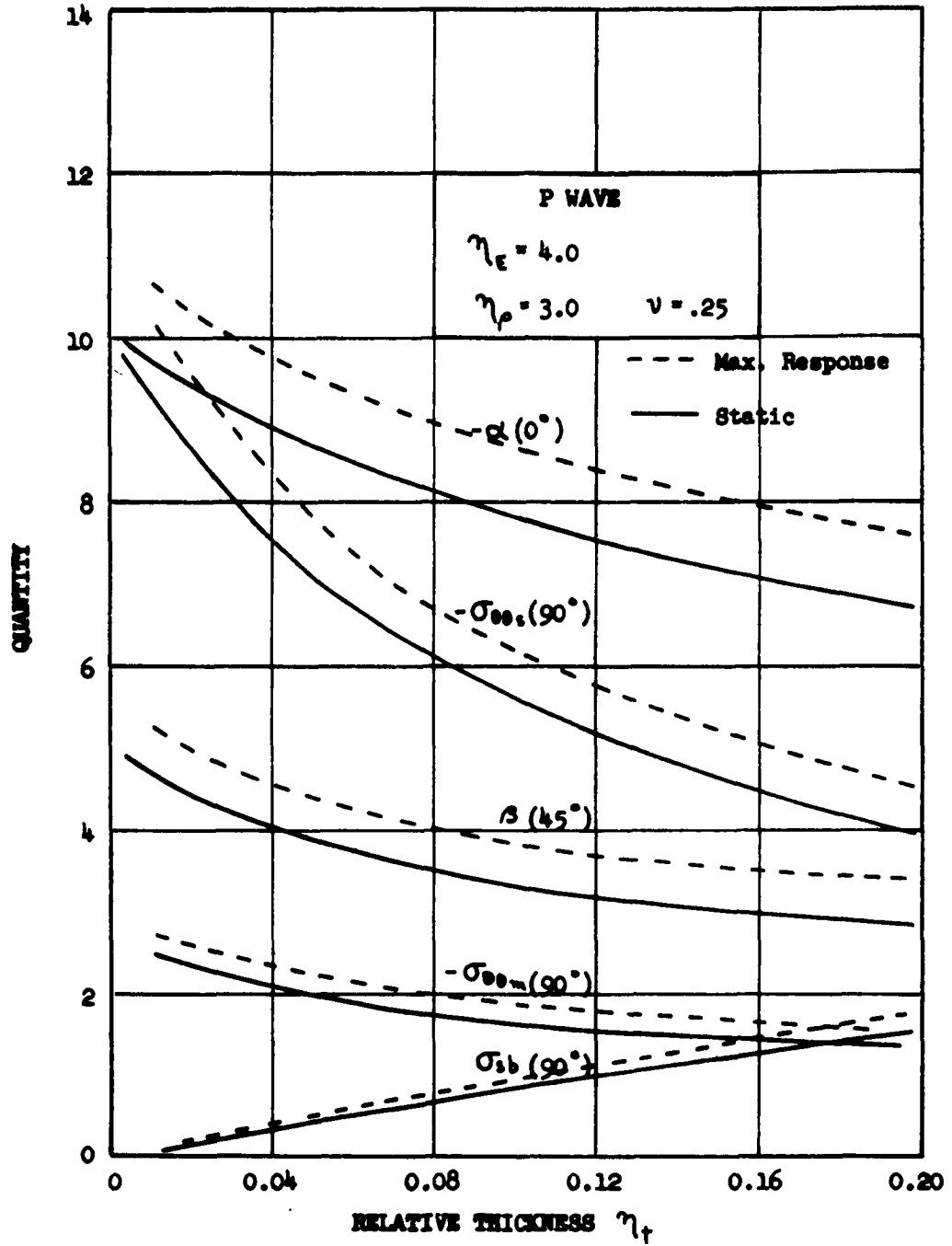


FIG. 38 EFFECT OF RELATIVE THICKNESS OF SHELL

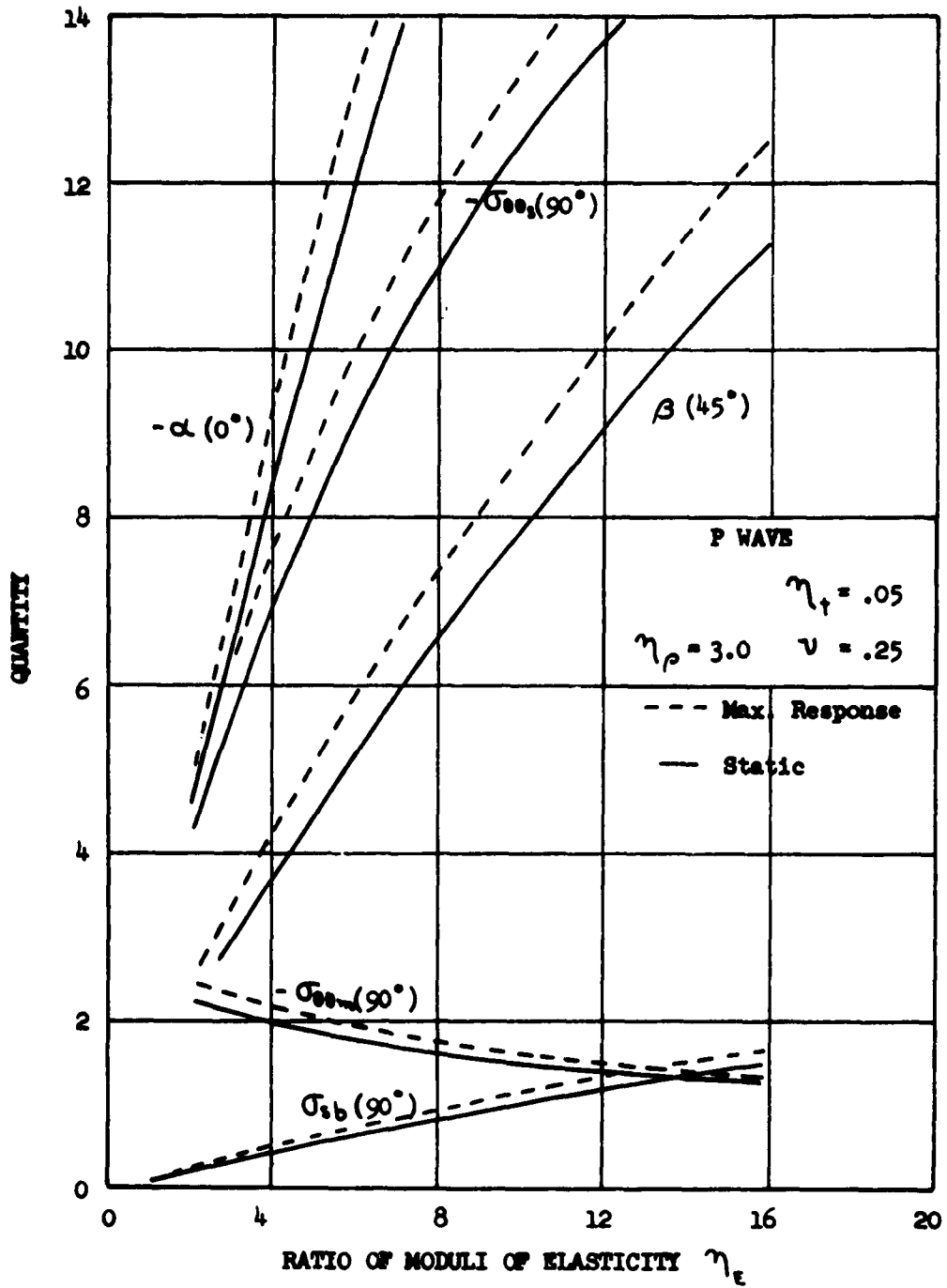


FIG. 39 EFFECT OF RATIO OF MODULI OF ELASTICITY

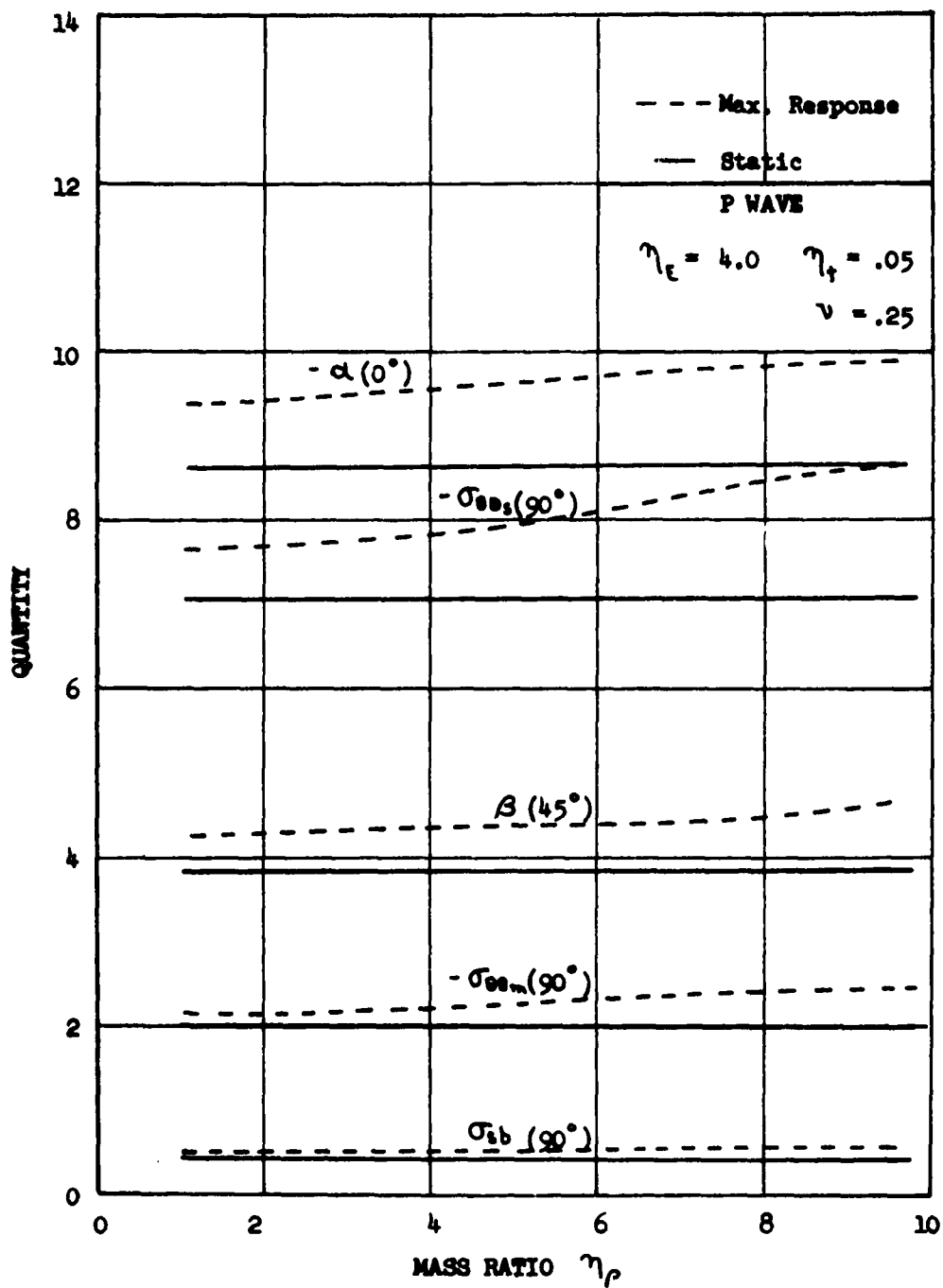


FIG. 40 EFFECT OF MASS RATIO

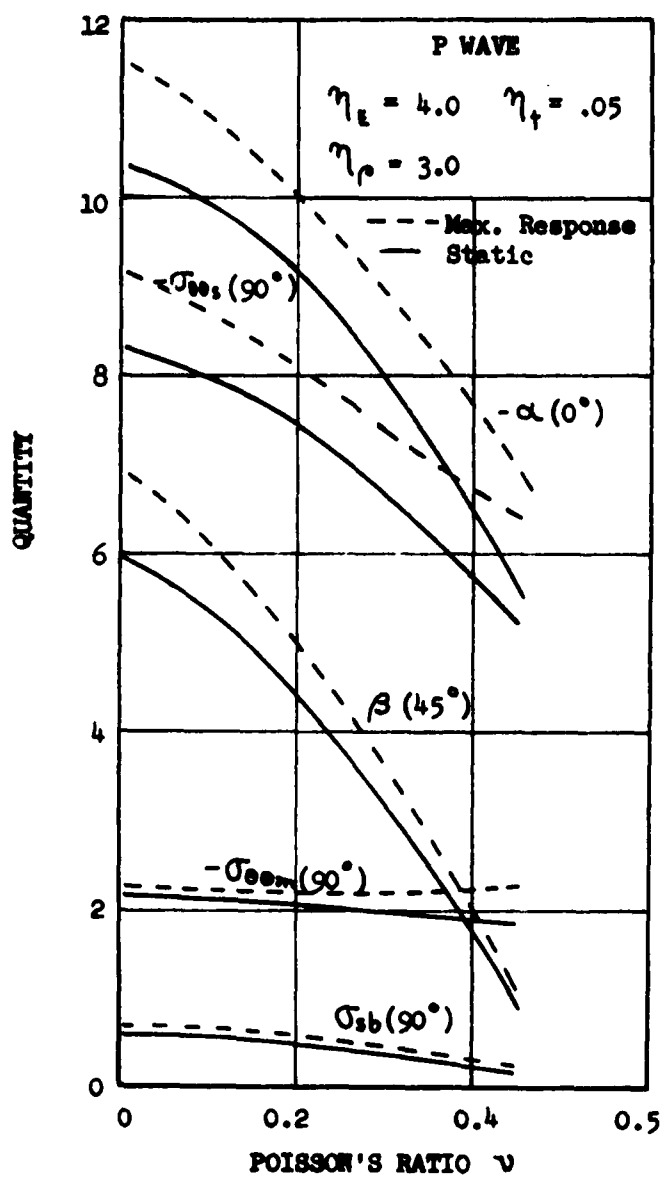


FIG. 41 EFFECT OF POISSON'S RATIO

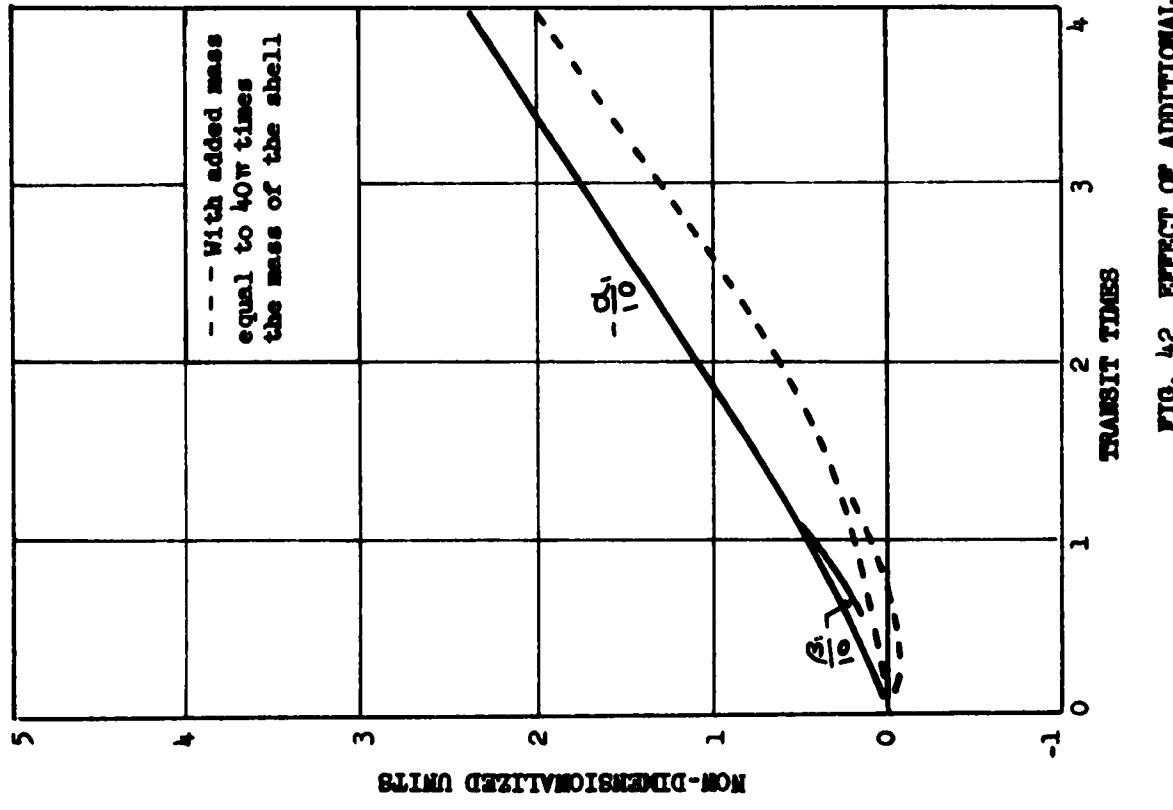
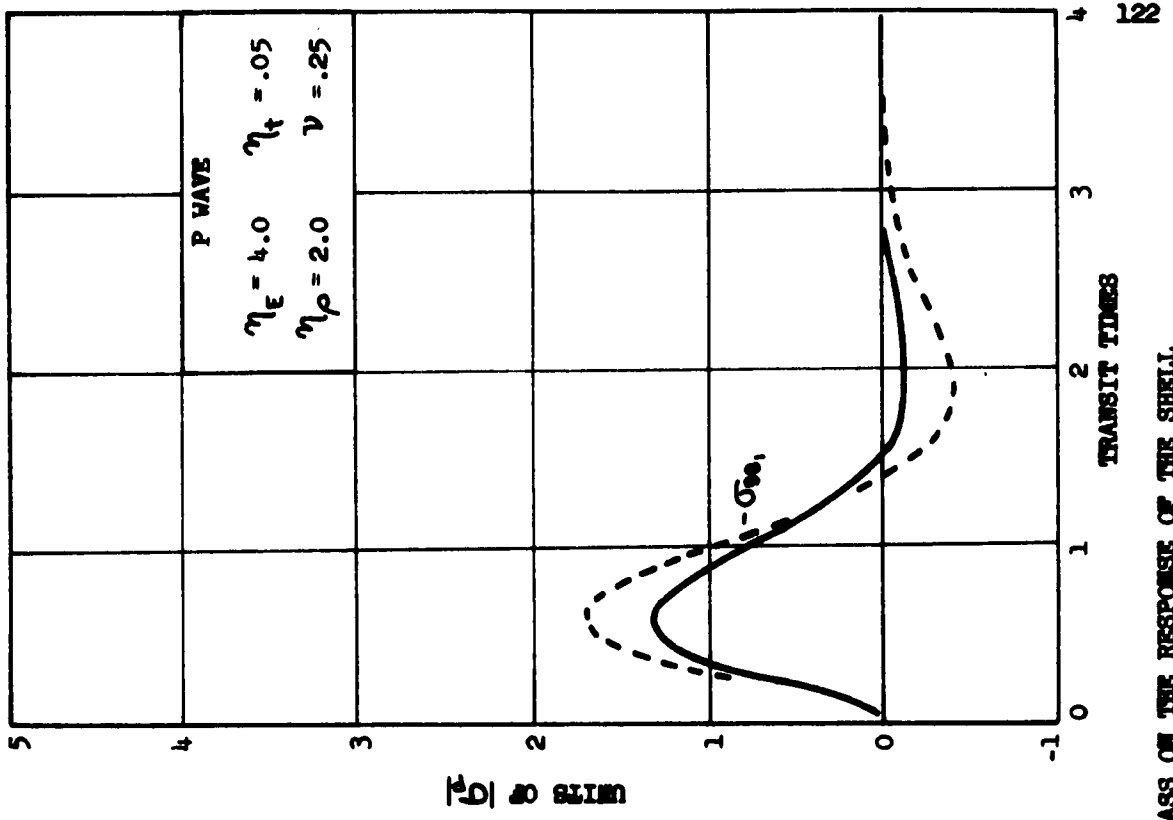


FIG. 4.2 EFFECT OF ADDITIONAL MASS ON THE RESPONSE OF THE SHELL

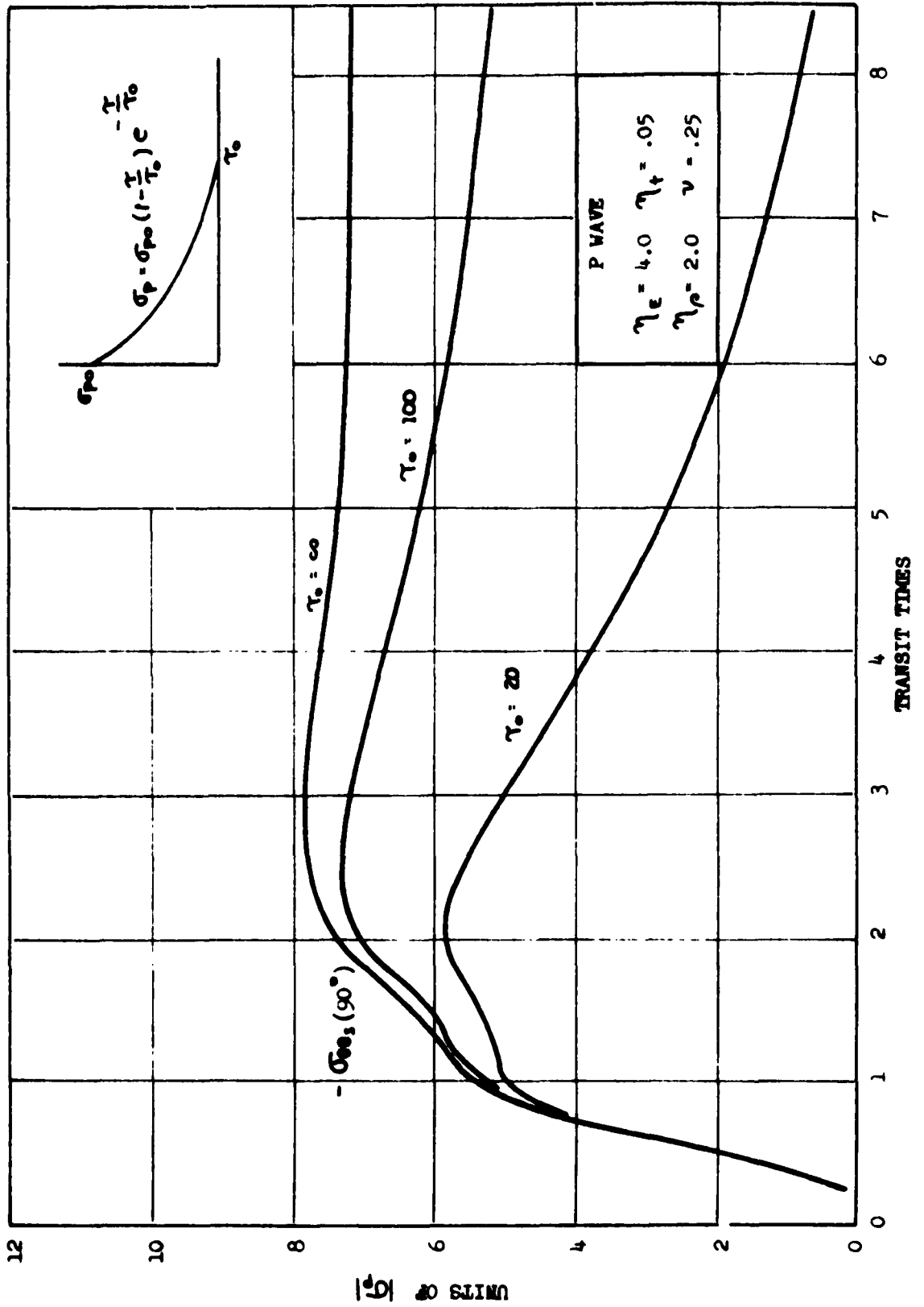


FIG. 43 EFFECT OF TIME VARYING INCIDENT STRESS WAVE ON SHELL HOOP STRESS

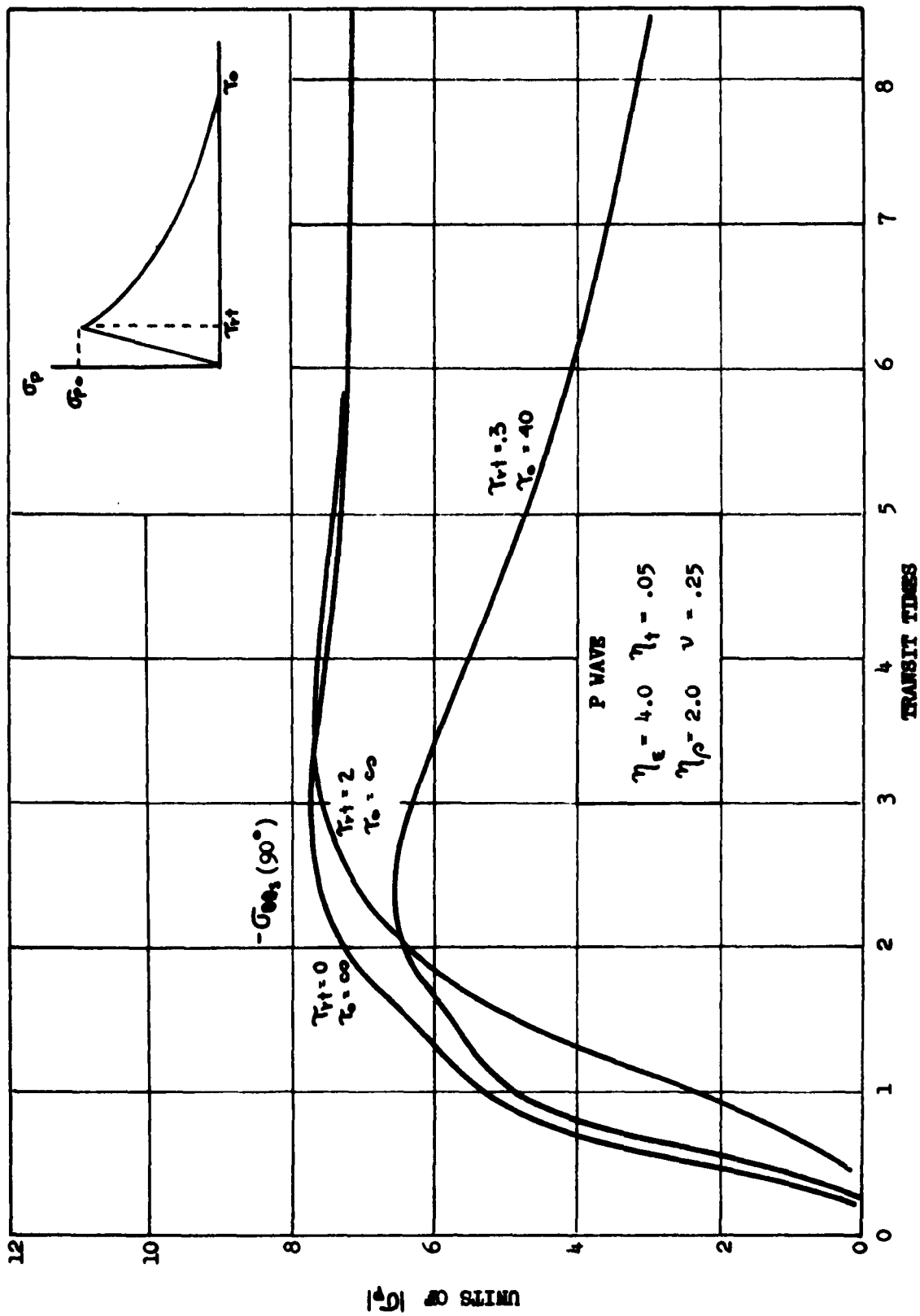


FIG. 44 EFFECT OF TIME VARYING INCIDENT STRESS WAVE ON SHELL HOOP STRESS

TRANSIT TIMES

8

7

6

5

4

3

2

1

0

UNITS OF  $|\sigma_p|$

$-\sigma_{\theta\theta_3} (90^\circ)$

$\tau_t = 0$   
 $\tau_0 = \infty$

$\tau_t = 2$   
 $\tau_0 = \infty$

$\tau_t = 3$   
 $\tau_0 = 40$

P WAVE

$\eta_e = 4.0$   $\eta_t = .05$

$\eta_p = 2.0$   $\nu = .25$

$\sigma_p$

$\sigma_p$

$\tau_0$

$\tau_t$

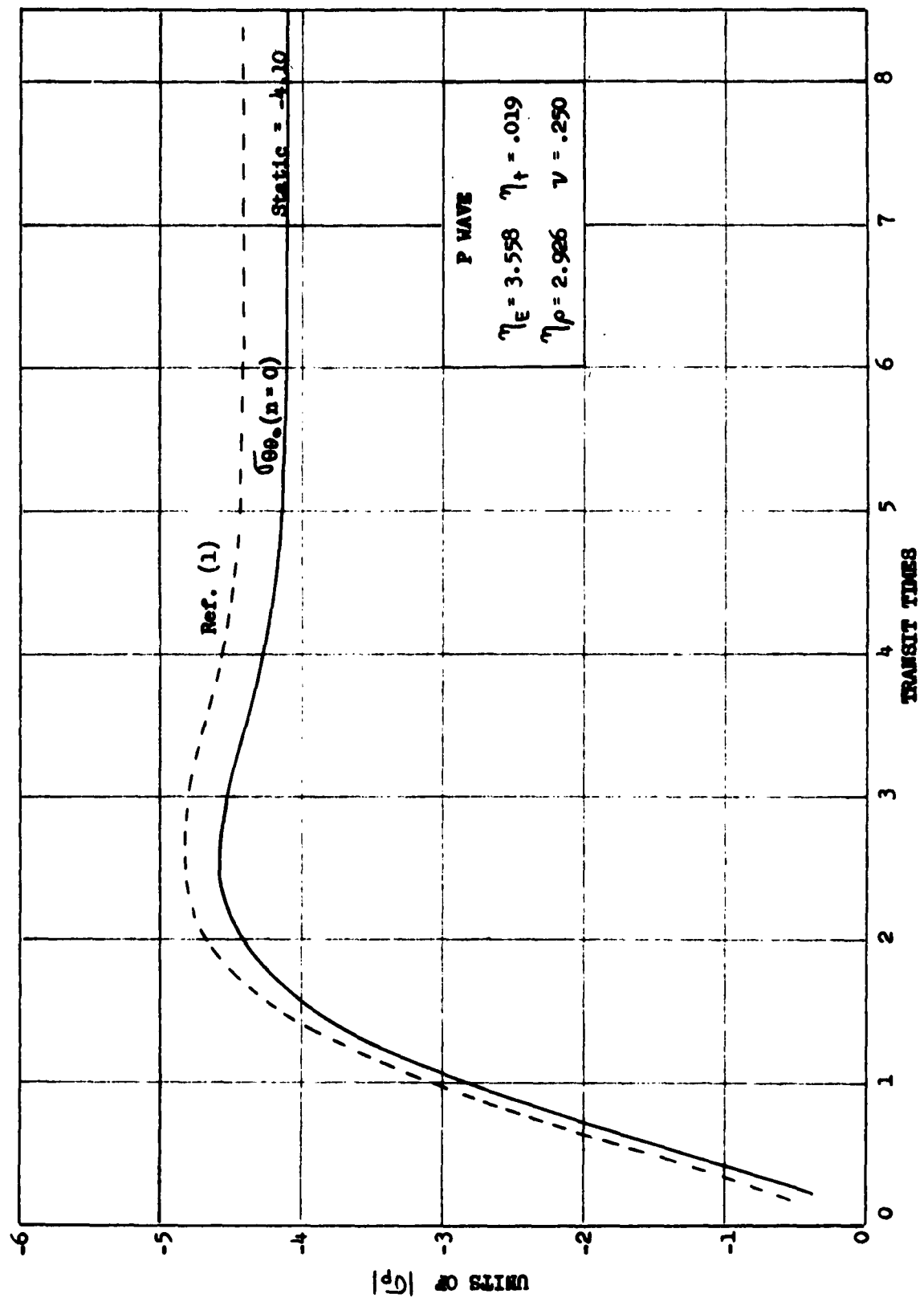


FIG. 45 COMPARISON WITH PREVIOUS WORK, HOOP STRESS (SHELL) FOR  $n = 0$

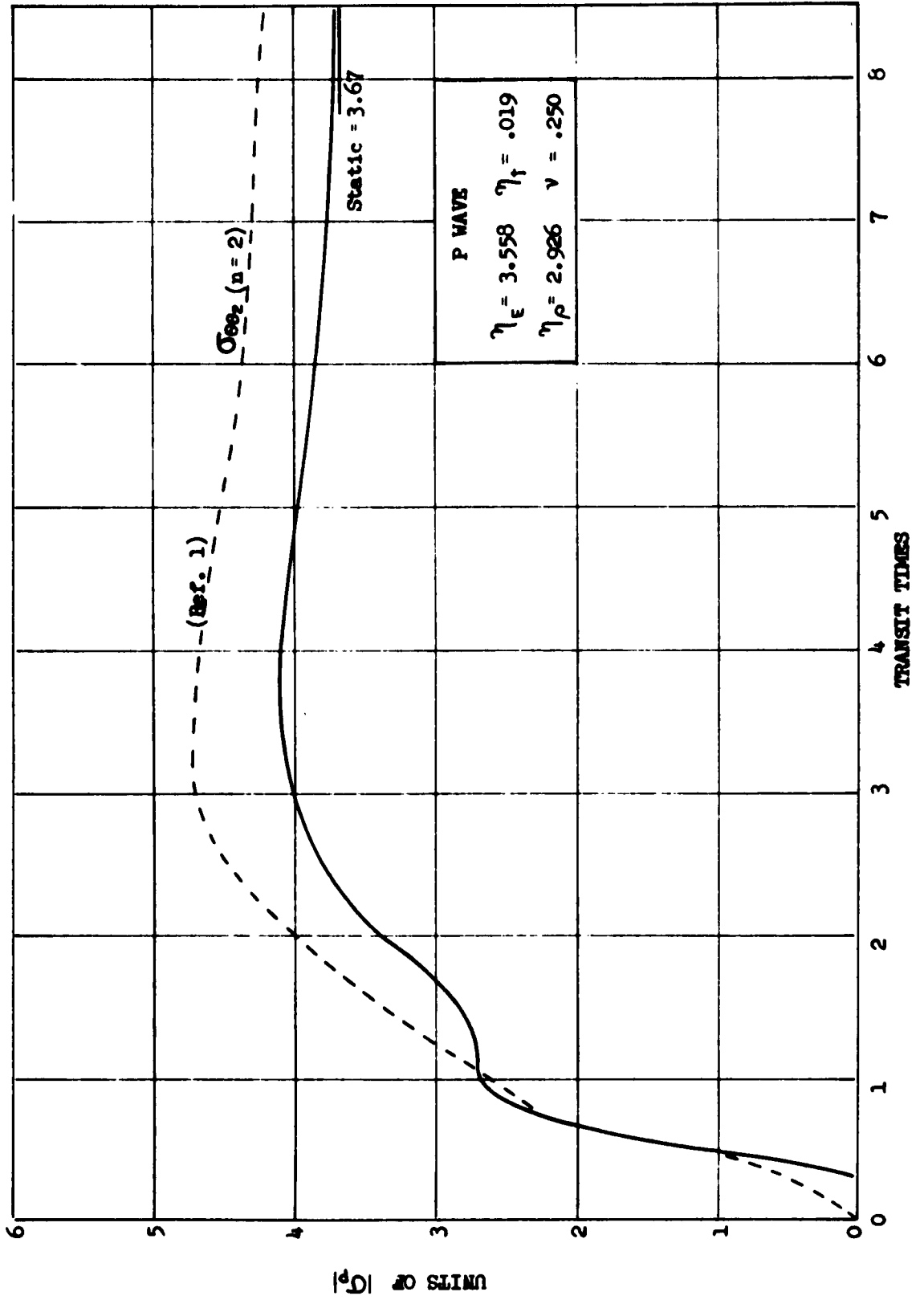


FIG. 46 COMPARISON WITH PREVIOUS WORK, HOOP STRESS (SHELL) FOR  $n = 2$

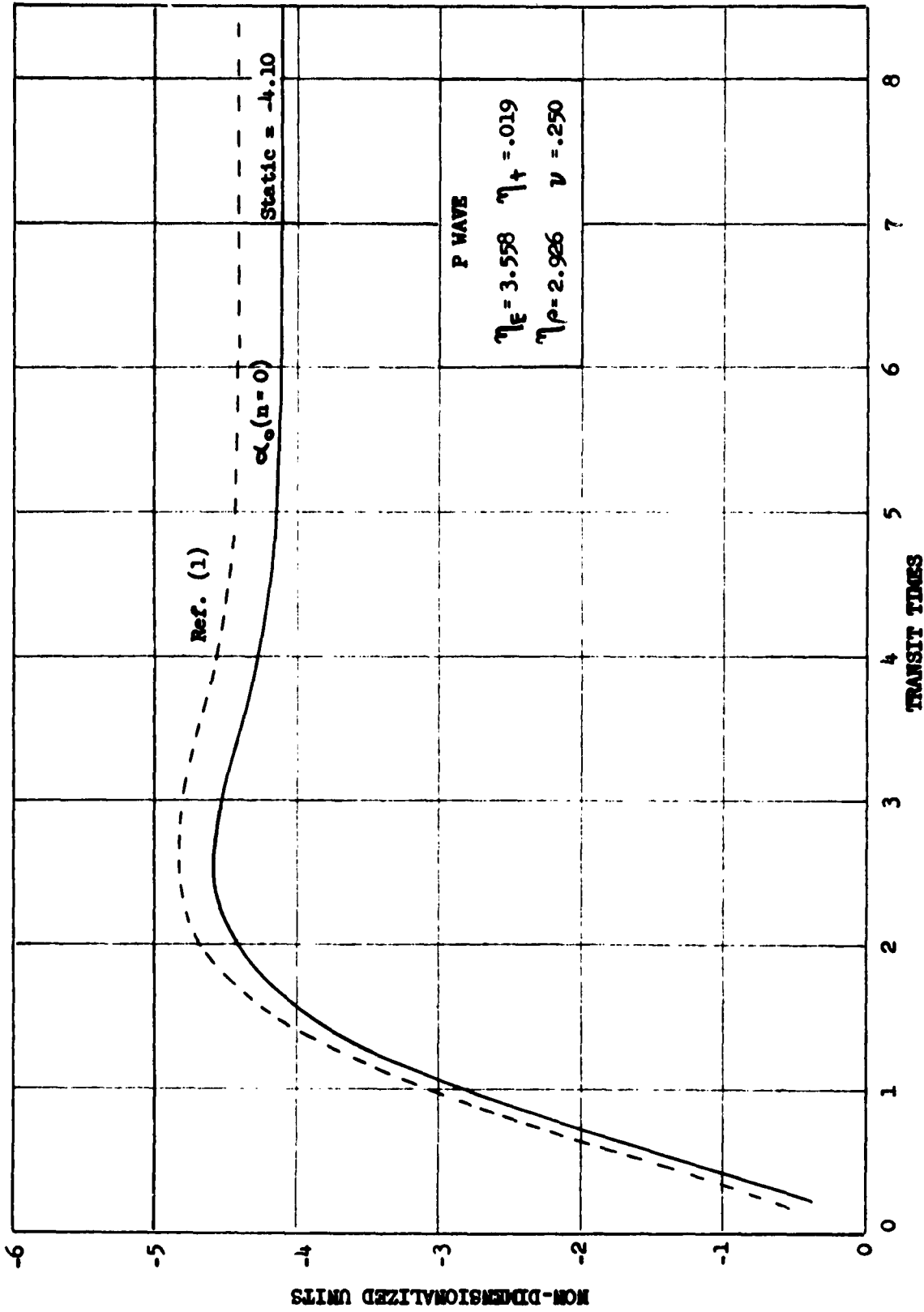


FIG. 47 COMPARISON WITH PREVIOUS WORK, RADIAL DISPLACEMENT FOR  $n = 0$

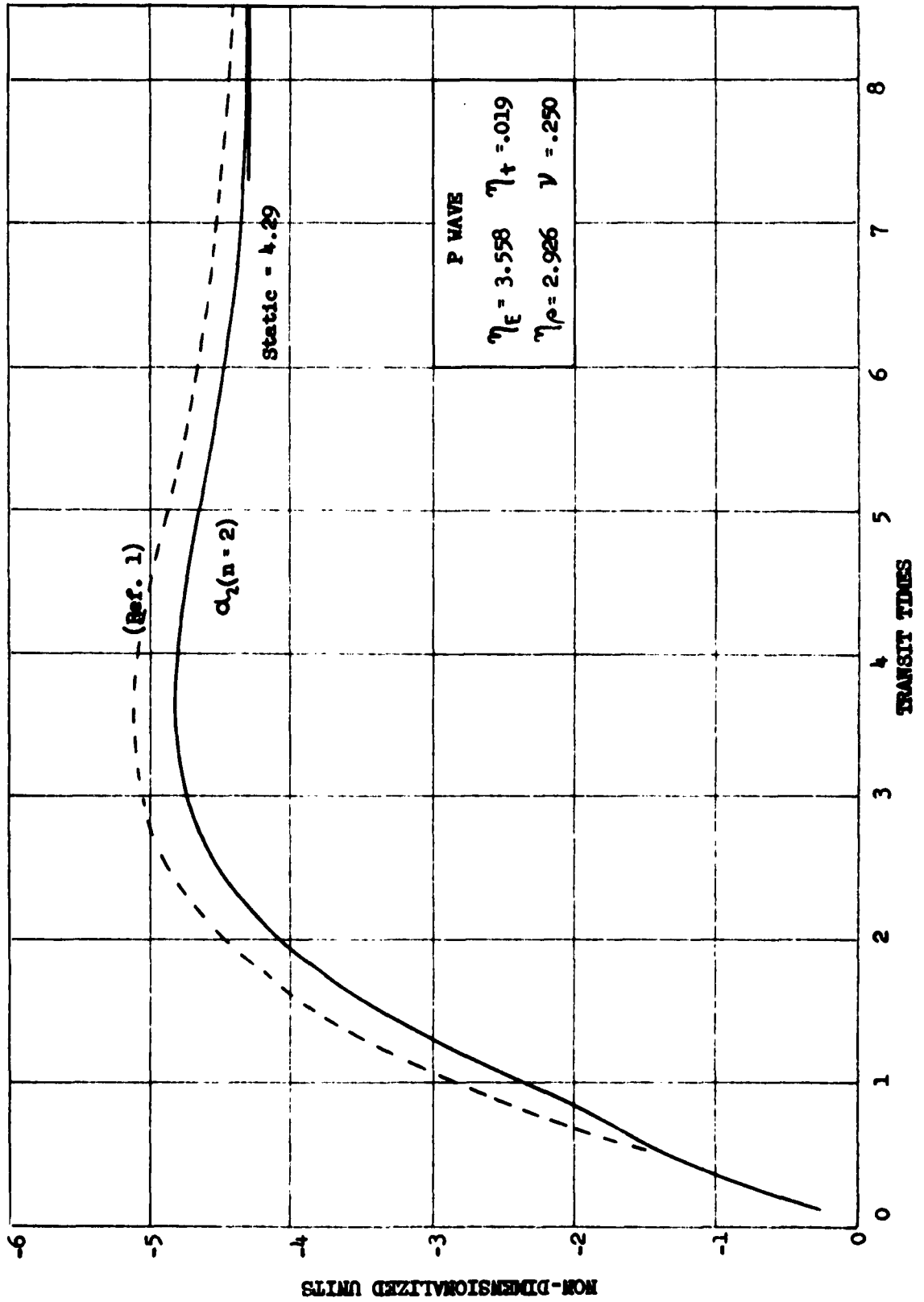


FIG. 4.6 COMPARISON WITH PREVIOUS WORK, RADIAL DISPLACEMENT FOR  $n = 2$

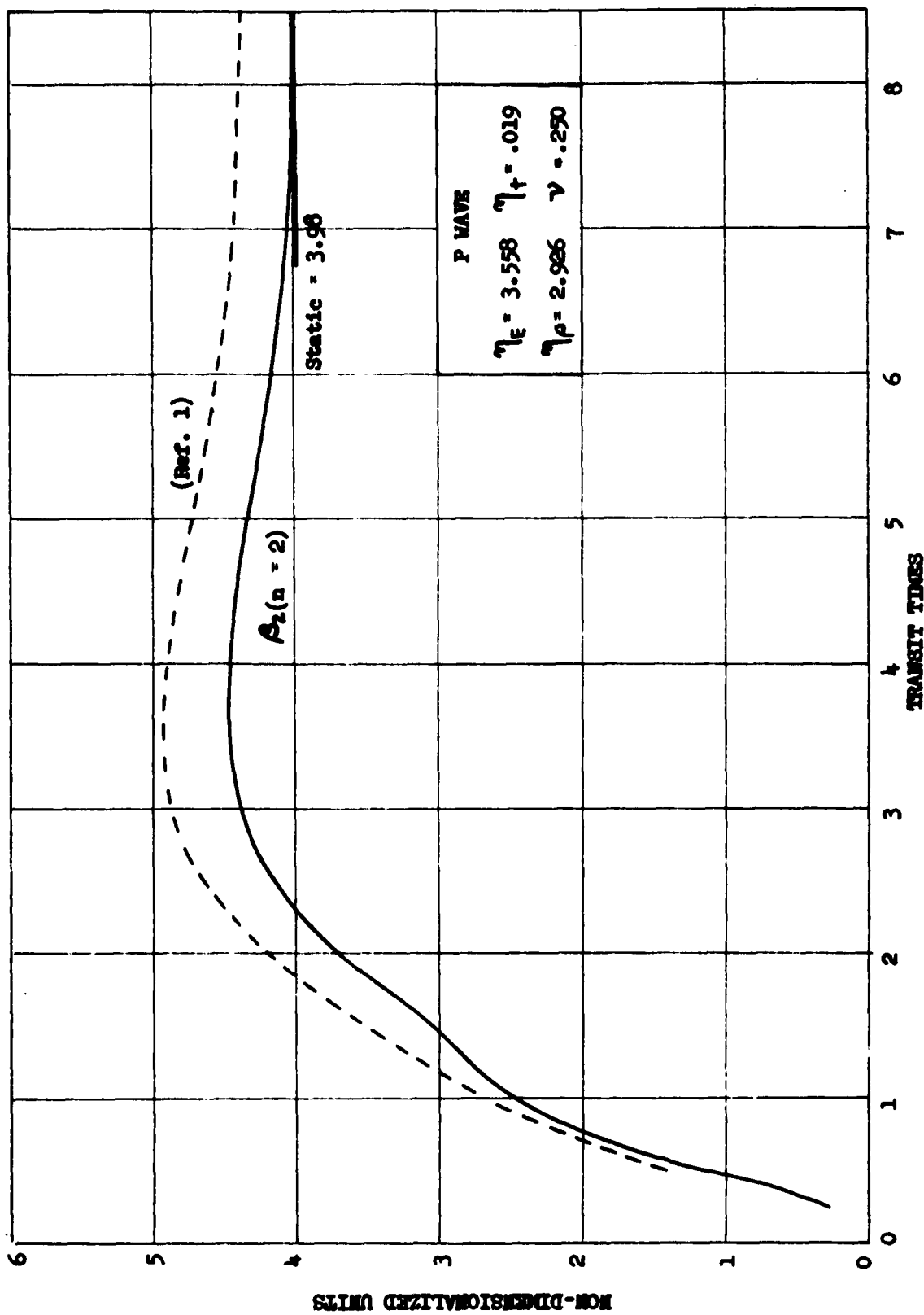


FIG. 49 COMPARISON WITH PREVIOUS WORK, TANGENTIAL DISPLACEMENT FOR  $n = 2$

Jan. 1963

Distribution List for Technical Reports Issued Under  
Contract Nonr 1834(03), Project NR-064-183

Argonne National Laboratory  
Bailey and Bluff  
Lamont, Illinois

Armed Forces Special Weapons Project  
P. O. Box 2610  
Washington, D. C.  
ATTN: Chief, Blast Branch (2)  
Chief, Weapons Effects Div. (1)

Armed Services Technical (5)  
Information Agency  
Arlington Hall Station  
Arlington 12, Virginia

Ballistic Research Laboratory  
Aberdeen Proving Ground  
Aberdeen, Maryland  
ATTN: Dr. C. W. Lampson

Battelle Memorial Institute  
505 King Avenue  
Columbus, Ohio  
ATTN: H. C. Cross

Chief of Bureau of Aeronautics  
Navy Department  
Washington 25, D. C.  
ATTN: DE-22 (1)  
DE-23, E.M. Ryan (1)  
TD-41, Tech. Lib. (1)

Chief, Bureau of Ordnance  
Navy Department  
Washington 25, D. C.  
ATTN: AD-3, Technical Library

Chief, Bureau of Ships  
Navy Department  
Washington 25, D. C.  
ATTN: Code 421 ( )  
Code 423 ( )  
Code 430 (1)  
Code 442 (1)  
Code 449 (1)  
Director of Research (2)

Chief, Bureau of Yards and Docks  
Navy Department  
Washington 25, D. C.  
ATTN: Code C-313 (1)  
Code P-314 (1)

Chief of Engineers  
Engineering Division  
Military Construction  
Washington 25, D. C.  
ATTN: ENGB (2)

Chief of Naval Research  
Department of the Navy  
Washington 25, D. C.  
ATTN: Code 423 (1)  
Code 432 (1)  
Code 438 (4)

Chief of Staff  
Department of the Army  
Research and Development Div.  
Washington 25, D. C.  
ATTN: Chief of Research  
and Development

Chief, Structures Division (2)  
Research Directorate  
Air Force Special Weapons Center  
Kirtland Air Force Base, New Mexico

Commander  
U. S. Naval Ordnance Test Station  
Inyokern, China Lake, California  
ATTN: Code 501

Commander  
U. S. Naval Ordnance Test Station  
Pasadena Annex  
3202 E. Foothill Boulevard  
Pasadena 8, California  
ATTN: Code P8087

Commander  
U. S. Naval Proving Grounds  
Dahlgren, Virginia

Forest Products Laboratory  
Madison, Wisconsin  
ATTN: L. J. Markwardt

Library, Engineering Foundation  
29 West 39th Street  
New York, New York

National Aeronautics and Space  
Administration  
Cleveland Municipal Airport  
Cleveland, Ohio  
ATTN: J. H. Collins, Jr.

National Aeronautics and Space  
Administration  
1512 H Street, N.W.  
Washington 25, D. C.

National Aeronautics and Space  
Administration  
Langley Field, Virginia  
ATTN: Dynamic Loads Branch (1)  
Structures Lab (1)

Naval Air Experimental Station  
Naval Air Material Center  
Naval Base  
Philadelphia 12, Pennsylvania  
ATTN: Head, Aeronautical  
Materials Laboratory

Naval Ordnance Laboratory  
White Oak, Maryland  
RFD 1, Silver Spring, Maryland  
ATTN: Mechanics Division (2)

Naval Ordnance Test  
Inyokern, China Lake, California  
ATTN: Scientific Officer

Office of Air Research  
Wright-Patterson Air Force Base  
Dayton, Ohio  
ATTN: Chief, Applied Mechanics Group

Office of the Chief of Engineers  
Assistant Chief for Public Works  
Department of the Army  
Bldg. T-7, Gravelly Point  
Washington 25, D. C.  
ATTN: Structural Branch, R.L. Bloor

Office of Naval Research (2)  
The John Crerar Library Building  
10th Floor, 86 E. Randolph Street  
Chicago 1, Illinois

Office of Chief of Ordnance  
Research and Development Service  
Department of the Army  
The Pentagon  
Washington 25, D. C.  
ATTN: ORDTB (2)

Officer in Charge  
Naval Civil Engineering Research  
and Evaluation Laboratory  
Naval Station  
Port Hueneme, California

Officer in Charge  
Office of Naval Research  
Branch Office, London  
Navy No. 100  
FPO, New York, New York

RAND Corporation  
Nuclear Energy Division  
1700 Main Street  
Santa Monica, California

Research and Development Board  
Department of Defense  
Pentagon Building  
Washington 25, D. C.  
ATTN: Library, Code 3D-1075

Superintendent  
Naval Gun Factory  
Washington 25, D. C.

Superintendent  
Post Graduate School  
U. S. Naval Academy  
Monterey, California

U. S. Atomic Energy Commission  
Division of Research  
Washington, D. C.

U. S. Coast Guard  
1300 E. Street, N.W.  
Washington, D. C.  
ATTN: Chief, Testing and  
Development Division

U. S. Maritime Commission  
Technical Bureau  
Washington, D. C.  
ATTN: Mr. V. Russo

Dr. W. Baldwin  
Metals Research Laboratory  
Case Institute of Technology  
Cleveland, Ohio

Prof. Lynn Beedle  
Fritz Engineering Laboratory  
Lehigh University  
Bethlehem, Pennsylvania

Prof. R. L. Bisplinghoff  
Massachusetts Inst. of Technology  
Cambridge 39, Mass.

Dr. Walter Bleakney  
Department of Physics  
Princeton University  
Princeton, New Jersey

Dean H. L. Bowman  
College of Engineering  
Drexel Institute of Technology  
Philadelphia, Pa.

Prof. E. J. Brunelle, Jr.  
Dept. of Aeronautic Engr.  
Princeton University  
Princeton, New Jersey

Prof. D. S. Clark  
Division of Mechanical Engineering  
Calif. Institute of Technology  
1201 E. California St.  
Pasadena, California

Dr. Francis H. Clauser  
Chairman, Dept. of Aeronautics  
The Johns Hopkins University  
School of Engineering  
Baltimore 18, Maryland

Prof. Morris Cohen  
Division of Metallurgy  
Massachusetts Inst. of Technology  
Cambridge 39, Mass.

Prof. Lloyd Donnell  
Department of Mechanics  
Illinois Inst. of Technology  
Technology Center  
Chicago 16, Illinois

Dr. J. E. Dorn  
University of California  
Berkeley, California

Dr. D. C. Drucker  
Chairman, Div. of Engineering  
Brown University  
Providence, Rhode Island

Dr. John E. Duberg  
Theoretical Mechanics Division  
Langley Research Center  
National Aeronautics and Space  
Administration  
Hampton, Virginia

Prof. W. J. Duncan  
Head, Dept. of Aeronautics  
James Watt Engineering Labs.  
The University  
Glasgow W.2, Scotland

Dr. L. Fox, Director  
Oxford University  
Computing Lab.  
Oxford, England

Dr. J. M. Frankland  
Mechanics Division  
National Bureau of Standards  
Washington 25, D. C.

Prof. A. M. Freudenthal  
Columbia University  
New York, New York

Dr. Robert E. Fulton  
Structural Mechanics Division  
NASA Langley Research Center  
Hampton, Virginia

General Electric Research Labs.  
1 River Road  
Schenectady, New York

Prof. M. Gensamer  
Department of Metallurgy  
Columbia University  
New York, New York

Dr. Martin Goland  
Vice President  
Southwest Research Inst.  
8500 Culebra Road  
San Antonio, Texas

Dr. J. N. Goodier  
School of Engineering  
Stanford University  
Stanford, California

Prof. L. E. Goodman  
Dept. of Mechanics and Materials  
University of Minnesota  
Minneapolis, Minnesota

Prof. A. E. Green  
Kings College  
Newcastle on Tyne 1, England

Dr. R. J. Hansen  
Massachusetts Inst. of Technology  
Cambridge 39, Mass.

Prof. R. P. Harrington, Head  
Department of Aeronautic Eng.  
University of Cincinnati  
Cincinnati 21, Ohio

Prof. R. M. Hermes  
University of Santa Clara  
Santa Clara, California

Prof. N. J. Hoff, Head  
Div. of Aeronautical Engineering  
Stanford University  
Stanford, California

Dr. W. H. Hoppmann  
Department of Mechanics  
Rensselaer Polytechnic Institute  
Troy, New York

Prof. L. S. Jacobsen  
Stanford University  
Stanford, California

Dr. Bruce Johnston  
301 W. Engineering Building  
University of Michigan  
Ann Arbor, Michigan

Prof. W. K. Krefeld  
College of Engineering  
Columbia University  
New York, New York

Dr. R. Latter  
RAND Corporation  
Nuclear Energy Division  
1700 Main St.  
Santa Monica, California

Prof. B. J. Lazan  
Department of Mechanics  
University of Minnesota  
Minneapolis 14, Minnesota

Prof. George Lee  
Department of Mechanics  
Rensselaer Polytechnic Institute  
Troy, New York

Dr. M. M. Lemcoe  
Atomics International  
Canoga Park, California

Dr. C. W. MacGregor  
Engineering Building  
University of Pennsylvania  
Philadelphia 4, Pa.

Prof. R. F. Mehl  
Metals Research Laboratory  
Carnegie Institute of Technology  
Pittsburgh, Pa.

Dr. M. L. Merritt  
Sandia Corporation  
Sandia Base  
Albuquerque, New Mexico

Prof. Jesse Ormondroyd  
University of Michigan  
Ann Arbor, Michigan

Prof. W. R. Osgood  
Department of Civil Engineering  
The Catholic University of America  
Washington 17, D. C.

Mr. R. E. Peterson  
ASTM Committee E-9 on Fatigue  
Westinghouse Research Laboratory  
East Pittsburgh, Pa.

Prof. W. Prager, Chairman  
Physical Sciences Council  
Brown University  
Providence, Rhode Island

Mr. J. T. Ranson  
Engineering Research Laboratory  
Experimental Station  
E. I. DuPont de Nemours  
Wilmington, Delaware

Dr. S. Raynor  
Prof. of Mechanical Engineering, Room 359  
Northwestern Technological Inst.  
Northwestern University  
Evanston, Illinois

Prof. E. Reissner  
Department of Mathematics  
Massachusetts Inst. of Technology  
Cambridge 39, Mass.

Prof. F. E. Richart, Jr., Head  
Department of Civil Engineering  
University of Michigan  
Ann Arbor, Michigan

Prof. Emilio Rosenblueth  
Instituto de Ingenieria  
Ciudad Universitaria  
Mexico D.F., Mexico

Prof. F. S. Shaw  
Professor of Civil Engineering  
The University of New South Wales  
Broadway, Sydney, N.S.W.  
Australia

Dr. J. D. Shreve, Jr.  
Sandia Corporation  
Sandia Base  
Albuquerque, New Mexico

Dr. C. B. Smith  
Department of Mathematics  
Walter Hall  
University of Florida  
Gainesville, Fla.

Dr. C. S. Smith  
Institute for Study of Metals  
University of Chicago  
Chicago, Illinois

Prof. R. V. Southwell  
The Old House, Trumpington  
Cambridge, England

Prof. E. Sternberg  
Division of Engineering  
Brown University  
Providence, Rhode Island

Prof. F. K. Teichmann  
Dept. of Aeronautical Engineering  
New York University  
University Heights, Bronx  
New York, New York

Dr. G. E. Uhlenbeck  
Engineering Research Institute  
University of Michigan  
Ann Arbor, Michigan

Mr. M. P. White  
Department of Civil Engineering  
University of Massachusetts  
Amherst, Massachusetts

Dr. Dana Young  
Technical Vice President  
Southwest Research Institute  
8500 Culebra Road  
San Antonio 6, Texas

University of Illinois

Mr. F. X. Finnigan  
Resident Representative  
Office of Naval Research

Prof. N. M. Newmark, Head  
Department of Civil Engineering

Dean W. L. Everitt  
College of Engineering

Dean F. T. Wall  
Graduate College

Project Staff

Dr. A. R. Robinson  
Dr. W. C. Schnobrich  
Dr. S. Sutcliffe  
Dr. A. S. Veletsos  
Dr. J. W. Melin